

G.N. BULANIK DURMUŐ

MODELING AND COMPARISON OF MICRO INVERTER AND STRING
INVERTER IN PHOTOVOLTAIC SYSTEMS

THE GRADUATE SCHOOL OF NATURAL AND APPLIED SCIENCES
OF
ATILIM UNIVERSITY



GİZEM NUR BULANIK DURMUŐ

A MASTER OF SCIENCE THESIS
IN
THE DEPARTMENT OF MECHANICAL ENGINEERING

JUNE 2019

ATILIM UNIVERSITY

MODELING AND COMPARISON OF MICRO INVERTER AND STRING
INVERTER IN PHOTOVOLTAIC SYSTEMS

A THESIS SUBMITTED TO
THE GRADUATE SCHOOL OF NATURAL AND APPLIED SCIENCES
OF
ATILIM UNIVERSITY

BY

GİZEM NUR BULANIK DURMUŞ

IN PARTIAL FULFILLMENT OF THE REQUIREMENTS
FOR
THE DEGREE OF MASTER OF SCIENCE
IN
MECHANICAL ENGINEERING

JUNE 2019

Approval of the Graduate School of Natural and Applied Sciences, Atilim University.

Prof. Dr. Ali Kara
Director

I certify that this thesis satisfies all the requirements as a thesis for the degree of **Master of Science in Mechanical Engineering Department, Atilim University.**

Prof. Dr. Sadık Engin Kılıç
Head of Department

This is to certify that we have read the thesis **MODELING AND COMPARISON OF MICRO INVERTER AND STRING INVERTER IN PHOTOVOLTAIC SYSTEMS** submitted by **GİZEM NUR BULANIK DURMUŞ** and that in our opinion it is fully adequate, in scope and quality, as a thesis for the degree of Master of Science.

Assoc. Prof. Dr. Özgür Aslan
Supervisor

Examining Committee Members:

Prof. Dr. Ayhan Albostan
Energy Systems Engineering, Atilim University

Assoc. Prof. Dr. Özgür Aslan
Mechanical Engineering, Atilim University

Prof. Dr. Adem Acır
Energy Systems Engineering, Gazi University

Assoc. Prof. Dr. Hakan Argeşo
Manufacturing Engineering, Atilim University

Asst. Prof. Dr. Besim Baranoğlu
Manufacturing Engineering, Atilim University

Date: June 28, 2019



I declare and guarantee that all data, knowledge and information in this document has been obtained, processed and presented in accordance with academic rules and ethical conduct. Based on these rules and conduct, I have fully cited and referenced all material and results that are not original to this work.

Name, Last Name : GİZEM NUR BULANIK DURMUŞ

Signature :

ABSTRACT

MODELING AND COMPARISON OF MICRO INVERTER AND STRING INVERTER IN PHOTOVOLTAIC SYSTEMS

Durmuş, Gizem Nur Bulanık

M.S., Department of Mechanical Engineering

Supervisor : Assoc. Prof. Dr. Özgür Aslan

June 2019, 96 pages

Photovoltaic panels are structures that convert solar energy directly into electrical energy using photovoltaic cells connected in series and parallel. Several reasons are affecting photovoltaic panel efficiency negatively. Shading on the panel temporarily or permanently is one of the reason reduction of the efficiency. Panels can be exposed to the shading due to the clouding, buildings, or any other obstacles like dust, bird or leaf. Additionally, constant shadowing generates a hot spot effect. This situation causes some failures in the long-term on the panel or the panel group. Another problem is about connecting photovoltaic panels. In mostly, photovoltaic panels are connected in series at the plant-based systems. Serial connected panels reach very high voltages, and the high voltage based failure can occur. In these systems, photovoltaic panels can be arranged in limited ways in photovoltaic systems where the string inverter is used. Conversely, micro inverters are panel based systems and more comfortable to install. There is not any necessity to arrange the panels concerning the inverter. Although micro inverters are preferred for small scale photovoltaic systems, in some cases, they are used for large scale photovoltaic systems. Since each panel produces its own AC power, the high voltage problem is eliminated. However, due to their high costs and lower efficiencies, they are not preferred especially in large scale plants. In this thesis, considering these problems, 24 kWp installed power photovoltaic system in Ankara

Province was simulated with three different shading densities with both string and micro inverters and these simulations were compared.

Keywords: micro-inverter, string-inverter, photovoltaic, solar energy



ÖZ

MİKRO İNVERTÖRLÜ VE DİZİ İNVERTÖRLÜ FOTOVOLTAİK SİSTEMLERİN MODELLENMESİ VE KARŞILAŞTIRILMASI

Durmuş, Gizem Nur Bulanık

Yüksek Lisans, Makine Mühendisliği

Tez Yöneticisi : Doç. Dr. Özgür Aslan

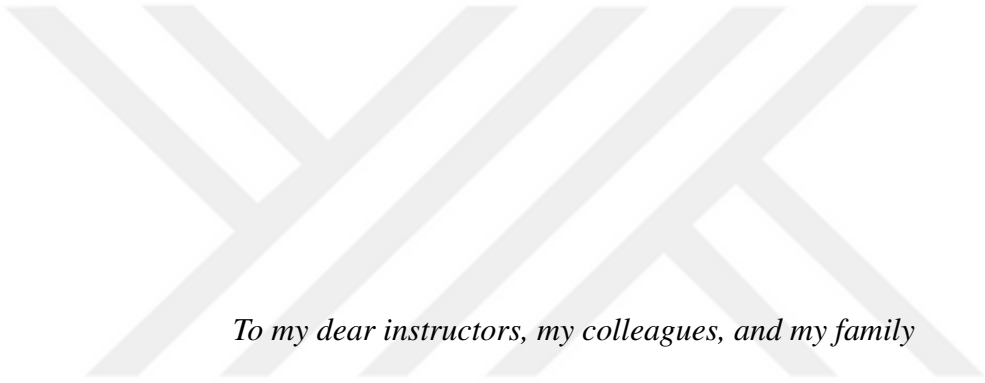
Haziran 2019, 96 sayfa

Fotovoltaik paneller, güneş enerjisini seri ve paralel bağlanmış fotovoltaik hücreler vasıtasıyla doğrudan elektrik enerjisine dönüştüren yapılardır. Fotovoltaik panel verimliliğini negatif yönde etkileyen birkaç neden vardır. Panelin üzerine düşen geçici veya sürekli gölgeleme, panel veriminin düşmesinin sebeplerinden bir tanesidir. Paneller, bulutlar, binalar, toz, kuş veya yaprak gibi engeller nedeniyle gölgelenmeye maruz kalabilir. Ek olarak, sürekli gölgeleme sıcak nokta etkisi yaratır. Bu durum uzun vadede panelde veya panel grubunda arızalara neden olmaktadır. Sistemlerde ortaya çıkan bir diğer problem, fotovoltaik panellerin birbirine bağlanması noktasında ortaya çıkar. Fotovoltaik paneller, özellikle büyük ölçekli fotovoltaik sistemlerde seri olarak bağlanır. Seri bağlı paneller çok yüksek gerilimlere ulaşır ve yüksek gerilime dayalı problemler ortaya çıkabilir. Dizi invertörün kullanıldığı fotovoltaik sistemlerde, fotovoltaik paneller sınırlı şekillerde yerleştirilebilir. Bunun karşısında, mikro invertörler panel tabanlı sistemlerdir ve kurulumu kolaydır. Panelleri invertöre göre yerleştirmeye gerek yoktur. Mikro invertörler, genellikle küçük ölçekli fotovoltaik sistemler için tercih edilse de, bazı durumlarda büyük ölçekli fotovoltaik sistemlerde de kullanılır. Her panel kendi AC gücünü ürettiğinden, yüksek voltaj sorunu ortadan kalkar. Fakat yüksek maliyetleri ve dizi invertörlere göre daha düşük olan verimleri

nedeniyle büyük ölçekli tesislerde tercih edilmemektedir. Bu tez çalışmasında, bu problemler göz önüne alınarak, Ankara İlinde 24 kWp kurulu güce sahip fotovoltaik bir sistemin, üç farklı gölge yoğunluğunda hem dizi invertör hem de mikro invertör ile bir paket program yardımıyla simülasyonları yapılmıştır. Yapılan simülasyon raporları doğrultusunda sistemler karşılaştırılmıştır.

Anahtar Kelimeler: mikro invertör, seri invertör, fotovoltaik, güneş enerjisi





To my dear instructors, my colleagues, and my family

ACKNOWLEDGMENTS

Firstly, I would like to thank my thesis advisor Assoc. Prof. Dr. Özgür Aslan.

I would also like to thank the experts who were involved in this thesis writing: Prof. Dr. Adem Acır, Mr. Mehmet Özeydın, Mrs. Füsün Bakır, Mr. Levent Erbük, Mr. Gökhan Özden.

Finally, I would like to thank my father Mr. Erol Bulanık, my mother Mrs. Firuzan Bulanık, my sister Mrs. İrem Bulanık, my husband Mr. Caner Durmuş, and my friends for their continuous support.

This thesis work would not have been possible without them.

Thank you.

TABLE OF CONTENTS

ABSTRACT	iii
ÖZ	v
DEDICATION	vii
ACKNOWLEDGMENTS	viii
TABLE OF CONTENTS	ix
LIST OF TABLES	xii
LIST OF FIGURES	xiii
CHAPTERS	
1 INTRODUCTION	1
2 PHOTOVOLTAIC ENERGY SYSTEMS	7
2.1 Photovoltaic Energy in the World	12
2.2 Photovoltaic Energy in Turkey	14
3 PHOTOVOLTAIC ENERGY SYSTEMS	17
3.1 Solar Cells	17
3.1.1 Solar cells according to structure	18
3.1.1.1 Monocrystalline cells	18
3.1.1.2 Polycrystalline cells	19
3.1.1.3 Thin film	19
3.2 Solar Angles	19
3.2.1 Latitude angle (\varnothing)	20
3.2.2 Declination angle (δ)	20
3.2.3 Clock angle (ω)	20
3.2.4 Azimuth angle (γ_S)	20

	3.2.5	Zenit angle (Θ_z)	21
3.3		Photovoltaic System Elements	21
	3.3.1	Photovoltaic panels	21
	3.3.2	Inverters	24
	3.3.3	Photovoltaic Mounting Systems	27
3.4		Photovoltaic Systems According to Network Dependence . .	28
	3.4.1	Grid-connected systems	28
	3.4.2	Network independent systems (Off-grid systems) .	28
	3.4.3	Hybrid systems	29
3.5		Problems in Photovoltaic Energy Systems	29
3.6		Effect of Temperature on the Panel	30
	3.6.0.1	Panels with a working temperature higher than 25 ° C	30
	3.6.0.2	Panels with a working temperature less than 25 ° C	33
4		MODELING AND COMPARISON OF PHOTOVOLTAIC SYSTEMS	37
4.1		Simulations with String Inverter	39
	4.1.1	A photovoltaic system modeled shadowless conditions with string inverter	39
	4.1.2	A photovoltaic system modeled with string inverter at first shadow density	41
	4.1.3	A photovoltaic system modeled with string inverter at second shadow density	44
4.2		Simulations with Micro Inverter	46
	4.2.1	A photovoltaic system modeled shadowless conditions with micro inverter	48
	4.2.2	A photovoltaic system modeled with micro inverter at first shadow density	49
	4.2.3	A photovoltaic system modeled with micro inverter at second shadow density	51
5		ANALYSIS, CONCLUSION AND RECOMMENDATIONS	56
5.1		Interpretation of Analysis	56
	5.1.1	String Inverter in Shadowless Condition	56

5.1.2	String Inverter in the First Shadow Density	57
5.1.3	String Inverter in the Second Shadow Density	59
5.1.4	Micro Inverter in Shadowless Condition	59
5.1.5	Micro Inverter in the First Shadow Density	60
5.1.6	Micro Inverter in the Second Shadow Density	61
5.2	Conclusion and Discussion	61
REFERENCES		64

APPENDICES

A	APPENDICES	67
A.1	Serial Shadowless	67
A.2	Serial 1st Density	72
A.3	Serial 2nd Density	77
A.4	Micro Shadowless	82
A.5	Micro 1st Density	87
A.6	Micro 2nd Density	92

LIST OF TABLES

TABLES

Table 2.1	List of installed capacity of solar power plants in the world by country [17]	12
Table 2.2	Annual Development Of Turkey's Installed Capacity [3]	14
Table 5.1	Simulated systems	57
Table 5.2	Performance rates	62

LIST OF FIGURES

FIGURES

Figure 1.2	Representation of Turkey by Primary Energy Sources - 2017 [1] . . .	1
Figure 1.3	Usage areas of solar energy	2
Figure 1.4	Turkey installed capacity by primary energy sources for the years 2007 and 2017 [3]	3
Figure 2.1	Electricity generation scheme from photovoltaic energy	7
Figure 2.2	Classification according to band spacing	9
Figure 2.3	Occurrence of an electron-gap pair	10
Figure 2.4	Combined n-type and p-type semiconductors	10
Figure 2.5	Photovoltaic energy conversion	11
Figure 2.6	A simple equivalent circuit model	11
Figure 2.7	Solar installed capacity by region [18]	13
Figure 2.8	Solar energy investments by year [18]	13
Figure 2.9	Solar energy potential map of Turkey [21]	15
Figure 2.10	Global Radiation Values Turkey (kWh / m^2 day) [22]	15
Figure 2.11	Turkey sunshine duration (time) [22]	16
Figure 2.12	PVGIS data for Turkey [23]	16
Figure 3.1	From cell to array Photovoltaic System Elements	17
Figure 3.2	Most common panel types according to cells	18
Figure 3.3	Monocrystalline cell	18
Figure 3.4	Polycrystalline cell	19
Figure 3.5	Thin film	19

Figure 3.6 Declination angle (δ)	20
Figure 3.7 Cell, panel and array	21
Figure 3.8 Panel layers [26]	22
Figure 3.9 Panel Production Line [28]	23
Figure 3.10 Polycrystalline cell production stages	24
Figure 3.11 Monocrystalline panel production stages	24
Figure 3.12 String inverter diagram	25
Figure 3.13 Shadow effect on string inverters	26
Figure 3.14 Central inverter	26
Figure 3.15 System with micro inverter	27
Figure 3.16 Roof and floor mounted sample system schemes	28
Figure 3.17 Network independent solar system diagram	29
Figure 3.18 Hot spot effect	30
Figure 3.19 Technical specifications of the panel	31
Figure 4.1 Energy and radiation values for PVGIS Ankara	38
Figure 4.2 Shadowless system parameters	39
Figure 4.3 Shadowless system diagram	40
Figure 4.4 Shadowless system losses diagram	41
Figure 4.5 Monthly simulation results in the shadowless system	42
Figure 4.6 Shading curve in shadowless system	42
Figure 4.7 System parameters at the first shadow density	43
Figure 4.8 System diagram of the first shadow density	43
Figure 4.9 System losses diagram	44
Figure 4.10 Simulation results on the basis of the first shadow density system	45
Figure 4.11 System parameters at the second shadow density	45
Figure 4.12 System diagram in the second shadow density	46
Figure 4.13 Scheme of system losses in the second shadow density	47
Figure 4.14 Simulation results on the basis of second shade density system	47

Figure 4.15 Shadowless system parameters with micro inverter	48
Figure 4.16 Shadowless system diagram with micro inverter	49
Figure 4.17 Shadowless system loss diagram with micro inverter	50
Figure 4.18 Shadowless system loss diagram with micro inverter	50
Figure 4.19 Shadowless system loss diagram with micro inverter	51
Figure 4.20 System diagram of the first shade density with micro inverter . . .	51
Figure 4.21 Diagram of system losses in the first shade density with micro inverter	52
Figure 4.22 Simulation results on the basis of the first shade density system with micro inverter	52
Figure 4.23 System parameters in second shadow density with micro inverter .	53
Figure 4.24 System loss diagram in second shadow density with micro inverter	53
Figure 4.25 System loss diagram in second shadow density with micro inverter	54
Figure 4.26 Simulation results in the second shade density system with micro inverter	55
Figure 5.1 String Inverter and shadowless system outputs	58
Figure 5.2 String Inverter and system outputs at the first shadow density . . .	58
Figure 5.3 String inverter and system outputs at the second shadow density . .	59
Figure 5.4 Micro inverter and shadowless system outputs	60
Figure 5.5 Micro inverter and system outputs at first shadow density	60
Figure 5.6 Micro inverter and system outputs at the second shadow density . .	61

CHAPTER 1

INTRODUCTION

The importance of alternative energy sources emerges, considering the limited fossil resources and the continuity of energy demand. The fossil resources are running out day by day. Considering their negative environmental impacts, potentials of the renewable energy sources of the countries gained importance over time and these resources have been used as well as fossil resources. For example, Turkey has a high potential for hydroelectric and the investments made in this direction. Hydroelectric energy, is one of the renewable energy source, becomes the most likely option for electricity production for Turkey (Figure 1.1). The use of solar energy as a renewable energy source in electricity generation has also become widespread in the last few years [1].

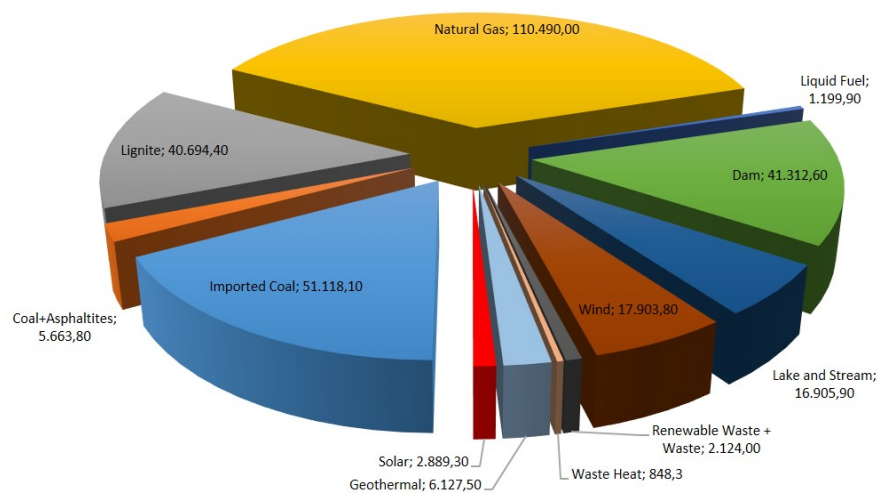


Figure 1.1: Representation of Turkey by Primary Energy Sources - 2017 [1]

Solar energy is the radiant energy released by fusion reactions in the center of the sun [2]. This energy can be transformed into other forms of energy, direct or indirect ways. For example, photovoltaic cells convert photon energy directly into electrical energy through their semiconductor structures. Starting with the work has been done in the 1950s, cell efficiencies increased, and solar panels have become a common way of generating electricity. The solar cells, which are commonly in crystalline or thin film form, joined together and composed the panels. Due to advances in technology and developments, the cost of increased cells has fallen over the years. Solar energy become important in Turkey since it can be used in many ways. Turkey has excellent potential for solar energy and a lot of positive development that occur over time. Although solar energy systems are divided into two main parts as electrical energy and heat energy, the following examples indicate the importance of the sun.



Figure 1.2: Usage areas of solar energy

Solar energy, which is used in almost any field, has been considered as photovoltaic energy in this thesis study.

Although the initial investment costs are high, the widespread use of photovoltaic plants is increasing due to the shortening of the depreciation periods and the high earnings in the long-term. The total installed capacity of Turkey is 85,2 GW by the end of April 2019, and according to the given data installed capacity of the solar energy is 3420 MW in 2017. The demand for energy increases with the population, and this demonstrates the importance of alternative sources. The statistics show that solar energy technology will have a more significant role in the future in Turkey, due to the high solar energy potential [3].

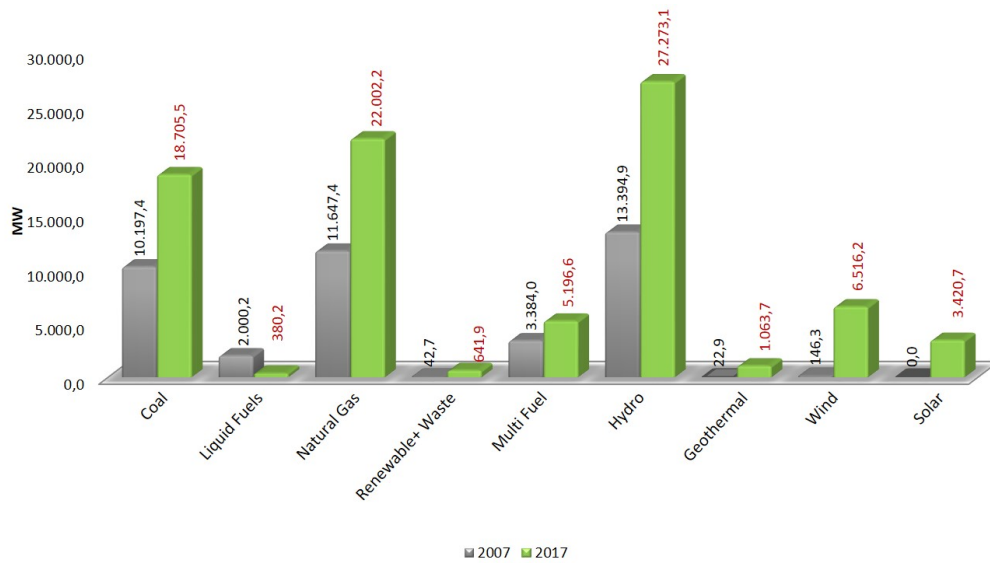


Figure 1.3: Turkey installed capacity by primary energy sources for the years 2007 and 2017 [3]

Problem Status / Description of the Subject

Almost all renewable energy sources depend on the sun. It is the basis of many renewable energy sources such as solar energy, wind energy, hydroelectric energy, tidal ocean energy, etc. In terms of its diameter and width, the sun, which is the only star in the solar system, is in the middle row compared to other systems and stars. As an infinite source, the sun has a core of about 20 million ° C and a surface temperature of 6000 ° C. To better emphasize the importance of the sun, the example of the annual energy from the sun is more than 150 times the current coal potential in the world. More importantly, our country is located between 36 ° and 42 ° north parallels, and it has a geographic position, it is accepted that between the 40 ° and 40 ° northern parallels as “sun zone” [4-6]. First works about the sun were mostly done to meet the need for space area. The primary purpose of that study was to meet the energy needs of satellites. However, the use of solar energy as a source of electricity is based on the oil crisis in the 1970s. Instead of the limited fossil resources, studies of inexhaustible and renewable energy resources are accelerated during this period. Today, increasing population and increasing energy need emphasize the importance of the sun [7].

In order to use the sun as a source of electricity, some elements required. The most

important of these are solar panels. Widely used panels are named according to cell types. These are monocrystalline cell panel, polycrystalline cell panel, and thin film panel. Monocrystalline cell panels are the most efficient in terms of cell efficiency in about 24 % yield. Since higher-yielding cells are not yet economically feasible, this study has been carried out over the comparison between existing panels. Panel selection can be made according to geographic location, desired panel efficiency, and price differences. The second important element after the panels is the inverter. Inverters are devices that provide grid compatibility by converting the direct current from the panels to alternating current. Inverters used in solar systems are divided into three: array inverters, central inverters, and micro inverters. The array inverters are connected to the inverter by connecting the panels in series depending on the input voltage. Central inverters, unlike series, are used in large power plant applications. In this type of inverter, the panel assemblies are first assembled in the junction boxes then the junction boxes are collected in a single central inverter. Micro inverters are connected to each panel separately and interconnected in parallel [6].

In this thesis, systems with string inverter and micro inverter under different shadow densities simulated with a package program.

Literature Survey

Gazis et al. demonstrated the importance of micro-inverters by performing both cost and performance analysis. They compared the micro and string inverters in their studies and concluded that micro inverter systems are more efficient in shaded conditions. In addition to the performance, they calculated that the payback period of the systems with string inverters is shorter than the systems with micro inverters [8]. According to Gozuk, micro-inverters operate at lower efficiency than string inverters. Even if this efficiency is achieved with the technologies developed by some micro inverter companies, they state that the micro inverter prices are four times more than the string inverters. In addition, they describe the installation of panels with micro inverter is easier. The reason for this is that the AC cable is supplied directly from the factory so that it is connected to the grid. [9] Arraez-Cancelliere et al. compared the cost of micro-inverters and string inverters to Colombia in a system with a power rating of 5.1 kWp. This comparison was carried out in two different scenarios: with shadow and without

shadow. They stated that micro inverters perform better in terms of levelized cost of energy (LCOE), but in Colombia terms, the payback period of both technologies is between 10 and 12 years. [10] Sharkawi and Hassan examined the effect of shadow on micro, series and central inverters in a 288 kW photovoltaic power plant. According to their study, the energy output of the string inverter in the large scale power plants is higher than the micro and central inverter. On the other hand, the power output of the micro inverter system is higher in small scale systems. Compared to the cost of the micro inverter system has been observed to have higher costs [11]. According to Krauter and Bendfeld, some micro-inverters, which compare performance and price between micro inverter brands, more expensive than the panel itself. [12] Famoso et al. Compared micro and string inverter performances with different strength and different photovoltaic panels in different azimuth angles at different shadow intensities. In the study conducted for Sicily, they observed that the micro inverter system has higher performance in both shaded and shadowless conditions. [13]

Aim of The Study

The purpose of this thesis study is to observe the energy outputs of six different solar power plants, with varying densities of shadow, having the same installed power with simulated micro inverter and string inverter. Based on the results of the simulations, the problems in solar energy systems were identified, and suggestions for improvement were made.

Simulations made with parameters kept apart from shading and inverters can be used as sample work for solar power plant designs. This theoretical study, which will be a reference for practical applications in solar energy investments, will help investors.

Importance of the Study

In this study, performance comparisons of string and micro inverters observed in different shadow densities. The systems where their performances compared will be an example for future solar energy investments. The study, which deals with the problems that may be encountered, also includes recommendations on the solution of these problems. This study, which can contribute to increasing solar energy investments, will serve as a model for investors to use in practice and theory. The comparison of

two different inverters with the same installed power will benefit the industrialists and researchers who will work on this issue. Thereby, they can select the most suitable system for themselves.

Assumptions

In this thesis, the PVSYST package program was used to compare the simulations of the systems. In comparison, in the six different systems with an installed power of 24 kWp, all inputs except inverters and inverters are considered to be the same. According to the program outcomes, comments will be made about the systems. By using these comments, we will compare which system performs better in shadows and how much it costs against its performance.

Limitations

In the comparisons made, the installations were carried out theoretically with simulations. Therefore, there may be differences between theory and practice. Approximate values of program outputs can be considered, and tolerances can be taken into account.

CHAPTER 2

PHOTOVOLTAIC ENERGY SYSTEMS

The solar and heat source for our world has a diameter of 6.955×10^5 km. The distance between the sun and the world is about 149 million km. The temperature in the kernel is 15 million K, with a temperature of approximately 5800 K at the surface. The energy of the sun based on fusion reactions. This reaction is a reaction to the formation of a new atomic nucleus as a result of the combination of two atomic nuclei. We can use the energy released as a result of these series reactions as heat and light energy. [14] Solar cells made from a semiconductor material. They are direct electricity generating systems. Electricity is produced as follows without any generator or a similar step. Photons reaching the earth from the sun, when they hit the solar cells, break the electron bond in the structure of the cell. As a result of the flow of free electrons, the electric current is produced.

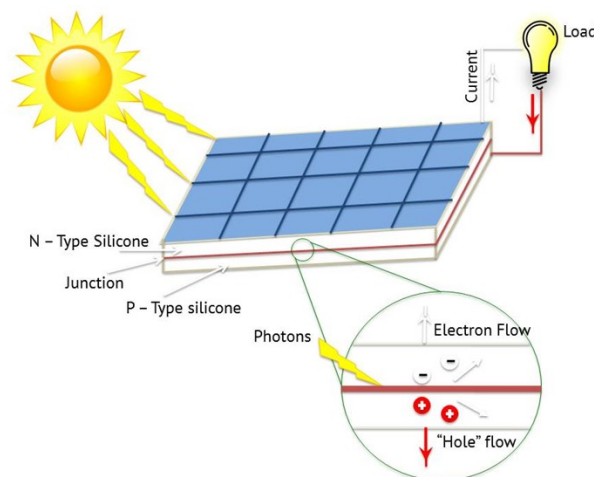


Figure 2.1: Electricity generation scheme from photovoltaic energy

Although electricity was produced using silicon crystal in the 1950s, in 1839 Becquerel discovered that the voltage between the two electrodes dipped in the electrolyte was due to the light coming on them. Similarly, G. W. Adams and R.E. in his experiment with selenium crystal, they made a study that revealed the existence of the relationship between light and voltage in 1876. In 1914, photovoltaic cell yield was around 1 % . Until 1954, photovoltaic cells have not used as today's. In 1954, in the experiments on the silicon crystal, the efficiency reached around 6 % and the solar cells which were converted into electrical energy with photons were accepted as a turning point for the works in later years. The first designs were made to support space work. Although solar cells were initially used for the energy requirements of spacecraft, photovoltaic cells showed their significant development due to the 1973 oil crisis. The crisis stemming from petroleum realized the orientation towards alternative energy sources and initiated studies in these areas. Even if the problems related to fossil resources were solved, solar energy continued to develop. As the process of converting the silicon crystal into a photovoltaic cell is costly, the work on thin film solar cells has been accelerated. [15]

The efficiency of photovoltaic cells made of semiconductor materials determines the amount of electrical energy into which photons from the sun are transformed. Besides, the electrical energy produced depends on geography, meteorology, and topography.

According to their conductivity, substances are divided into three as insulating, semiconductor and superconductor. At the atom, the electron closest to the center is bound by the strongest link. Therefore, the electrons are weakened as they move away from the center. These outermost electrons determine the structure of matter and are called valence electrons. These electrons can move easily between adjacent atoms in metals with good conductors. These free electrons can be circulated at their own energy levels. Since free electrons can easily respond to incoming light and reflect light back, there is not any energy zone in the metals where the electrons are separate from the positive charges. Therefore, free electrons in metal materials are good for electron exchange, but not for photovoltaic transformations. The energy level between the energy level of the electrons in the insulating and semiconductor materials and the next energy level that they can be found in the energies for electrons. The energy band that contains the valence electrons is called the "valence band" and the band next to

the forbidden energy band is called the conduction band. The width of the forbidden energy band is the measure that determines whether the material is semiconductor or insulating. The energy band that contains the valence electrons is called the “valence band” and the band next to the forbidden energy band is called the conduction band. The width of the forbidden energy band is the measure that determines whether the material is semiconductor or insulating.

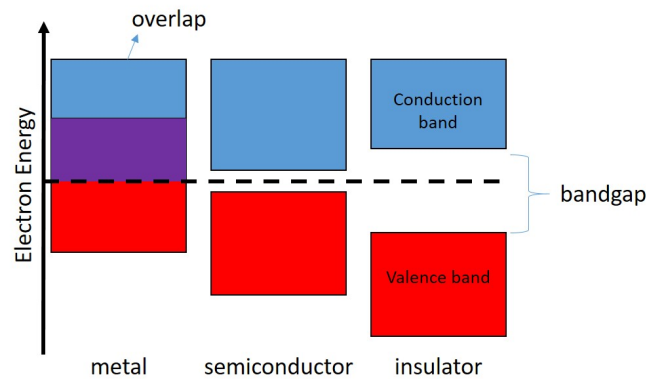


Figure 2.2: Classification according to band spacing

In photovoltaic systems, the energy of photons charged with carrying energy in the solar radiation, if greater or equal than the forbidden energy range, transmits it to an electron in the valence band and discharges it from the conductivity band. If the prohibited energy range of the material is greater than 2.5eV (electron volts), it is insulated. Photons can be considered as energy-carrying packages. They may have low and high energy. When the sun falls on semiconductor material, the photons transfer the energy they carry to the electrons in the material. The electrons that rise in energy try to rise to a higher energy band. If it reaches energy that exceeds the forbidden energy range, it breaks off its own valence band and reaches the conductivity band. After the electron passes to the other band, the remaining positive charge (+) is called “gap”. In summary, if the energy of the photon that falls on the material transfers enough energy to pass the electron-free energy range, an electron-gap pair is formed. If the energy supplied with the photon does not suffice to pass the electron-free energy range, it will not contribute to the photovoltaic transformation. The most suitable semiconductors for photovoltaic conversion are those with a band spacing of 1.4eV and 1.6eV. The excess energy is transferred to the conductive material as heat energy.

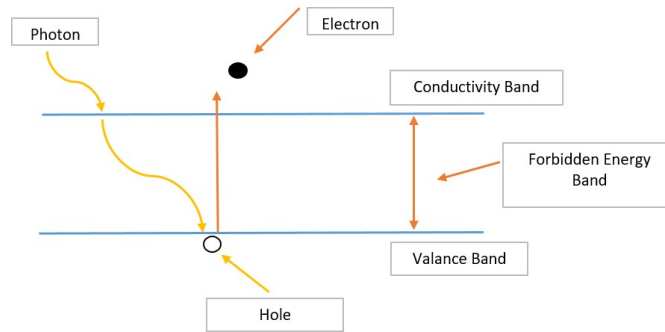


Figure 2.3: Occurrence of an electron-gap pair

Crystalline photovoltaic cells consist of type n and p-type conductors. The n-type semiconductors are formed by the addition of metals in the fifth group of the periodic table to the Si structure. P-type semiconductors are created by the addition of metals with valence electrons 3 to Si structure. When n-type and p-type semiconductors are combined, they form an uncharged transition at the junctions.

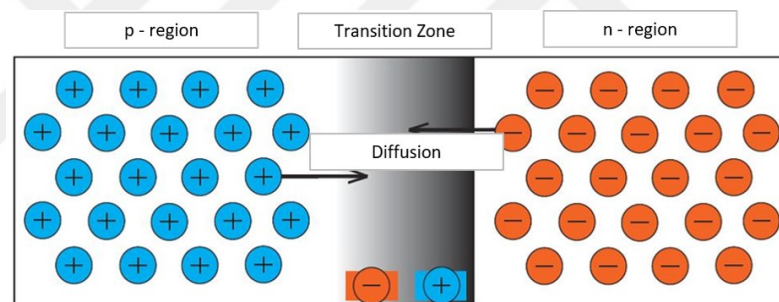


Figure 2.4: Combined n-type and p-type semiconductors

Part of the p-type semiconductor cavities flows towards the n-type semiconductor, while some of the electrons in the n-type semiconductor flow towards the p-type semiconductor. The electrons absorb photons from the sun in the p-n semiconductor. The photon transfers its energy to the electron and breaks the electron bonds. The released electrons flow into the region of the n-type semiconductor, whereby the cavities flow into the p-type semiconductor. This phenomenon is called a photovoltaic effect. The voltage difference between two semiconductor zones creates a voltage, and when this circuit is completed with a load, the current starts to flow.[16]

For a photovoltaic cell, the given figure indicates a simple equivalent circuit model.

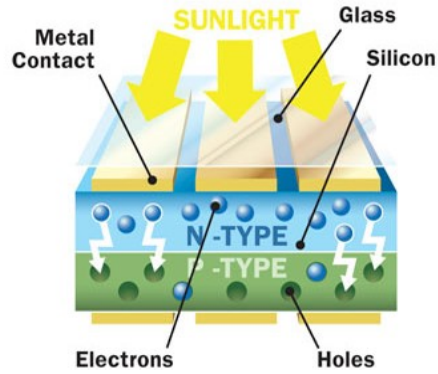


Figure 2.5: Photovoltaic energy conversion

The components are, real diode connected in parallel to ideal current source. Two parameters are related with this circuit:

- 1) Short circuit current (I_{sc})
- 2) Open circuit voltage (V_{oc})

When the leads of the equivalent circuit for the PV cell are shorted together, no current flows in the (real) diode since $V_d = 0$, so the whole current from the ideal source flows through the shorted leads. Since the short-circuit current must equal I_{sc} , the magnitude of the ideal current source itself must be equal to I_{sc} . When the leads from the PV cell are left open, the load current, I , is null and the V on the load is equal to $V_{oc} = V_d$. [35]

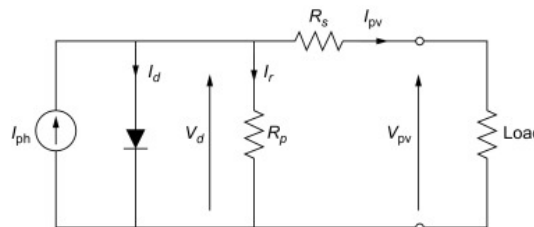


Figure 2.6: A simple equivalent circuit model

2.1 Photovoltaic Energy in the World

With the developing industry and increasing population, energy requirements have increased. Therefore, the importance of energy resources all over the world has been playing a critical role. The search for clean and renewable resources has become even more essential, considering the exhaustion of existing resources and environmental damage. In this way, renewable energy is preferred to replace fossil fuels. The reason is that fossil resources harmful to human health and the environment. Renewable resources are transformed into energy sources through specific processes. The Sun is an alternative energy source that is popular in recent years. Geographical location plays an important role in these resources. Especially for the sun, certain regions of the world can be considered lucky. The duration of the sun, the intensity of the radiation, are essential factors affecting efficiency. The use of the sun as a source of electricity can be seen in almost all countries. While some of the systems are used as off-grid, the power of grid-connected systems can be confirmed by official sources. The country with the highest installed capacity in the world is the People's Republic of China with an installed power of more than 78 GW. The top 15 countries listed according to their installed powers are given in Table 2.1.

Table 2.1: List of installed capacity of solar power plants in the world by country [17]

	Country	Update	Installed Power (MW)
1	China	December 2017	131.000
2	The United States of America	December 2017	51.000
3	Japan	December 2017	49.000
4	Germany	November 2018	45.550
5	Italy	December 2017	19.700
6	India	December 2017	18.300
7	The United Kingdom	December 2017	12.700
8	France	December 2017	8.000
9	Australia	December 2017	7.200
10	Spain	July 2017	6.730
11	South Korea	December 2017	5.600
12	Turkey	December 2018	5.095
13	Belgium	December 2017	3.800
14	Netherlands	December 2017	2.900
15	Canada	December 2017	2.900
16	Thailand	December 2017	2.700

According to the 2018 data, Turkey ranks 12th in line. Generating energy from the sun is common in European countries. Although factors such as the geographic location of the country, effective sunshine duration affect the yield, photovoltaic energy production may be limited in the regions which can be considered as sun-drenched or vice versa. The installed power capacities of the areas are as follows.

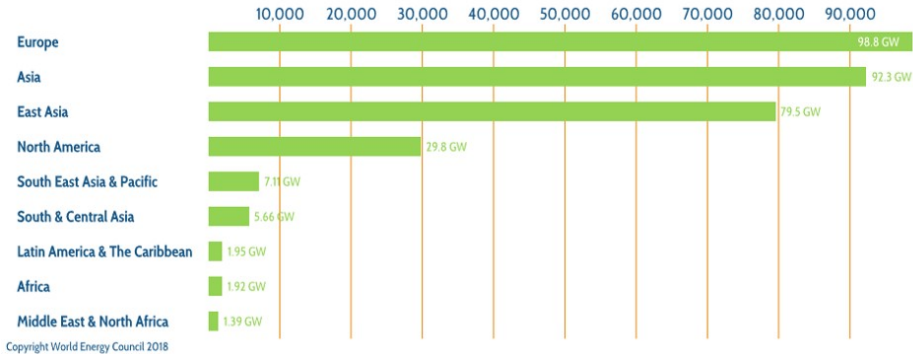


Figure 2.7: Solar installed capacity by region [18]

When the cumulative installed powers compared, Europe is close to 100 GW. Asia is pushing the 100 GW limit in second place. In addition to this, East Asia 79,5 GW, North America 29,8 GW, 7,11 GW in South East Asia and Pacific, 1,95 GW in Latin America and North America, 1,92 GW in Africa and finally the Middle East and North Africa has an installed power of 1.39 GW.

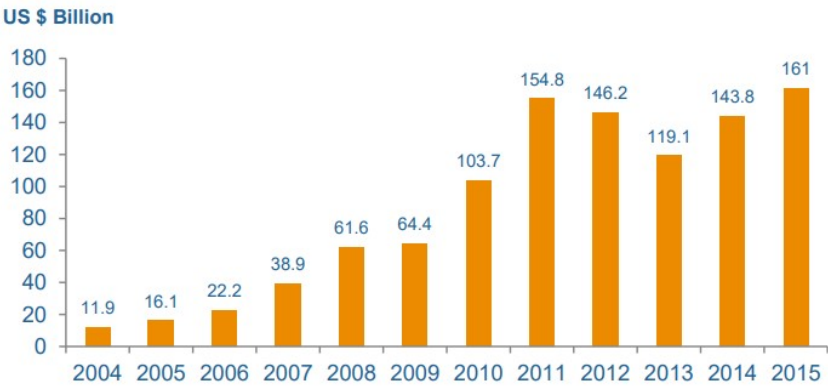


Figure 2.8: Solar energy investments by year [18]

Solar energy investments, which have been increasing all year around the world, in-

creased to 161 billion USD in 2015, while this figure was 11.9 billion USD in 2004. Solar energy investments are growing rapidly all over the world.

2.2 Photovoltaic Energy in Turkey

Energy demand in Turkey has increased with the growing population. Table 2.2 shows the comparison between 2006 and 2016 for energy sources. According to TEIAS data, natural gas is the most used energy source. In 2006, solar energy had no share in installed capacity and 2016 it reached 832.5 MW installed capacity.

Table 2.2: Annual Development Of Turkey's Installed Capacity [3]

Unit :MW										
	Coal	Liquid Fuels	Natural Gas	Renewable + Waste +Waste Heat	Multi Fuel	Hydro	Geothermal	Wind	Solar	Total
2007	10.197,4	2.000,2	11.647,4	42,7	3.384,0	13.394,9	22,9	146,3	-	40.835,7
%	24,97	4,90	28,52	0,10	8,29	32,80	0,06	0,36	-	100,00
2017	18.705,5	380,2	20.732,4	641,9	6.466,4	27.273,1	1.063,7	6.516,2	3.420,7	85.200,0
%	21,95	0,45	24,33	0,75	7,59	32,01	1,25	7,65	4,01	100,00

As of the end of 2018, 5868 solar power plants produced 7477 GWh electricity, and 2,5 % of the electricity production obtained from the sun. [19]

Due to its geographical location, Turkey is fortunate in terms of solar energy, the annual average sunshine hours to 2640 hours, 1311 kWh / m^2 of solar radiation has. Compared with European countries, Turkey is among the highest solar energy potential of countries. However, despite this potential, solar energy use is higher in European countries which are unlucky in terms of solar energy. Solar Energy Potential Atlas Turkey according to 2010 data, in the case of Turkey benefit from a readily available solar potential annual average of 380 billion kWh of electricity can be produced. The distribution of solar energy potential is not enough. [20]

The most active region of Turkey is Southeastern Anatolia. The other areas with the best solar potential are Mediterranean, Eastern Anatolia, Central Anatolia, Aegean, and the last Black Sea Region.

Monthly radiation values are given in Figure 2.9. energy per day (kWh) amounts given for one day. Accordingly, it is expected that the highest amount of electricity

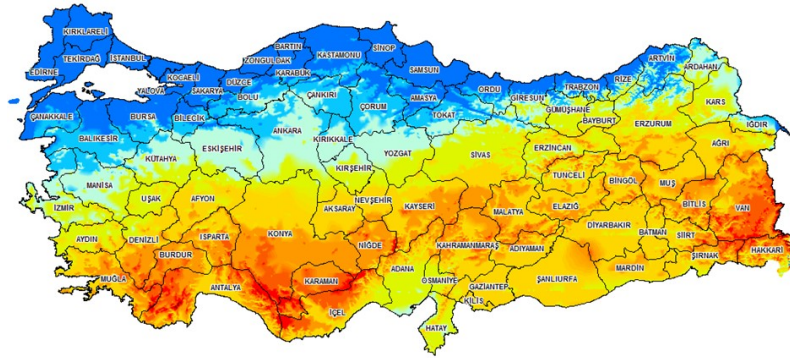


Figure 2.9: Solar energy potential map of Turkey [21]

will be produced in the summer when the radiation comes from the sun with the best solar angle.

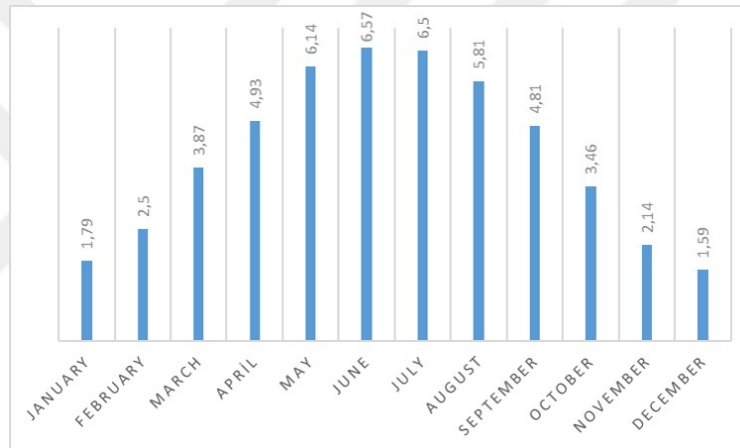


Figure 2.10: Global Radiation Values Turkey (kWh / m² day) [22]

In another chart, average sunshine times were given based on months. Another critical measure of sunbathing time is the effective sunbathing time depending on the sunbathing time. According to the PVGIS data, there are 5,31 hours of effective sunshine time. In other words, on a light day of 11.31 hours, only 5.31 hours of energy can be produced effectively. PVGIS data are given in Figure 2.10.

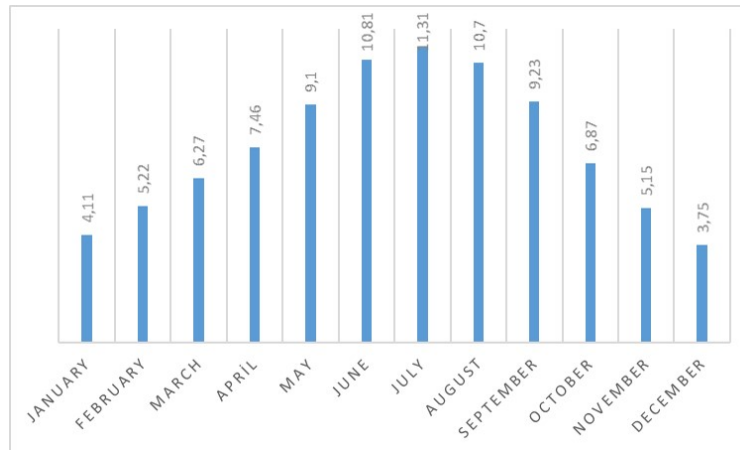


Figure 2.11: Turkey sunshine duration (time) [22]

Fixed system: inclination=35°, orientation=0°				
Month	E_d	E_m	H_d	H_m
Jan	2.36	73.1	2.90	89.9
Feb	2.86	80.0	3.55	99.5
Mar	3.84	119	4.95	154
Apr	4.24	127	5.55	166
May	4.69	145	6.32	196
Jun	5.08	152	6.92	208
Jul	5.31	165	7.39	229
Aug	5.38	167	7.48	232
Sep	4.99	150	6.84	205
Oct	4.18	130	5.49	170
Nov	3.32	99.5	4.20	126
Dec	2.37	73.5	2.94	91.1
Yearly average	4.06	123	5.39	164
Total for year		1480		1970

Figure 2.12: PVGIS data for Turkey [23]

CHAPTER 3

PHOTOVOLTAIC ENERGY SYSTEMS

In this part, the main elements of the photovoltaic energy system will be examined.

3.1 Solar Cells

Solar cells are semiconductor materials that convert the photons from the sun into electrical energy. The efficiency of the semiconductor material alters according to its components. This yield can be up to 25 %. The smallest unit of photovoltaic energy systems is the cells. With the combination of cells, the string is formed by the combination of the strings and the panels. [24]

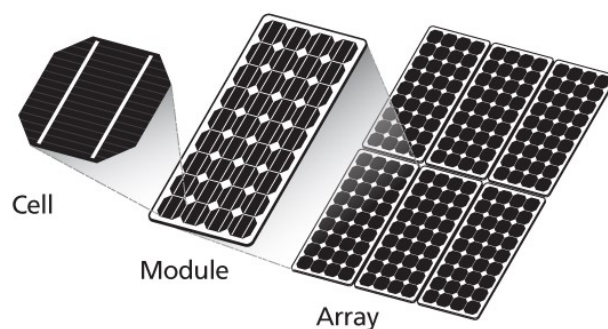


Figure 3.1: From cell to array Photovoltaic System Elements

3.1.1 Solar cells according to structure

Commonly used materials for solar cells are silicon (Si), cadmium telluride (CdTe) and gallium arsenite (GaAs). Material differences used to affect the yield. Efforts are continuing to increase efficiency by decreasing the cost. The selected material and panels are produced considering the meteorological conditions of the region to be used. Polycrystalline, monocrystalline, and thin-films are the most used materials. [24]

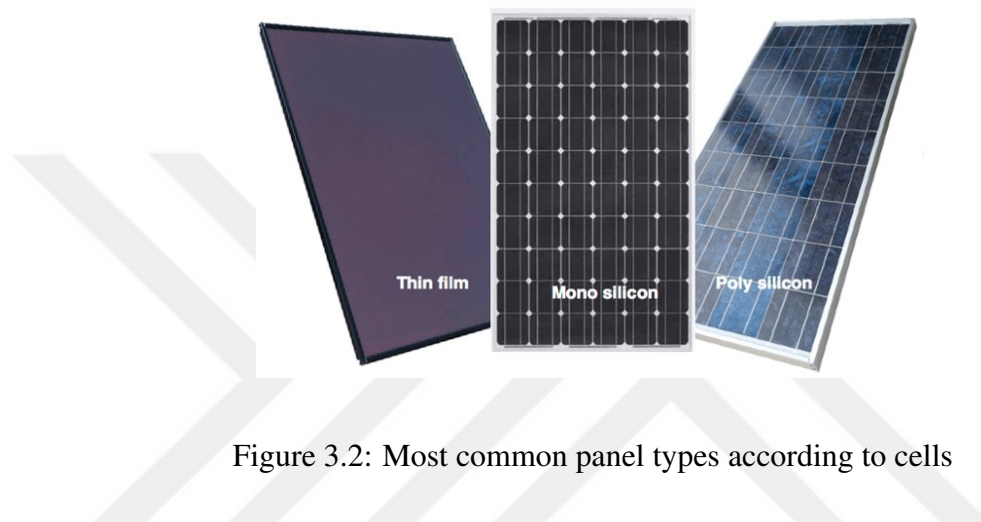


Figure 3.2: Most common panel types according to cells

3.1.1.1 Monocrystalline cells

Cells, also called single crystal silicon, have a homogeneous atomic structure. Their yields are around 20 %, and they have the best yield among the crystal cells. While they are high in cost, they are ideal for producing higher power in limited spaces. It is preferred for yield and long-term use. [24]

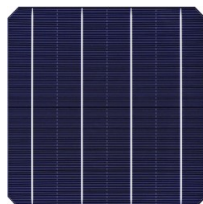


Figure 3.3: Monocrystalline cell

3.1.1.2 Polycrystalline cells

The multi-crystalline silicon cells have a non-homogeneous atomic structure and are composed of more than one crystal. Their yield is lower than that of monocrystalline cells. These cells, which have a yield of around 16 %, are widely preferred because their costs are lower. [24]



Figure 3.4: Polycrystalline cell

3.1.1.3 Thin film

Unlike monocrystalline and polycrystalline cells, amorphous silicon material is used. It has lighter but lower efficiency. They are the least affected cells from high and low temperatures. Because less material is used and easy installation, this material can be preferred. [24]

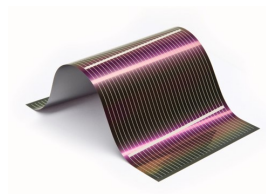


Figure 3.5: Thin film

3.2 Solar Angles

Sun angles are angles used to determine the position of the sun. The angles from the sun vary depending on the parameters such as latitude, longitude, date time, where a plane is located. These angles are latitude angle (ϕ), declination angle δ , clock angle

ω , angle of inclination β , surface azimuth angle γ , angle of incidence Θ , zenith angle ω_z , solar height angle α_s and solar azimuth angle γ_s . [25]

3.2.1 Latitude angle (\emptyset)

The equator is taken as a reference line, the north of the equator is considered positive, and its south is considered negative. It varies $-90^\circ \leq \emptyset \leq 90^\circ$. [25]

3.2.2 Declination angle (δ)

The angle between the equatorial plane and the sun direction. This angle is 0 at equinox. It varies $-23,45^\circ \leq \delta \leq 23,45^\circ$ [25]

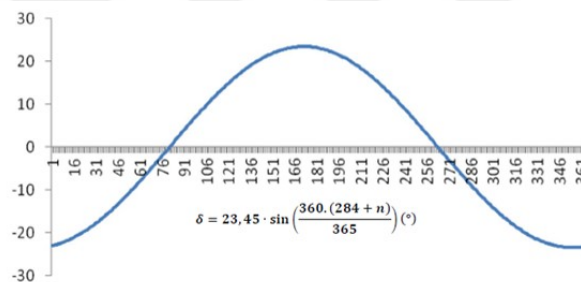


Figure 3.6: Declination angle (δ)

3.2.3 Clock angle (ω)

It is between -180° and 180° , which is negative before 12:00 and positive after 12:00. [25]

3.2.4 Azimuth angle (γ_s)

It is between the direction indicated by the compass needle and the clockwise direction from the north. The azimuth angle is 0° in the north and 180° in the south. [25]

3.2.5 Zenit angle (Θ_z)

The angle between the vertical axis and the direction of the sun. It is 90° in the sunrise and sunset, 0° at the 12:00. [25]

3.3 Photovoltaic System Elements

Photovoltaic panels, inverters, mounting systems and batteries (for off-grid systems) are the essential elements of a solar power plant.

3.3.1 Photovoltaic panels

Solar panels are composed of components that convert the photon energy from the sun into electrical energy. As a result of parallel or series binding of the cells, they are named according to the combined cell types. For example, the photovoltaic panel formed by polycrystalline cells is called a polycrystalline panel.

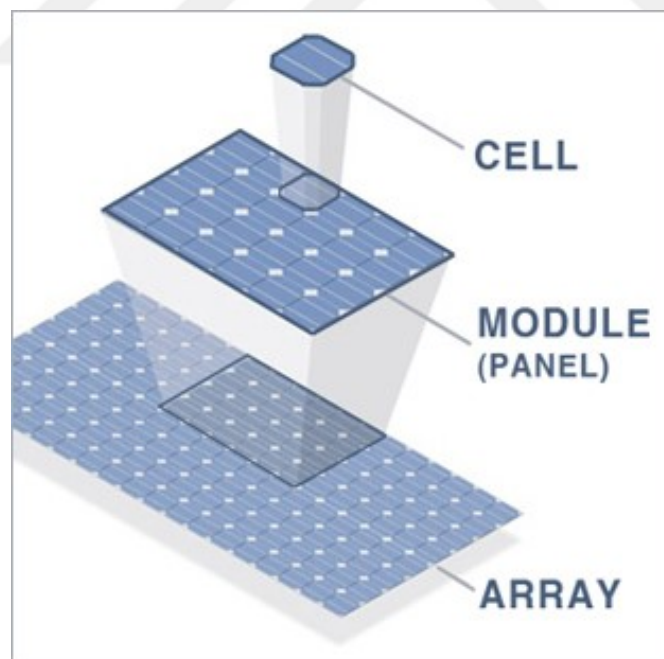


Figure 3.7: Cell, panel and array

Except for thin-film panels, after the cell connections are made, the panel is finalized

with the addition of the upper and lower layers. At the top coated glass, then continued with respectively the EVA for the capsulation process and the ribbons for the connections of the cells, one more fold in the EVA and lastly the back sheet. Figure 3.8 shows the layers of the panel.

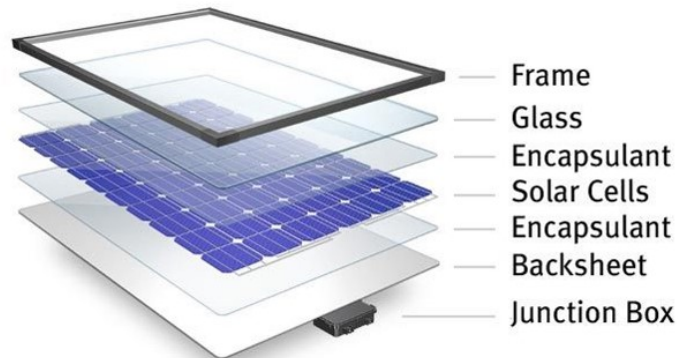


Figure 3.8: Panel layers [26]

The glass used on the front surface is to protect the other layers of the panel against external influences. It is designed to get the best efficiency so as not to reflect the light coming from the sun. EVA with ethyl vinyl acetate components is used for the capsulation process. The EVA layer is placed above and below the cells. Then the cells are then encapsulated. Thus, power losses are prevented and a protection layer is obtained for the cells. The back sheet film on the back has polyvinyl fluoride components. It is an insulating material, and it is used to protect the panel and cells from external influences. [27]

An example of panel production is in figure 3.9, respectively.

Glass is the first element to enter the production line from glass feed. When the glass placed on the conveyor belt, a layer of EVA is laid on it. The EVA and the glass comes the tabber station for cell line-up and soldering. Tabbing ribbons provide intercellular conductivity. Visual inspection is performed after cell arrays. Bus ribbons are used to connect cell groups connected by tabbing ribbons, and the panel array enters the soldering station for this operation. The panel comes the electroluminescent station for the control of the electrical connections. Then enters the laminator after the controls by laying one more layer of EVA and back sheet on it. After lamination, the back



Figure 3.9: Panel Production Line [28]

sheet and EVA, which are excess, are shaved. Frames are attached to the panel, the junction box is inserted and the sun is reflected into the simulation station. The panel is finished and stacked. [28]

The most widely used solar panels are polycrystalline cells, monocrystalline cells, and thin film panels.

Polycrystalline Cell Panels

Melted silicon is poured into the mold and allowed to cool. The silicon, which is cooled as a block, is first separated into thin slices and then becomes a cell. Because of the heterogeneous crystalline structure during cooling, a discontinuity occurs between the vessels, which prevents the transmission of electricity. This is why their yield is lower than that of monocrystalline cell panels. [29]

Monocrystalline cell panels

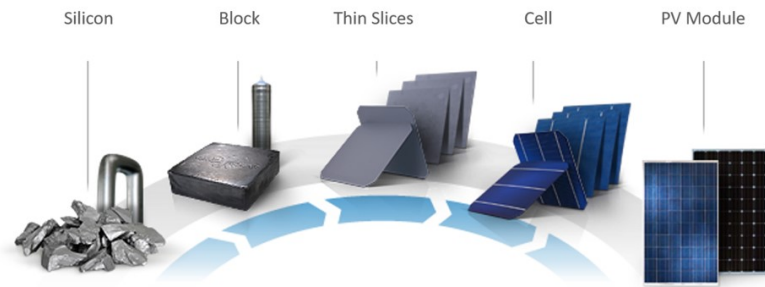


Figure 3.10: Polycrystalline cell production stages

It has a single crystalline structure. The crystal nuclei are grown at a very low speed. As it has a single crystalline structure, it has high conductivity in itself. For this reason, the yield is higher than polycrystalline panels. [8]

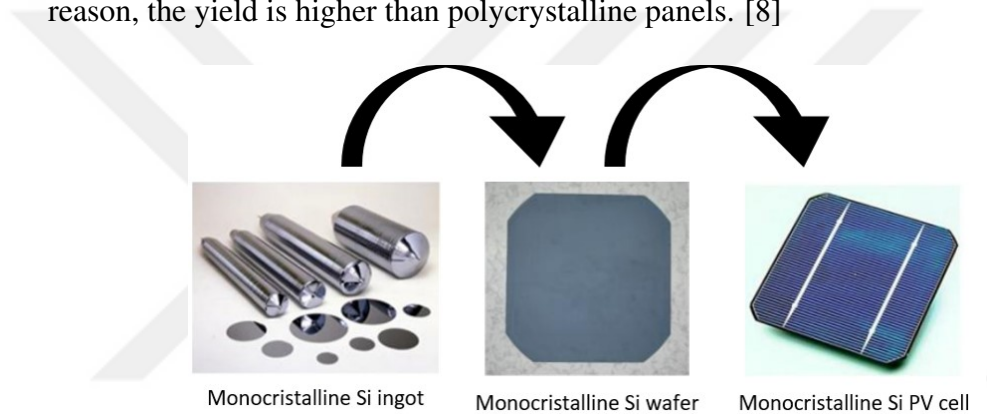


Figure 3.11: Monocrystalline panel production stages

Thin Film Panels

In these panels, materials such as amorphous silicon, cadmium tellur, copper indium di-selenoid are used. The reason for this is that the light absorption of these materials is very high. Costs are lower. Lower yields than polycrystalline and mono-crystalline panels are the major impediment to their spread. [29]

3.3.2 Inverters

Inverters are electronic devices that convert the direct current produced by the solar panels into alternating current for use in the network. Inverters are divided into two

depending on whether the system is connected to the grid or not. In non-grid systems, off-grid inverters are selected according to the panel power. In grid-connected systems, inverters are divided into three as string inverters, central inverters, and micro inverters.

String inverters

These are the inverters in which the panels enter into groups. It is selected according to the total DC voltages of the panels. It is more widely used in large-scale plants. The panels form a series of connected arms, which are connected parallel to the inverter. The following diagram is an example of the connection patterns of string inverters.

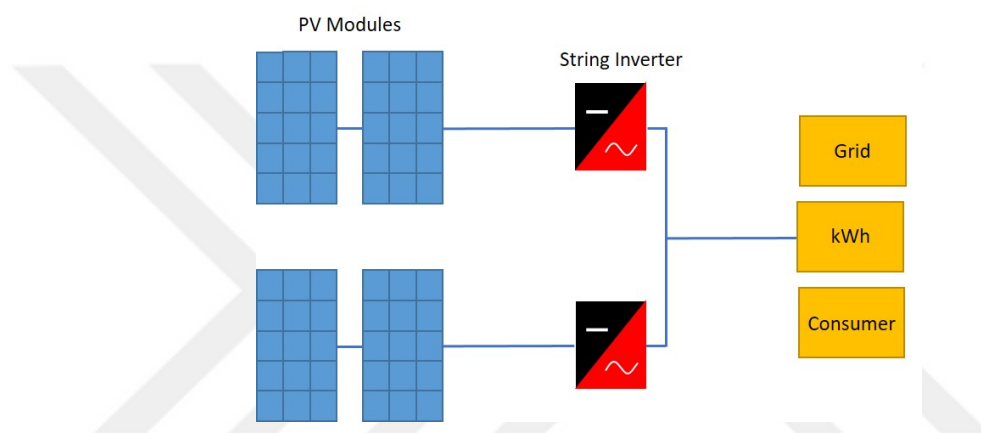


Figure 3.12: String inverter diagram

Voltages are summed where the panels connected to the series. For example, in the case that 20 panels are connected at varying voltages depending on temperature, very high voltage levels are reached. Besides, due to the series connection of the panels, the shadow on any panel affects the production of the power in the entire serial connected arm. This is explained in Figure 3.13.

In Figure 3.13, the shadow falling on a single panel in a series-connected arm affects the output power of the panel arm as a whole panel group, not as a single panel.

Another disadvantage of string inverters is cabling. The panels are connected by DC cables. DC cable losses are higher than AC cables, and DC cables are more expensive [30].

Considering the cabling problem, the panel group should be kept close to the inverter.

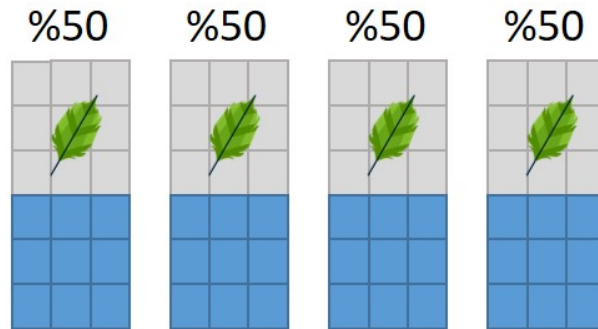


Figure 3.13: Shadow effect on string inverters

In systems with string inverters, installation and wiring are also of great importance and are limiting in projects.

The advantages of string inverters are their lower costs and higher inverter efficiency than other inverter technologies. These essential benefits that can be considered as the preferred reason are the features that are required in all solar power plants.

Central Inverters

They are used in large scale applications. The panel groups are joined in the junction boxes. After the connection boxes, it is connected to the central inverters and enters the transformer. They can be managed from a single center.



Figure 3.14: Central inverter

Micro Inverters

It is an inverter type that allows the connection of one or two panels. Failure or shading on a single panel does not affect other panels. It does not allow the connection of more than two or many panels in series or central inverters. Each panel is advantageous in such cases as it will feed the network by converting its DC current to AC current. Because the DC cable will only be used between the panel and the micro inverter behind the panel, DC cable losses and DC cable costs are largely avoided. Installation in power plants is easier than other inverters. This is because each panel carries the inverter itself.

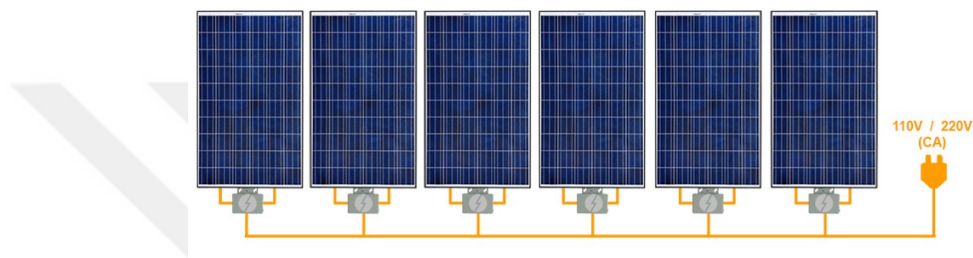


Figure 3.15: System with micro inverter

As shown in Figure 3.15, the micro-inverters on the panels can be connected directly to the grid by AC cables. The shade on the panel only affects itself as each panel can deliver its own energy output directly to the network. High-voltage connections are avoided, as the panels do not generate series-connected arms.

In addition to these advantages, they are not yet widely used due to their higher costs and lower device efficiencies to other inverters. Micro-inverters with very high prices, especially in large-scale power plants, are now commonly used in homes or small-scale applications.

3.3.3 Photovoltaic Mounting Systems

Solar panels are fixed with different mounting systems. These systems are divided into roof applications and floor applications. Floor mounting can be done with concrete feet or foot feet. Which of the concrete-footed or standing foot systems to choose

the ground, the shape of the ground, etc. depends on situations. In roof applications, panel installation is performed by selecting the mounting elements according to the direction and type of the roof.



Figure 3.16: Roof and floor mounted sample system schemes

3.4 Photovoltaic Systems According to Network Dependence

Solar energy systems are divided into two according to grid connection. The grid-connected systems transmit the electricity produced by the network during the day. Systems that are independent of the network are short-lived systems to meet the need for electricity temporarily. The energy stored in the battery can be used during the night.

3.4.1 Grid-connected systems

In these systems, DC from the panels is converted to AC by the help of inverters. In the systems installed in houses or industrial systems, the energy needed is used, and the excess is transferred to the interconnected system with the same frequency and voltage as the grid by the decoupling system. In these power plant installations, the energy is transmitted directly to the network.

3.4.2 Network independent systems (Off-grid systems)

These systems are intended for the production, storage, or direct use of energy in places where there is no electricity transmission. For example, in the irrigation systems, when the required voltage value is reached, the engine starts. The engine run-

ning during the sun's efficient hours slows down and stops from losing the right angle of the sun. In the stored systems, the electrical energy produced during the day is stored in the batteries, and even if there is no sun, this stored energy can be used.

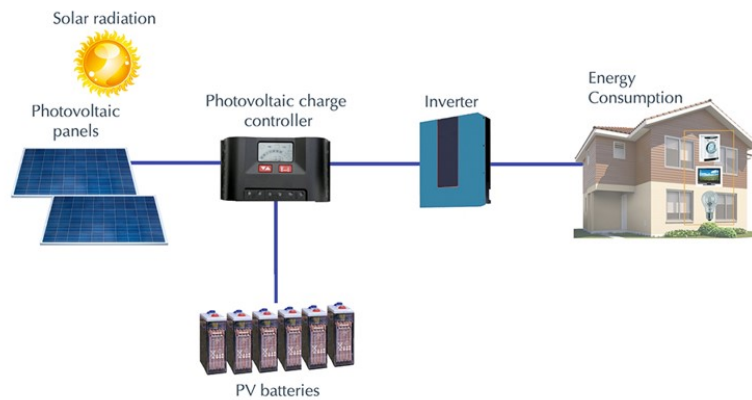


Figure 3.17: Network independent solar system diagram

3.4.3 Hybrid systems

Hybrid systems can act as both off-grid and grid-dependent systems. In contrast, a hybrid system can also be designed as a system that can be used together with a solar system and a diesel generator.

3.5 Problems in Photovoltaic Energy Systems

Problems such as pollution in the systems, energy losses due to shade, cable losses, improper installation, and hot spot effects are encountered. In a power plant installed in a dusty or dirty environment, energy losses and hot spot effects can be experienced due to the fact that the panels are not cleaned regularly. The hot spot effect can be defined as, when the current produced by one of the cell is lower than the other cells, the panel starts to act as a load not generating but consuming, and the voltage is reversed. In this case, the temperature of the cell increases. If this condition persists, the cell will then damage the panel. The system will continue to be harmed unless interfered with the system. This is called a hot spot effect. Here, the common reason for a cell to produce less current than other cells in the presence of elements such as

birds, impurities. [31]

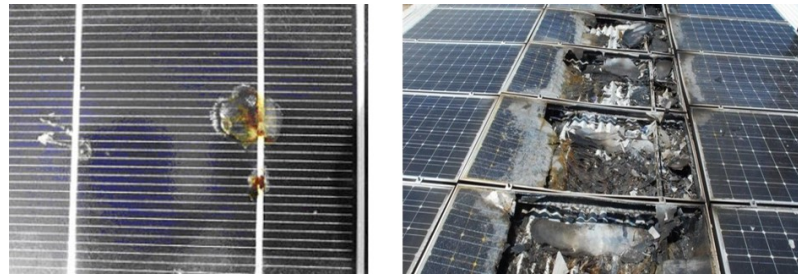


Figure 3.18: Hot spot effect

3.6 Effect of Temperature on the Panel

In this section, panel performance concerning temperature will be observed. Photovoltaic panels are also electronic devices and are affected by temperature. This effect, which causes the voltage to increase and decrease, is of great importance, especially in inverter connections. In the series inverters, the input voltage range is given. The voltage range with lower and upper limits is designed to respond to the varying voltages of the series-connected panel group at different temperatures. The solar panels are tested under conditions 25°C temperature, $1000\text{W}/\text{m}^2$ and 1.5AM in standard test conditions (STC). However, these values are not working conditions. The panels made by the installation convert a specific part of the energy from the sun into electrical energy. Some energy is transformed into heat energy. This event, which causes the panel to heat up, increases the current while reducing the voltage and decreasing the output power of the panel. [32]

To better explain this effect, the effect of the temperature on the panel is described below for values which are higher and lower than 25°C .

3.6.0.1 Panels with a working temperature higher than 25°C

The temperature value used in the calculations for the following example is 45°C . The characteristics of the discussed panel are as follows.

For example, when a panel with a power of 285Wp is considered,

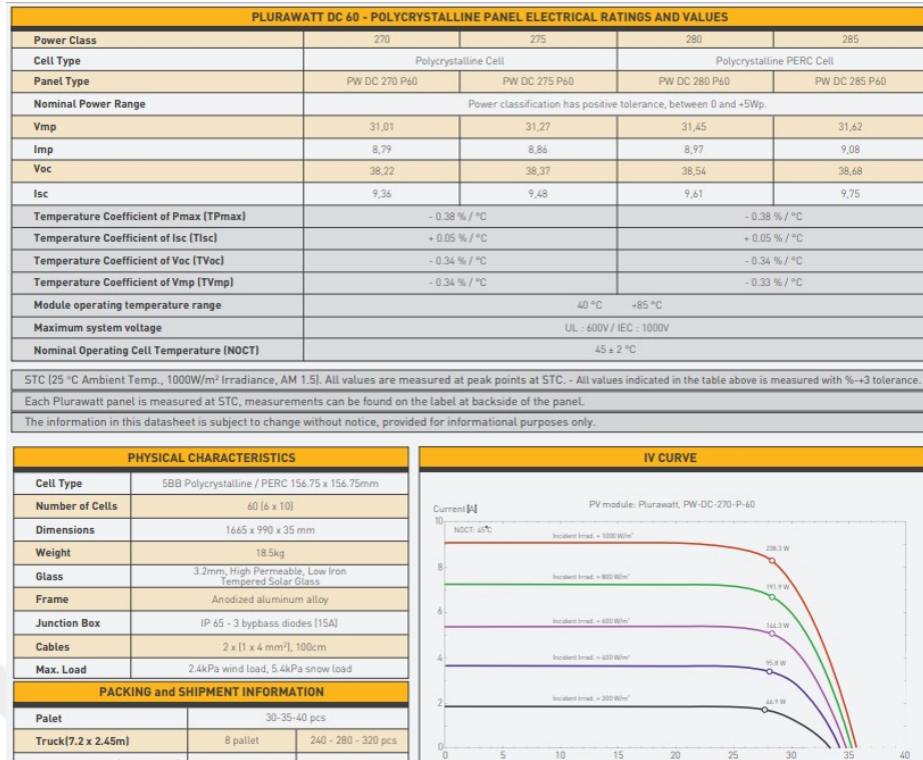


Figure 3.19: Technical specifications of the panel

Maximum power temperature coefficient (TP_{max}) : $-0.38\%/^{\circ}C$

Short circuit current temperature coefficient (TI_{sc}) : $+0.05\%/^{\circ}C$

Temperature coefficient of open circuit voltage (TV_{oc}) : $-0,34\%/^{\circ}C$

Working voltage temperature coefficient (TV_{mp}) : $-0.33\%/^{\circ}C$

Temperature difference:

$$[45^{\circ}C - 25^{\circ}C] = 20^{\circ}C \quad (3.1)$$

$$P_{out} = P \times (1 - (\Delta T) \times TP_{max}) \quad (3.2)$$

where ΔT is absolute temperature difference.

$$P_{out} = 285Wp \times (1 - (20^{\circ}C) \times (0.37\%/^{\circ}C)) \quad (3.3)$$

$$P_{out} = 263.91Wp \quad (3.4)$$

As shown in equation (3.4), the output power was 285 Wp under standard test conditions, and the output power at 45 ° C decreased to 263.91 Wp.

Similarly,

$$V_{out} = Voltage \times (1 - (\Delta T) \times TV_{mp}) \quad (3.5)$$

$$V_{out} = 31,62V \times (1 - (20^{\circ}C) \times (0.33\%/^{\circ}C)) \quad (3.6)$$

$$V_{out} = 29.53V \quad (3.7)$$

The voltage of 31.62 V in STC is reduced to 29.53 V due to temperature. The change in current is as follows.

$$I_{out} = Current \times (1 + (\Delta T) \times TI_{sc}) \quad (3.8)$$

$$I_{out} = 9.75A \times (1 - (20^{\circ}C) \times (0.05\%/^{\circ}C)) \quad (3.9)$$

$$I_{out} = 9.84A \quad (3.10)$$

The current at equation 3.10, 9,08 A in STC is increased to 9.84 A with the effect of temperature. These changes in the output power of a single panel have much larger effects on a system basis. For example, in a system of 25 kWp, approximately 88 panels with a power of 285 Wp shall be used. When calculating for 4 parallel arms and 22 connected groups:

STC:

$$22panels \times 31,62V = 695,64V \quad (3.11)$$

$$4arms \times 9,75A = 39A \quad (3.12)$$

where arms are connected in parallel.

At 45 °C :

$$22panels \times 29,53V = 649,72V \quad (3.13)$$

$$4arms \times 9.84A = 39.4A \quad (3.14)$$

where arms are connected in parallel.

Differences:

$$695.64V - 649.72V = 45.91V \quad (3.15)$$

$$39.4A - 39A = 0.4A \quad (3.16)$$

Differences between voltage and current as in Eq. 3.15 and Eq. 3.16. The output power yield is equal to as in 3.17.

$$(263,91Wp/285Wp) \times 100 = 7.4\% \quad (3.17)$$

Accordingly, there is a 7.4 % decrease in a single panel.

3.6.0.2 Panels with a working temperature less than 25 ° C

The temperature value used in the calculations for the following example is -10 ° C. The characteristics of the panel discussed are as in Figure 3.19. For example, when a

panel with a power of 270 Wp is considered,

Maximum power temperature coefficient (TP_{max}) : $-0.38\%/^{\circ}C$

Short circuit current temperature coefficient (TI_{sc}) : $+0.05\%/^{\circ}C$

Open circuit voltage temperature coefficient (TV_{oc}) : $-0.31\%/^{\circ}C$

Operating voltage temperature coefficient (TV_{mp}) : $-0.34\%/^{\circ}C$

Temperature difference:

$$[-10^{\circ}C - 25^{\circ}C] = -35^{\circ}C \quad (3.18)$$

$$(P_{out}) = Power \times (1 + (\Delta T) \times TP_{max}) \quad (3.19)$$

$$P_{out} = 270Wp \times (1 + (-35^{\circ}C) \times (-0.38\%/^{\circ}C)) \quad (3.20)$$

$$P_{out} = 305.91Wp \quad (3.21)$$

As shown in Eq. 3.4, the output power of the panel was 270 Wp under standard test conditions, and the output power at -10 C increased to 305.91 Wp.

Similarly,

$$V_{out} = Voltage \times (1 + (\Delta T) \times TV_{mp}) \quad (3.22)$$

$$V_{out} = 31.01V \times (1 + (-35^{\circ}C) \times (-0.34\%/^{\circ}C)) \quad (3.23)$$

$$V_{out} = 34.70V \quad (3.24)$$

The voltage of 31,01 V in STC increased to 34,70 V with the effect of temperature.
The change in current is as follows:

$$I_{out} = Current \times (1 + (\Delta T) \times TI_{sc}) \quad (3.25)$$

$$I_{out} = 9.36A \times (1 + (-35^{\circ}C) \times (0.05\%/^{\circ}C)) \quad (3.26)$$

$$I_{out} = 9.20A \quad (3.27)$$

Current at 9.36 A at Eq. 3.10 in STC decreased to 9.20 A with the effect of temperature. These changes in the output power of a single panel have much larger effects on a system basis. For example, in a system of 25 kW_p, approximately 92 panels with 270 W_p power will be used. When calculating for 4 parallel arms and 23 series connected groups:

STC:

$$23panels \times 31,01V = 713,23V \quad (3.28)$$

$$4arms \times 9.36A = 37.44A \quad (3.29)$$

where arms are connected in parallel.

At 45 °C :

$$23panels \times 34,70V = 798,1V \quad (3.30)$$

$$4arms \times 9,20A = 36,8A \quad (3.31)$$

where arms are connected in parallel.

Differences:

$$798.1V - 713.23V = 84.87V \quad (3.32)$$

$$37.44A - 36.8A = 0.64A \quad (3.33)$$

Differences between voltage and current 3.31 and Eq. as in 3.32. The output power output is equal to Eq. 3.33.

$$(270W_p/305.9W_p) \times 100 = 11.74\% \quad (3.34)$$

Accordingly, the efficiency of a single panel increased by 11.74%.

Examples explain the effect of temperature on the panel for situations where the temperature is low and high above. Accordingly, temperature and voltage are inversely proportional; The panels are described to operate at higher efficiency in the cold.

CHAPTER 4

MODELING AND COMPARISON OF PHOTOVOLTAIC SYSTEMS

In this section, the system with 24 kWp installed power using 260 Wp polycrystalline panels in Ankara was investigated in different shade densities using a string inverter and micro inverter. The costs of the simulated systems were analyzed and compared.

The data of Ankara for 1 kWp using the Photovoltaic Geographical Information System - Interactive Maps data are as in Figure 4.1. System losses are estimated as 24.3% in total including 9,6% low radiation and temperature, 2,7% reflection losses, 14% cable and system element losses such as an inverter.

E_d : Daily average electricity generation (kWh)

E_m : Monthly average electricity generation (kWh)

H_d : Global irradiation per day (kWh / m²)

H_m : Global radiation per square meter (kWh / m²)

This data is calculated for 1 kWp installed power. For this reason, " E_d " can be considered as an effective sunshine duration. For example, the average time of an average of 2,8 hours/day in February is 5.27 hours/day in August. When a calculation is made in short, the total installed DC power is expected to be around 23.4 kWp.

$$92panels \times 260Wp \div panels \times \%98yield = 23,4kWp \quad (4.1)$$

The following is a summary of the six different system simulations detailed below:

Fixed system: inclination=30°, orientation=0°				
Month	E_d	E_m	H_d	H_m
Jan	2.05	63.6	2.52	78.0
Feb	2.80	78.5	3.48	97.5
Mar	3.84	119	4.90	152
Apr	4.15	124	5.42	163
May	4.67	145	6.31	195
Jun	5.09	153	6.92	208
Jul	5.34	166	7.42	230
Aug	5.27	163	7.34	227
Sep	4.81	144	6.55	196
Oct	3.82	118	4.97	154
Nov	3.04	91.3	3.82	115
Dec	2.06	63.9	2.54	78.6
Yearly average	3.92	119	5.19	158
Total for year		1430		1890

Figure 4.1: Energy and radiation values for PVGIS Ankara

24 kWp systems modeled using 92 panels and string inverters:

- a- Shadowless system: It is designed not to shade on the panels.
- b- System at the first shade density: It is designed to drop the tree shade on the panels at certain times depending on the angle of the sun.
- c- System with the second shade density: It is designed to drop the shade of trees and wind turbines at certain times depending on the angle of the sun on the panels.

24 kWp systems modeled using 92 panels and micro inverters:

- a- Shadowless system: It is designed not to shade on the panels.
- b- System at the first shade density: It is designed to drop the tree shade on the panels at specific times depending on the angle of the sun.
- c- System with the second shade density: It is designed to drop the shade of trees and

wind turbines at specific times depending on the angle of the sun on the panels.

In the simulations made using 92 260 Wp panels at three different shade densities, the panels are placed at 30° angle with the ground, in the south direction, and the azimuth angle is 0°. The roof has a total area of 155 m². 23 series of panels in four groups have the area 150 m² was placed at the roof.

The shadowless system diagram with 24 kWp installed power on the roof in Ankara province is as shown in Figure 4.2.

Simulation parameters			
Collector Plane Orientation	Tilt	30°	Azimuth 0°
Models used	Transposition	Perez	Diffuse Perez, Meteonom
Horizon	Free Horizon		
Near Shadings	Linear shadings		
PV Array Characteristics			
PV module	Si-poly	Model	PW-DC-260-P-60
<small>Original PV/syst database</small>	Manufacturer	Plurawatt	
Number of PV modules	In series	23 modules	In parallel 4 strings
Total number of PV modules	Nb. modules	92	Unit Nom. Power 260 Wp
Array global power	Nominal (STC)	23.92 kWp	At operating cond. 21.42 kWp (50°C)
Array operating characteristics (50°C)	U mpp	636 V	I mpp 34 A
Total area	Module area	150 m²	Cell area 134 m ²
Inverter			
<small>Original PV/syst database</small>	Model	Sunny Tripower 25000TL-JP-30	
Characteristics	Manufacturer	SMA	
Inverter pack	Operating Voltage	390-800 V	Unit Nom. Power 25.0 kWac
	Nb. of inverters	2 * MPPT 50 %	Total Power 25 kWac

Figure 4.2: Shadowless system parameters

4.1 Simulations with String Inverter

String inverters are mainly used in high power solar power plants. However, it is also used for lower power plants. Below are simulations for three different shade densities.

4.1.1 A photovoltaic system modeled shadowless conditions with string inverter

The shadowless system diagram with 24 kWp installed power on the roof in Ankara province is as shown in Figure 4.2. Following the information given in Figure 4.2, panel layout is made in Figure 4.3.

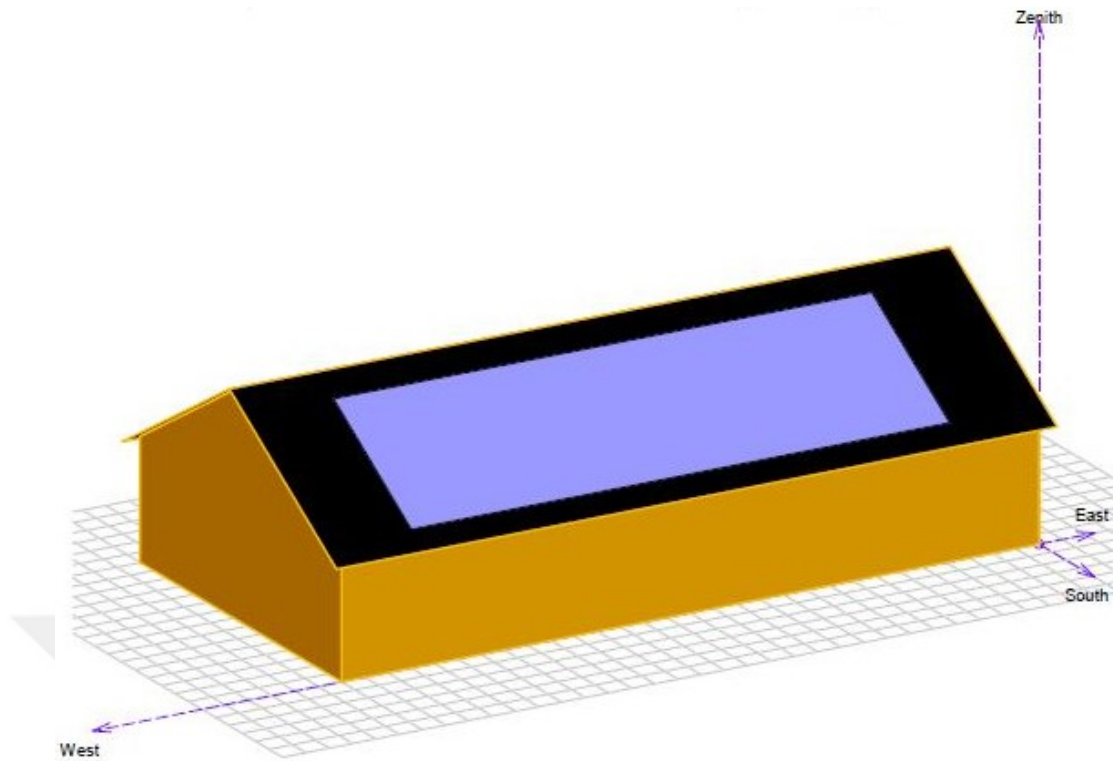


Figure 4.3: Shadowless system diagram

As seen in Figure 4.3, modeling was carried out with the assumption that there is not an object to shade in front of the panels. Shape losses such as cloud, bird, dust, system losses such as cable inverters and other losses are given in Figure 4.4.

In summary, as seen in Figure 4.2, the installed DC power is 23,92 kWp. In the Annex-1 simulation output, the annual energy generation capability of this system is 44,06 MWh / year under standard test conditions, while the rated energy falls to 38,13 MWh / year after losses.

Simulation results and annual total results are given in Figure 4.5.

The shading curve gives a synthetic evaluation of the shading distribution over the season and the time of day throughout the year. Interpolations cause the occasional appearance of the lines in discrete calculation points. When the angle of arrival of the sun is high, the overall efficiency will be high even if the losses are high.

Loss diagram over the whole year

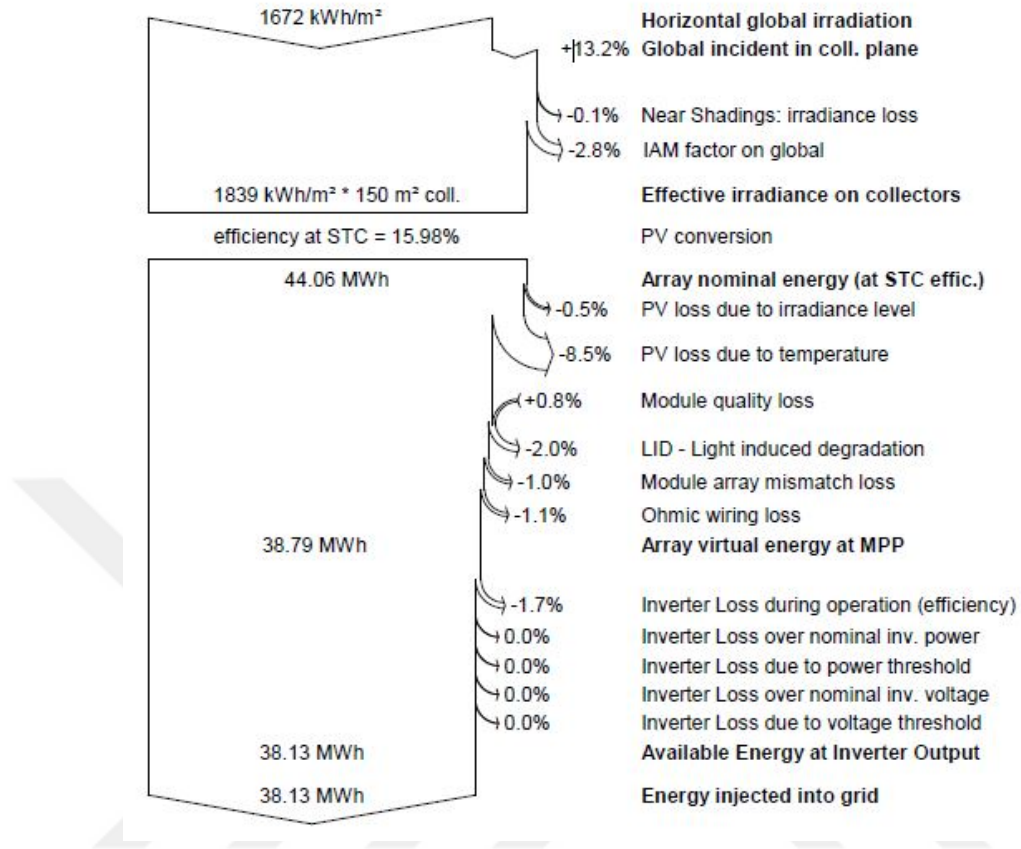


Figure 4.4: Shadowless system losses diagram

4.1.2 A photovoltaic system modeled with string inverter at first shadow density

In the province of Ankara, 24 kWp installed on the roof, the system is simulated by adding an object to the shading system. System inputs are as in Figure 4.7.

Panel layout according to the information given in Figure 4.7 is shown as Figure 4.8.

The tree in front of the building, as seen in Figure 4.8 will drop shadows on the panels at certain times of the day. Shape losses such as cloud, bird, dust, system losses such as cable inverters, and other losses are given in Figure 4.9.

In summary, in the Annex-2 simulation output, the annual energy generation capability of this system is 42.31 MWh / year under standard test conditions, while the rated

Balances and main results

	GlobHor kWh/m ²	T Amb °C	GlobInc kWh/m ²	GlobEff kWh/m ²	EArray MWh	E_Grid MWh	EffArrR %	EffSysR %
January	53.9	0.70	75.6	73.5	1.690	1.657	14.90	14.61
February	72.8	2.40	97.6	94.8	2.172	2.134	14.83	14.57
March	127.1	5.80	148.9	144.8	3.176	3.120	14.22	13.97
April	151.5	10.80	163.5	158.4	3.426	3.368	13.97	13.74
May	197.8	16.40	196.6	190.5	3.997	3.931	13.55	13.33
June	217.5	20.00	206.1	199.7	4.089	4.022	13.23	13.01
July	236.5	24.40	229.0	222.2	4.426	4.353	12.88	12.67
August	214.8	24.50	229.1	223.0	4.415	4.342	12.85	12.63
September	163.2	20.40	197.2	192.1	3.891	3.828	13.16	12.94
October	113.5	12.60	154.9	150.9	3.241	3.188	13.94	13.72
November	73.2	6.90	114.8	111.6	2.486	2.445	14.44	14.20
December	50.5	2.00	79.5	77.1	1.777	1.744	14.90	14.62
Year	1672.4	12.30	1892.8	1838.5	38.785	38.132	13.66	13.43

Legends: GlobHor Horizontal global irradiation EArray Effective energy at the output of the array
T Amb Ambient Temperature E_Grid Energy injected into grid
GlobInc Global incident in coll. plane EffArrR Effic. Eout array / rough area
GlobEff Effective Global, corr. for IAM and shadings EffSysR Effic. Eout system / rough area

Figure 4.5: Monthly simulation results in the shadowless system

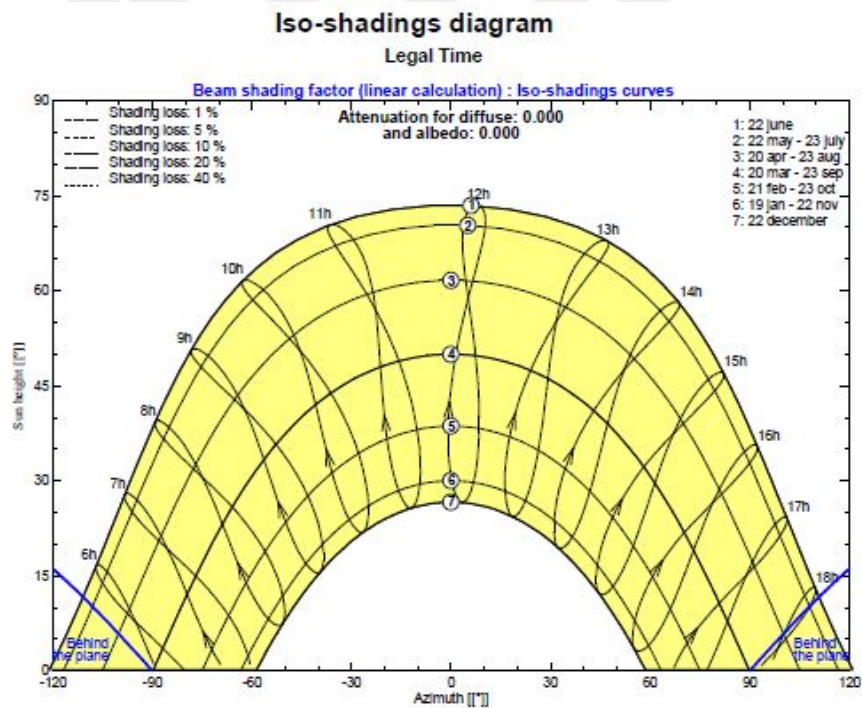


Figure 4.6: Shading curve in shadowless system

energy falls to 36.71 MWh / year after losses. The annual decrease in the amount of energy produced is due to the shadow of the tree. All parameters except for the

Simulation parameters				
Collector Plane Orientation	Tilt	30°	Azimuth	0°
Models used	Transposition	Perez	Diffuse	Perez, Meteonorm
Horizon	Free Horizon			
Near Shadings	Linear shadings			
PV Array Characteristics				
PV module	Si-poly	Model	PW-DC-260-P-60	
<small>Original PV/syst database</small>	Manufacturer	Plurawatt		
Number of PV modules	In series	23 modules	In parallel	4 strings
Total number of PV modules	Nb. modules	92	Unit Nom. Power	260 Wp
Array global power	Nominal (STC)	23.92 kWp	At operating cond.	21.42 kWp (50°C)
Array operating characteristics (50°C)	U mpp	636 V	I mpp	34 A
Total area	Module area	150 m²	Cell area	134 m ²
Inverter				
<small>Original PV/syst database</small>	Model	Sunny Tripower 25000TL-JP-30		
Characteristics	Manufacturer	SMA		
Inverter pack	Operating Voltage	390-800 V	Unit Nom. Power	25.0 kWac
	Nb. of inverters	2 * MPPT 50 %	Total Power	25 kWac

Figure 4.7: System parameters at the first shadow density

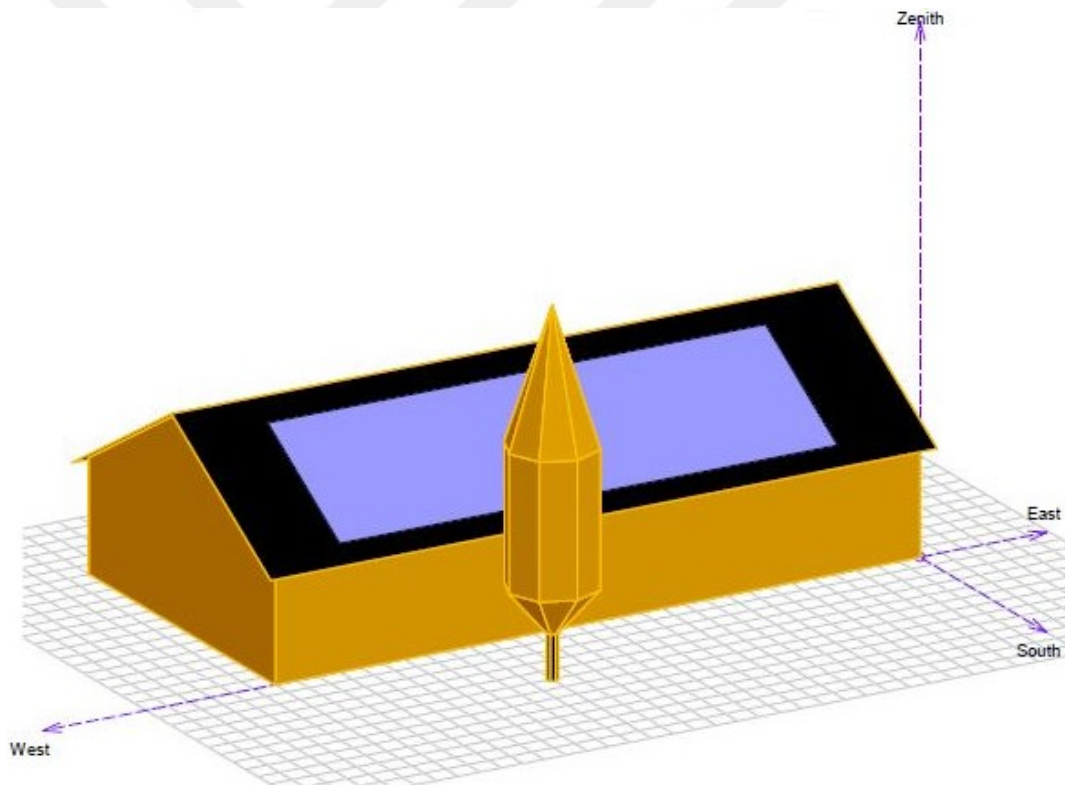


Figure 4.8: System diagram of the first shadow density

shading body were kept constant. Simulation results and annual total results are given in Figure 4.10.

Loss diagram over the whole year

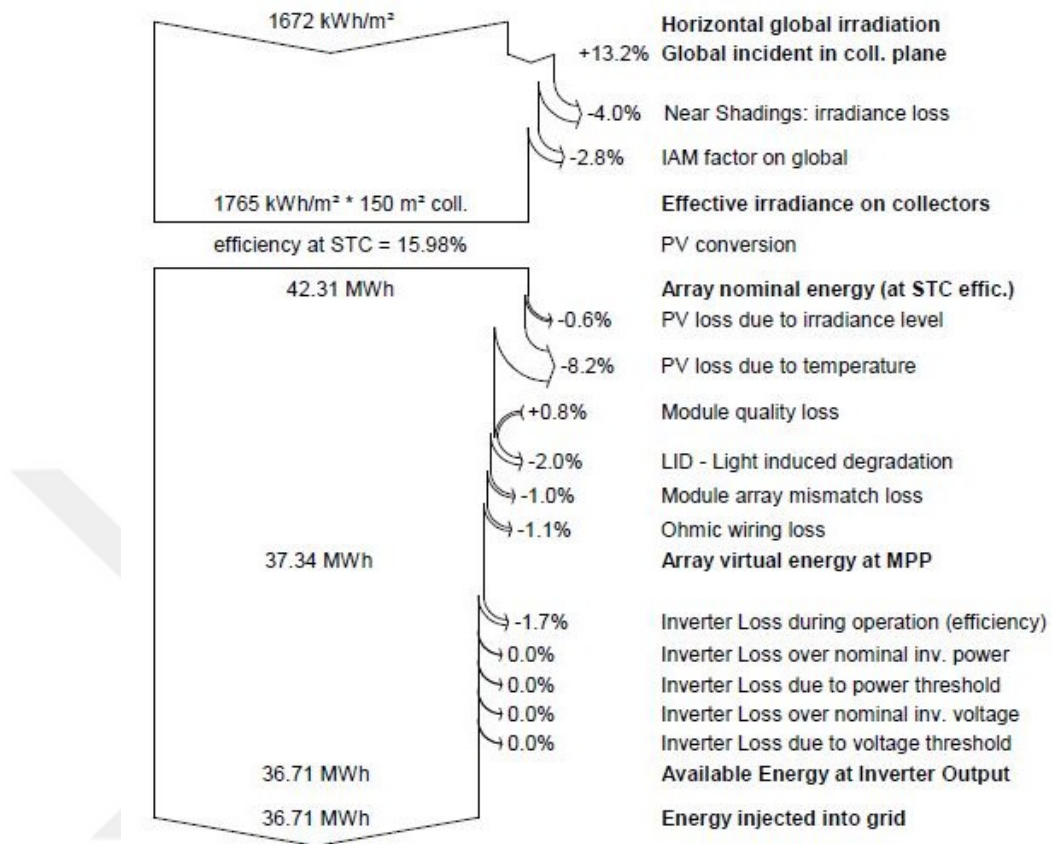


Figure 4.9: System losses diagram

4.1.3 A photovoltaic system modeled with string inverter at second shadow density

In the province of Ankara, 24 kWp installed on the roof, the system has been simulated by adding two bodies that will provide shading. The system inputs are as in Figure 4.11.

In accordance with the information given in Figure 4.11, panel layout is shown as Figure 4.12.

As shown in Figure 4.12, the tree and wind turbine in front of the building will drop shadows over the panels at certain times of the day. Figure 4.12 presents the dia-

Balances and main results

	GlobHor kWh/m ²	T Amb °C	GlobInc kWh/m ²	GlobEff kWh/m ²	EArray MWh	E_Grid MWh	EffArrR %	EffSysR %
January	53.9	0.70	75.6	66.8	1.550	1.519	13.66	13.39
February	72.8	2.40	97.6	87.9	2.026	1.989	13.83	13.58
March	127.1	5.80	148.9	138.8	3.058	3.005	13.69	13.45
April	151.5	10.80	163.5	154.5	3.348	3.292	13.65	13.43
May	197.8	16.40	196.6	186.8	3.924	3.859	13.31	13.09
June	217.5	20.00	206.1	196.2	4.023	3.958	13.02	12.80
July	236.5	24.40	229.0	218.9	4.367	4.296	12.71	12.50
August	214.8	24.50	229.1	219.8	4.360	4.288	12.69	12.48
September	163.2	20.40	197.2	186.2	3.790	3.729	12.81	12.61
October	113.5	12.60	154.9	140.5	3.044	2.994	13.10	12.88
November	73.2	6.90	114.8	100.3	2.257	2.219	13.10	12.89
December	50.5	2.00	79.5	68.7	1.596	1.566	13.38	13.13
Year	1672.4	12.30	1892.8	1765.3	37.342	36.713	13.15	12.93

Legends: GlobHor Horizontal global irradiation EArray Effective energy at the output of the array
T Amb Ambient Temperature E_Grid Energy injected into grid
GlobInc Global incident in coll. plane EffArrR Effic. Eout array / rough area
GlobEff Effective Global, corr. for IAM and shadings EffSysR Effic. Eout system / rough area

Figure 4.10: Simulation results on the basis of the first shadow density system

Simulation parameters

Collector Plane Orientation	Tilt	30°	Azimuth	0°
Models used	Transposition	Perez	Diffuse	Perez, Meteonorm
Horizon	Free Horizon			
Near Shadings	Linear shadings			
PV Array Characteristics				
PV module	Si-poly	Model	PW-DC-260-P-60	
<small>Original PV/syst database</small>	Manufacturer	Plurawatt		
Number of PV modules	In series	23 modules	In parallel	4 strings
Total number of PV modules	Nb. modules	92	Unit Nom. Power	260 Wp
Array global power	Nominal (STC)	23.92 kWp	At operating cond.	21.42 kWp (50°C)
Array operating characteristics (50°C)	U mpp	636 V	I mpp	34 A
Total area	Module area	150 m²	Cell area	134 m ²
Inverter				
<small>Original PV/syst database</small>	Manufacturer	Sunny Tripower 25000TL-JP-30		
Characteristics	Operating Voltage	390-800 V	Unit Nom. Power	25.0 kWac
Inverter pack	Nb. of inverters	2 * MPPT 50 %	Total Power	25 kWac

Figure 4.11: System parameters at the second shadow density

gram about the loss of shadows such as cloud, bird, dust, system losses such as cable inverters and other losses.

To sum up, in the Annex-3 simulation output, the annual energy generation capability of this system is 42.57 MWh / year under standard test conditions, while the nominal

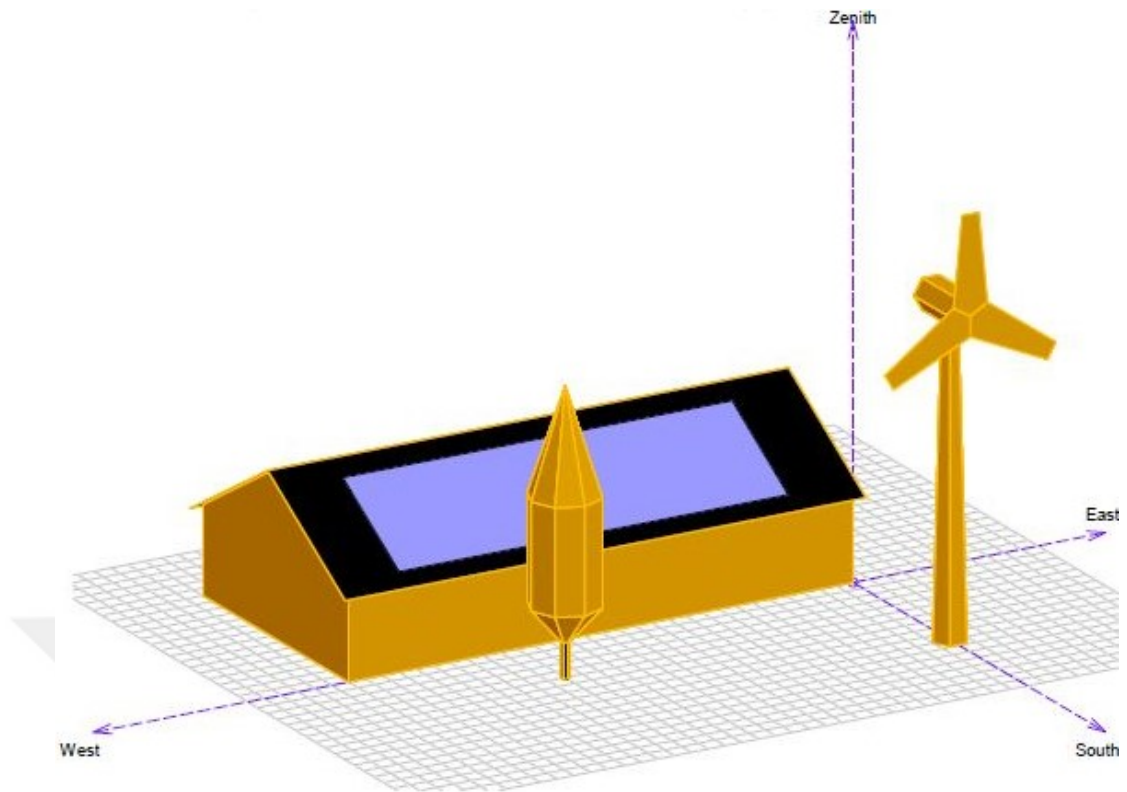


Figure 4.12: System diagram in the second shadow density

energy falls to 36.10 MWh / year after losses. The decrease in the amount of energy produced per year is due to the shadow of the tree and the turbine. All parameters except the shadowing objects were kept constant. Simulation results and annual total results are given in Figure 4.14.

4.2 Simulations with Micro Inverter

Micro inverter technology is a new technology according to string inverters. Therefore, their yield is not as high as string inverters. The simulation results in the three shadows density are given below. The installed DC power decreased to 23.92 kWp because the inverter efficiency was lower despite 260 Wp panels.

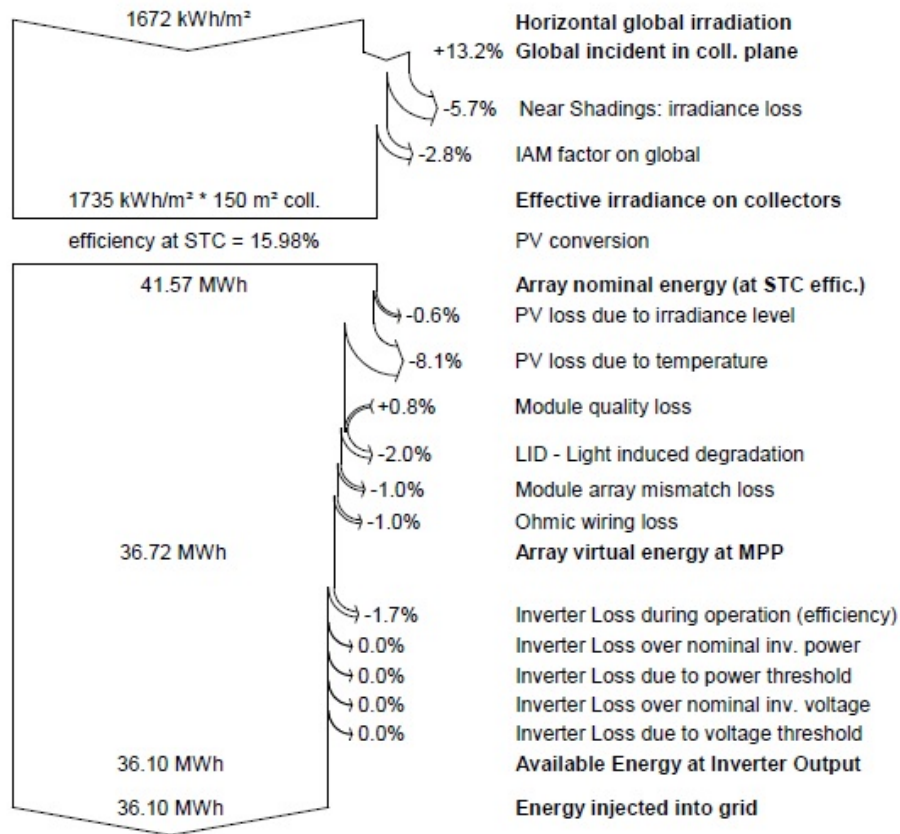


Figure 4.13: Scheme of system losses in the second shadow density

	GlobHor kWh/m ²	T Amb °C	GlobInc kWh/m ²	GlobEff kWh/m ²	EArray MWh	E_Grid MWh	EffArrR %	EffSysR %
January	53.9	0.70	75.6	64.4	1.498	1.468	13.21	12.94
February	72.8	2.40	97.6	84.1	1.943	1.908	13.27	13.03
March	127.1	5.80	148.9	135.7	2.995	2.943	13.41	13.18
April	151.5	10.80	163.5	153.2	3.321	3.265	13.55	13.32
May	197.8	16.40	196.6	185.5	3.899	3.835	13.22	13.00
June	217.5	20.00	206.1	195.0	4.001	3.935	12.94	12.73
July	236.5	24.40	229.0	217.7	4.347	4.276	12.65	12.45
August	214.8	24.50	229.1	218.7	4.341	4.269	12.63	12.42
September	163.2	20.40	197.2	183.4	3.741	3.681	12.65	12.44
October	113.5	12.60	154.9	134.1	2.915	2.868	12.54	12.34
November	73.2	6.90	114.8	96.0	2.166	2.130	12.58	12.37
December	50.5	2.00	79.5	66.9	1.555	1.526	13.04	12.80
Year	1672.4	12.30	1892.8	1734.6	36.722	36.105	12.93	12.72

Legends: GlobHor Horizontal global irradiation
T Amb Ambient Temperature
GlobInc Global incident in coll. plane
GlobEff Effective Global, corr. for IAM and shadings
EArray Effective energy at the output of the array
E_Grid Energy injected into grid
EffArrR Effic. Eout array / rough area
EffSysR Effic. Eout system / rough area

Figure 4.14: Simulation results on the basis of second shade density system

PV Array Characteristics			
PV module	Si-poly	Model	PW-DC-260-P-60
<small>Original PV_{syst} database</small>	Manufacturer	Plurawatt	
Number of PV modules	In series	1 modules	In parallel 92 strings
Total number of PV modules	Nb. modules	92	Unit Nom. Power 260 Wp
Array global power	Nominal (STC)	23.92 kWp	At operating cond. 21.42 kWp (50°C)
Array operating characteristics (50°C)	U mpp	28 V	I mpp 774 A
Total area	Module area	150 m²	Cell area 134 m ²
Inverter			
<small>Custom parameters definition</small>	Model	MICRO-0.25-I-OUTD-US-240	
Characteristics	Manufacturer	ABB	
Inverter pack	Operating Voltage	12-60 V	Unit Nom. Power 0.250 kWac
	Nb. of inverters	92 units	Total Power 23 kWac
PV Array loss factors			
Thermal Loss factor	Uc (const)	20.0 W/m ² K	Uv (wind) 0.0 W/m ² K / m/s
Wiring Ohmic Loss	Global array res.	0.60 mOhm	Loss Fraction 1.5 % at STC
LID - Light Induced Degradation			Loss Fraction 2.0 %
Module Quality Loss			Loss Fraction -0.8 %
Module Mismatch Losses			Loss Fraction 1.0 % at MPP
Incidence effect, ASHRAE parametrization	IAM =	1 - bo (1/cos i - 1)	bo Param. 0.05
User's needs :	Unlimited load (grid)		

Figure 4.15: Shadowless system parameters with micro inverter

4.2.1 A photovoltaic system modeled shadowless conditions with micro inverter

In the shadowless system with an installed capacity of 23,92 kWp on the roof in Ankara province, the panel layout is as seen in Figure 4.16. The system parameters are as in Figure 4.15.

As it is seen in Figure 4.16, modeling was carried out with the assumption that there is not an object to shade in front of the panels. Figure 4.17 presents a diagram of the system losses and other losses such as cloud, bird, dust, cable inverters.

In summary, as seen in Figure 4.17, the installed DC power is 23.92 kWp. In the Annex-4 simulation output, the annual energy generation capability of this system is 44,06 MWh / year under standard test conditions, while the nominal energy falls to 36,9 MWh / year after losses. Simulation results and annual total results are given in Figure 4.18.

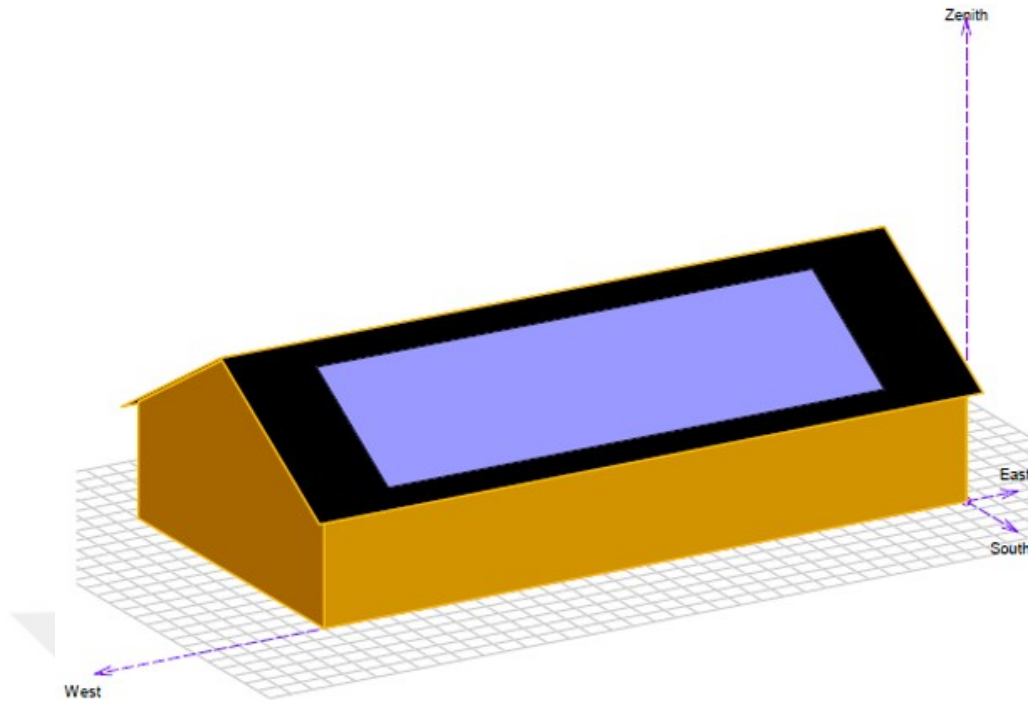


Figure 4.16: Shadowless system diagram with micro inverter

4.2.2 A photovoltaic system modeled with micro inverter at first shadow density

In the system with a first shade density of 23,92 kWp installed on the roof in Ankara province, the panel layout is as seen in Figure 4.20. The system parameters are as in Figure 4.19.

As seen in Figure 4.20, an object was placed in front of the panels and modelled. Figure 4.21 presents the diagram about the loss of shadows such as cloud, bird, dust, system losses such as cable inverters and other losses.

In summary, as seen in Figure 4.21, the installed DC power is 23.92 kWp. The annual energy generation capability of this system in the Annex-5 simulation output is 44,06 MWh / year under standard test conditions, while the nominal energy falls to 35,5 MWh / year after the losses. Simulation results and annual total results are given in Figure 4.22.

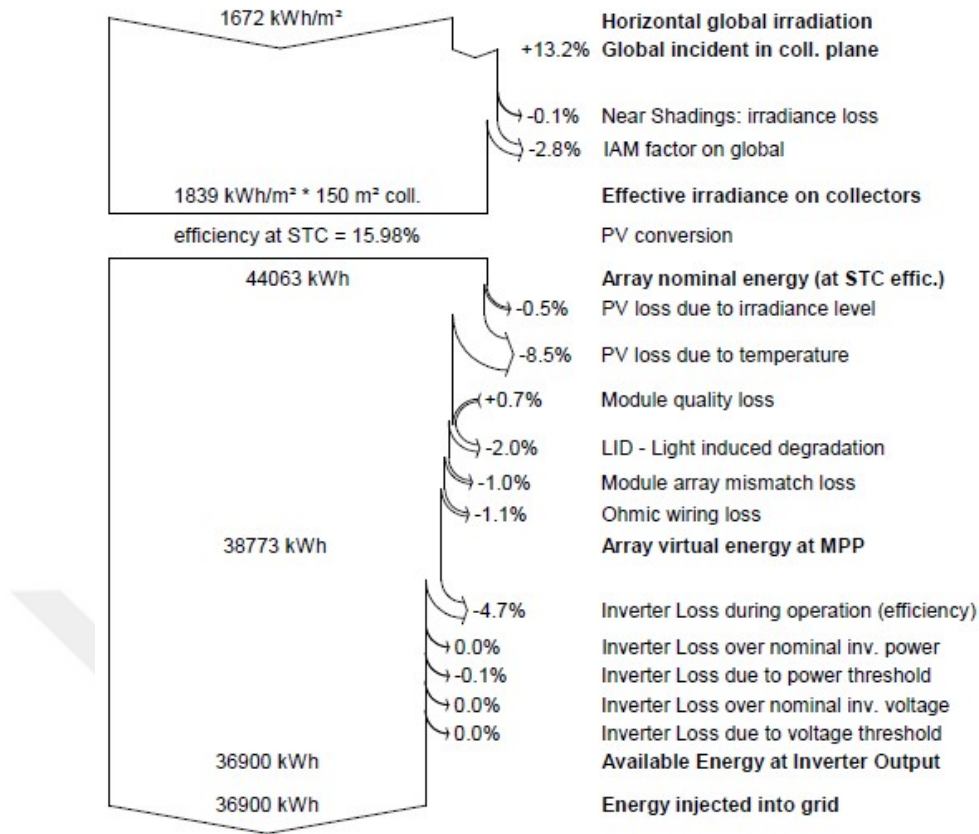


Figure 4.17: Shadowless system loss diagram with micro inverter

	GlobHor kWh/m ²	T Amb °C	GlobInc kWh/m ²	GlobEff kWh/m ²	EArray kWh	E_Grid kWh	EffArrR %	EffSysR %
January	53.9	0.70	75.6	73.5	1690	1586	14.90	13.98
February	72.8	2.40	97.6	94.8	2171	2060	14.83	14.07
March	127.1	5.80	148.9	144.8	3174	3021	14.21	13.53
April	151.5	10.80	163.5	158.4	3424	3260	13.97	13.29
May	197.8	16.40	196.6	190.5	3995	3803	13.55	12.90
June	217.5	20.00	206.1	199.7	4088	3891	13.22	12.59
July	236.5	24.40	229.0	222.2	4425	4213	12.88	12.26
August	214.8	24.50	229.1	223.0	4414	4213	12.84	12.26
September	163.2	20.40	197.2	192.1	3891	3717	13.15	12.57
October	113.5	12.60	154.9	150.9	3240	3091	13.94	13.30
November	73.2	6.90	114.8	111.6	2485	2368	14.43	13.75
December	50.5	2.00	79.5	77.1	1776	1676	14.89	14.05
Year	1672.4	12.30	1892.8	1838.5	38773	36900	13.66	13.00

Legends: GlobHor Horizontal global irradiation EArray Effective energy at the output of the array
T Amb Ambient Temperature E_Grid Energy injected into grid
GlobInc Global incident in coll. plane EffArrR Effic. Eout array / rough area
GlobEff Effective Global, corr. for IAM and shadings EffSysR Effic. Eout system / rough area

Figure 4.18: Shadowless system loss diagram with micro inverter

PV Array Characteristics			
PV module	Si-poly	Model	PW-DC-260-P-60
Original PV/syst database	Manufacturer	Plurawatt	
Number of PV modules	In series	1 modules	In parallel 92 strings
Total number of PV modules	Nb. modules	92	Unit Nom. Power 260 Wp
Array global power	Nominal (STC)	23.92 kWp	At operating cond. 21.42 kWp (50°C)
Array operating characteristics (50°C)	U mpp	28 V	I mpp 774 A
Total area	Module area	150 m²	Cell area 134 m ²
Inverter			
Custom parameters definition	Model	MICRO-0.25-I-OUTD-US-240	
Manufacturer	ABB		
Operating Voltage	12-60 V	Unit Nom. Power	0.250 kWac
Nb. of inverters	92 units	Total Power	23 kWac
PV Array loss factors			
Thermal Loss factor	Uc (const)	20.0 W/m ² K	Uv (wind) 0.0 W/m ² K / m/s
Wiring Ohmic Loss	Global array res.	0.60 mOhm	Loss Fraction 1.5 % at STC
LID - Light Induced Degradation			Loss Fraction 2.0 %
Module Quality Loss			Loss Fraction -0.8 %
Module Mismatch Losses			Loss Fraction 1.0 % at MPP
Incidence effect, ASHRAE parametrization	IAM =	1 - bo (1/cos i - 1)	bo Param. 0.05
User's needs :	Unlimited load (grid)		

Figure 4.19: Shadowless system loss diagram with micro inverter

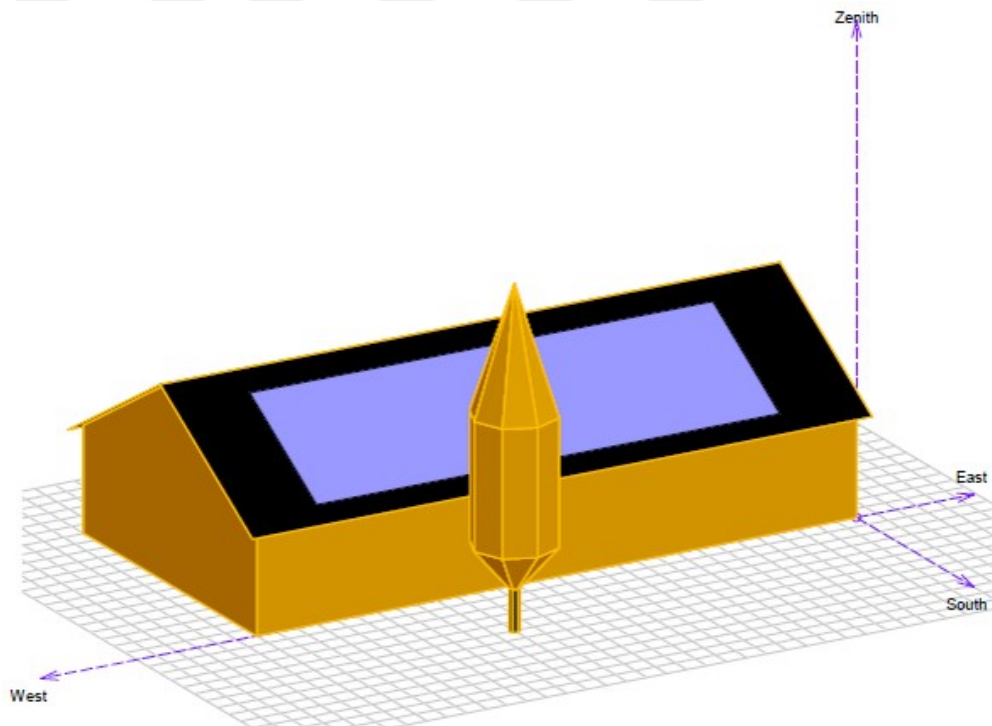


Figure 4.20: System diagram of the first shade density with micro inverter

4.2.3 A photovoltaic system modeled with micro inverter at second shadow density

In the system with a second shade density of 23,92 kWp installed on the roof in Ankara province, the panel layout is as seen in Figure 4.24. The system parameters

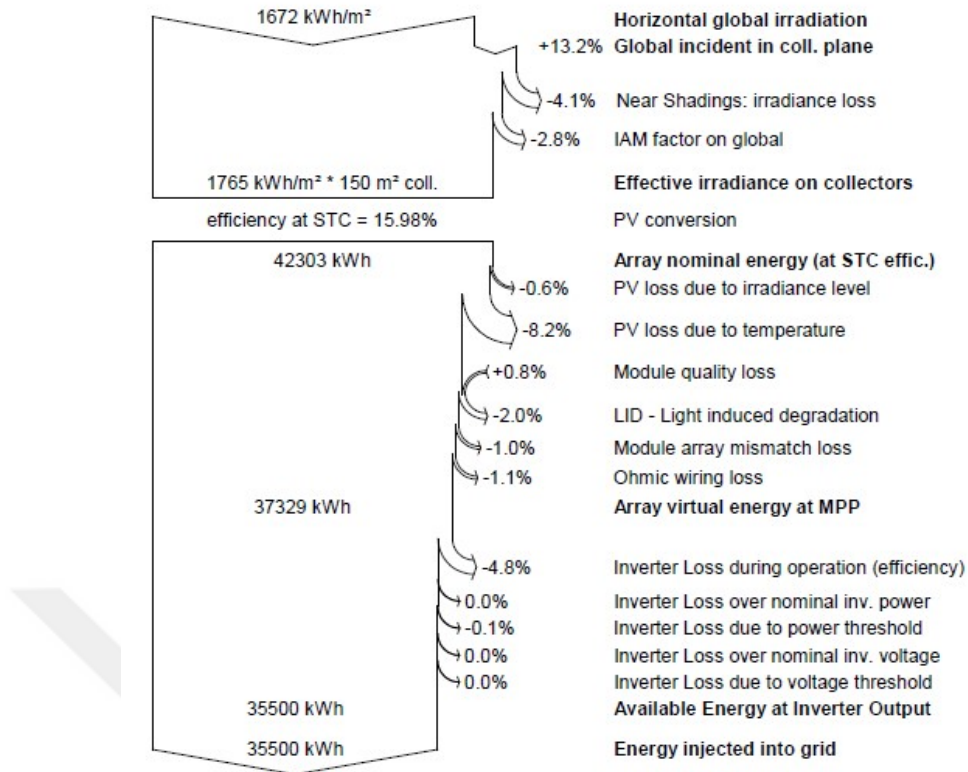


Figure 4.21: Diagram of system losses in the first shade density with micro inverter

	GlobHor kWh/m ²	T Amb °C	GlobInc kWh/m ²	GlobEff kWh/m ²	EArray kWh	E_Grid kWh	EffArrR %	EffSysR %
January	53.9	0.70	75.6	67.0	1552	1453	13.68	12.81
February	72.8	2.40	97.6	87.9	2026	1919	13.83	13.10
March	127.1	5.80	148.9	138.7	3055	2905	13.68	13.01
April	151.5	10.80	163.5	154.2	3341	3179	13.63	12.96
May	197.8	16.40	196.6	186.7	3922	3732	13.30	12.65
June	217.5	20.00	206.1	196.2	4022	3827	13.01	12.38
July	236.5	24.40	229.0	218.8	4366	4156	12.71	12.10
August	214.8	24.50	229.1	219.4	4353	4153	12.66	12.09
September	163.2	20.40	197.2	185.9	3784	3614	12.79	12.22
October	113.5	12.60	154.9	140.6	3043	2901	13.09	12.48
November	73.2	6.90	114.8	100.7	2264	2154	13.15	12.51
December	50.5	2.00	79.5	69.0	1602	1507	13.43	12.64
Year	1672.4	12.30	1892.8	1765.1	37329	35500	13.15	12.50

Legends: GlobHor Horizontal global irradiation EArray Effective energy at the output of the array
T Amb Ambient Temperature E_Grid Energy injected into grid
GlobInc Global incident in coll. plane EffArrR Effic. Eout array / rough area
GlobEff Effective Global, corr. for IAM and shadings EffSysR Effic. Eout system / rough area

Figure 4.22: Simulation results on the basis of the first shade density system with micro inverter

PV Array Characteristics			
PV module	Si-poly	Model	PW-DC-260-P-60
<small>Original PV/syst database</small>	Manufacturer	Plurawatt	
Number of PV modules	In series	1 modules	In parallel 92 strings
Total number of PV modules	Nb. modules	92	Unit Nom. Power 260 Wp
Array global power	Nominal (STC)	23.92 kWp	At operating cond. 21.42 kWp (50°C)
Array operating characteristics (50°C)	U mpp	28 V	I mpp 774 A
Total area	Module area	150 m²	Cell area 134 m ²
Inverter			
<small>Custom parameters definition</small>	Model	MICRO-0.25-I-OUTD-US-240	
Characteristics	Manufacturer	ABB	
Inverter pack	Operating Voltage	12-60 V	Unit Nom. Power 0.250 kWac
	Nb. of inverters	92 units	Total Power 23 kWac
PV Array loss factors			
Thermal Loss factor	Uc (const)	20.0 W/m ² K	Uv (wind) 0.0 W/m ² K / m/s
Wiring Ohmic Loss	Global array res.	0.60 mOhm	Loss Fraction 1.5 % at STC
LID - Light Induced Degradation			Loss Fraction 2.0 %
Module Quality Loss			Loss Fraction -0.8 %
Module Mismatch Losses			Loss Fraction 1.0 % at MPP
Incidence effect, ASHRAE parametrization	IAM =	1 - bo (1/cos i - 1)	bo Param. 0.05
User's needs :	Unlimited load (grid)		

Figure 4.23: System parameters in second shadow density with micro inverter are as in Figure 4.23.

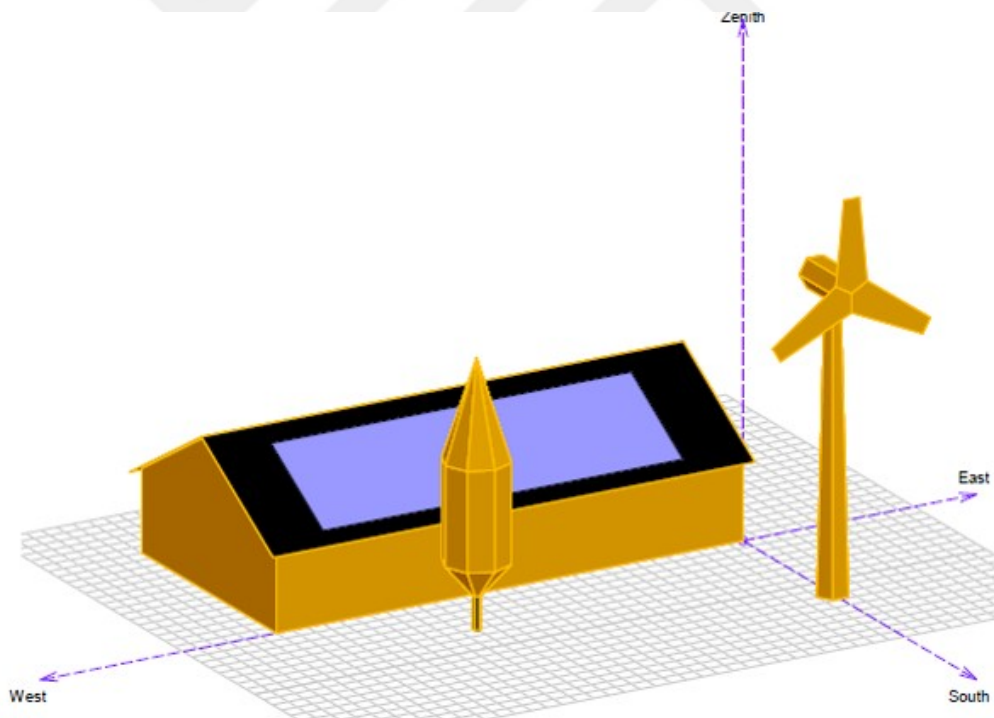


Figure 4.24: System loss diagram in second shadow density with micro inverter

As shown in Figure 4.24, the objects drop shadow to the panels, and modeling was done. Figure 4.25 presents a diagram of the system losses and other losses such as

cloud, bird, dust, cable inverters.

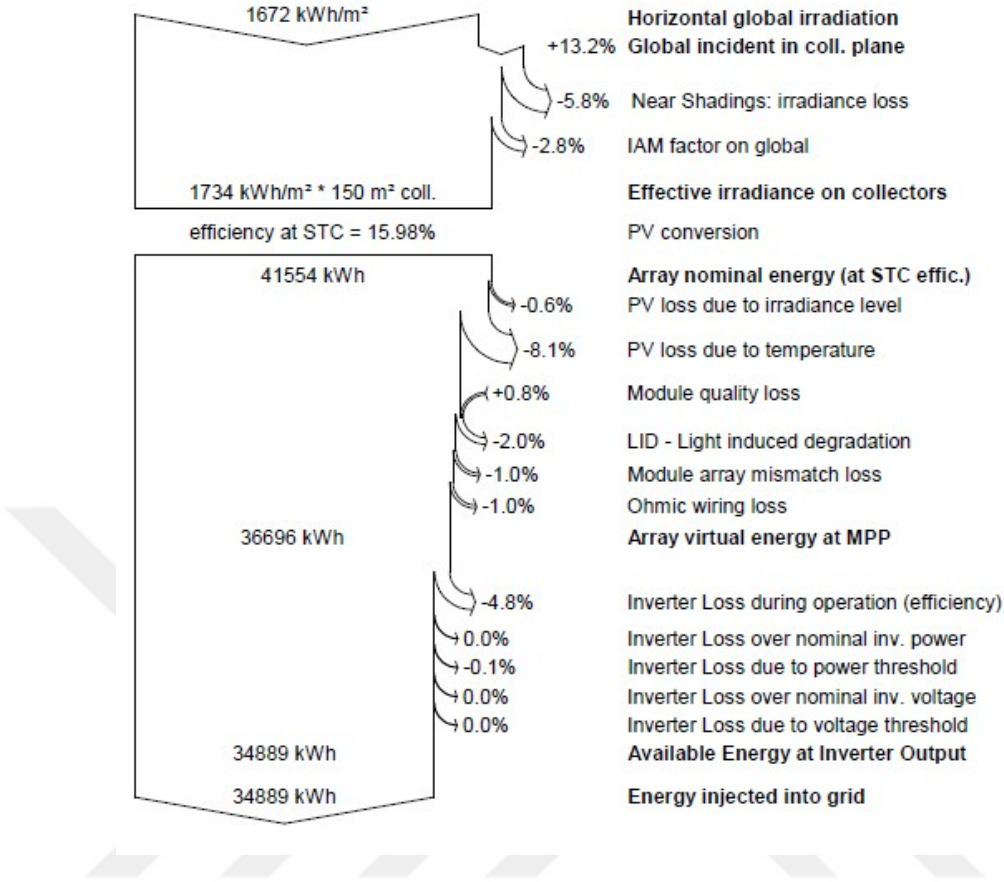


Figure 4.25: System loss diagram in second shadow density with micro inverter

In summary, as seen in Figure 4.25, the installed DC power is 23,92 kWp. The annual power generation capability of this system in the Annex-6 simulation output is 44,06 MWh / year under standard test conditions, while the nominal energy falls to 34,9 MWh / year after losses. Simulation results and annual total results are given in Figure 4.26.

CHAPTER 5

ANALYSIS, CONCLUSION AND RECOMMENDATIONS

5.1 Interpretation of Analysis

In this thesis, the following assumptions were made for the two types of inverters that were compared: any parameters other than the inverter type should be the same in the systems, shadow intensities should affect the systems at the same rate; The inputs of the simulations are summarized as follows.

As seen in Table 5.1, all parameters are the same except micro inverter, string inverter, and the connection forms of the panels. Although the powers entering the systems are the same, the difference in AC power is caused by the used inverters. When the efficiency of the inverters used in Annex-7 and Appendix-8 is examined, it is seen that the string inverter works with higher efficiency, and thus, the energy outputs are higher.

These systems will be examined separately below. The burgundy column seen in the figures gives the produced useful energy in kWh / kWp / day unit, and the green column gives the daily system losses (inverters, cables, etc.) in kWh / kWp / day unit and the purple column gives the collections losses in kWh/ kWp / day unit.

5.1.1 String Inverter in Shadowless Condition

System outputs are shown in Figure 5.1.

This is the system where the loss of inverter and panel is the minimum. In July and

Table 5.1: Simulated systems

	System Inputs with Micro Inverter System	System Inputs with Serial Inverter
The angle of the panels with the ground (tilt, °)	30°	30°
Azimuth angle (°)	0°	0°
Geographic Area	Ankara 29,9°N - 32,9°E	Ankara 29,9°N - 32,9°E
Meteorological Data Used	PVGIS CM SAF, satellite 1998-2011 - Synthetic	PVGIS CM SAF, satellite 1998-2011 - Synthetic
Photovoltaic panel	Plurawatt PW-DC-260-P-60	Plurawatt PW-DC-260-P-60
Number of panels connected in series	1	23
Number of parallel connected arrays	92	4
Total number of panels	92	92
Total installed power (kWp)	23,92 kWp	23,92 kWp
Total power in working conditions (@ 50 ° C, kWp)	21,42 kWp	21,42 kWp
Voltage at maximum power point (Umpp, V)	28 V	636 V
Current at maximum power point (Impp, A)	774 A	34 A
Total area covered by panels m ²	150 m ²	150 m ²
Inverter	ABB-MICRO-0.25-I-OUTD-US-240	SMA-Sunny Tripower 25000TL-JP-30
Inverter voltage operating range	12-60 V	390-800 V
Output power of a single inverter	0.250 kWac	25.0 kWac
Total Output Power of Inverters	23 kWac	25 kWac

August, the highest energy production per month is 6 kWh / kWp / day. Normalized productions (per installed kWp) for 23.92 kWp, produced useful energy is 4.37 kWh / kWp / day, system loss (inverter,..) is 0.07 kWh / kWp / day and collection loss (PV-array losses) is 0,74 kWh / kWp / day.

5.1.2 String Inverter in the First Shadow Density

Monthly system outputs are given in Figure 5.2.

Inverter and panel losses are higher due to first shade density. In July and August, the

Normalized productions (per installed kWp): Nominal power 23.92 kWp

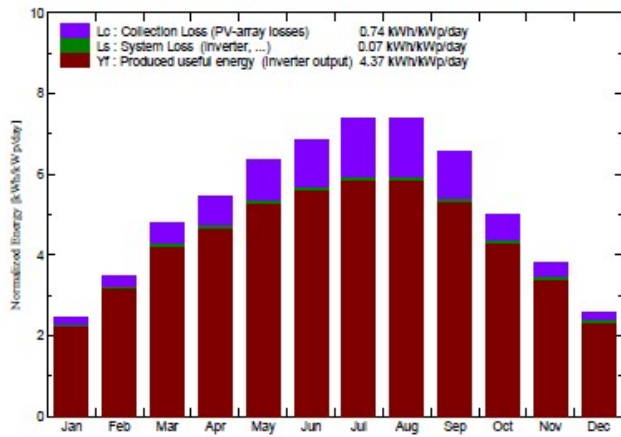


Figure 5.1: String Inverter and shadowless system outputs

Normalized productions (per installed kWp): Nominal power 23.92 kWp

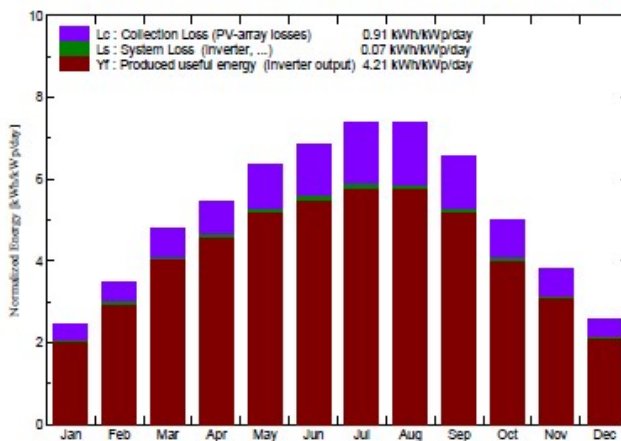


Figure 5.2: String Inverter and system outputs at the first shadow density

highest energy production per month is 6 kWh / kWp / day. Normalized productions (per installed kWp) for 23.92 kWp, produced useful energy is 4.21 kWh / kWp / day, system loss (inverter,..) is 0.07 kWh / kWp / day and collection loss (PV-array losses) is 0,91 kWh / kWp / day. The loss of the inverter is the same as in the previous system, because the loss of the panel is more likely to be due to the fact that the inverter does not change, but the power generation capabilities decrease because of the shadowing on the panels.

5.1.3 String Inverter in the Second Shadow Density

Monthly system outputs are given in Figure 5.3.

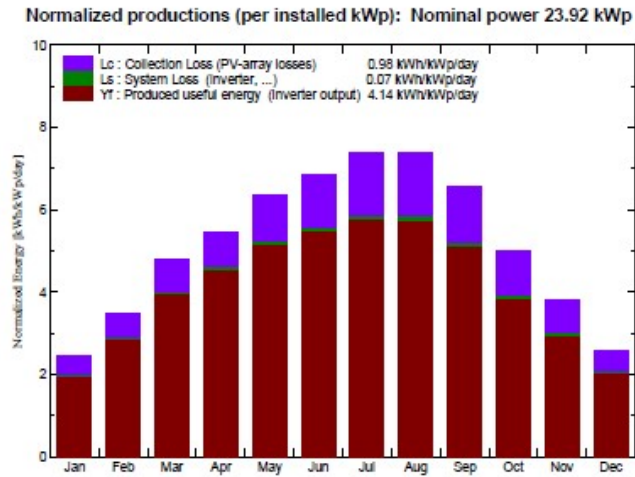


Figure 5.3: String inverter and system outputs at the second shadow density

Inverter and panel losses are higher than the first two systems. In July and August, the highest per capita energy generation rate is less than 6 kWh / kWp / day. When evaluated throughout the year, the produced useful energy is 4.14 kWh / kWp / day, system loss is 0.07 kWh / kWp / day and collection loss (PV-array losses) is 0.98 kWh / kWp / day.

5.1.4 Micro Inverter in Shadowless Condition

Monthly system outputs are given in Figure 5.4.

This is a micro inverter system with the highest performance of inverter and panel. In July and August, the ratio of production per installed kWp is about 5.5 kWh / kWp / day. When evaluated throughout the year, the produced useful energy is 4.23 kWh / kWp / day, system loss is 0.21 kWh / kWp / day and collection loss (PV-array losses) is 0.74 kWh / kWp / day.

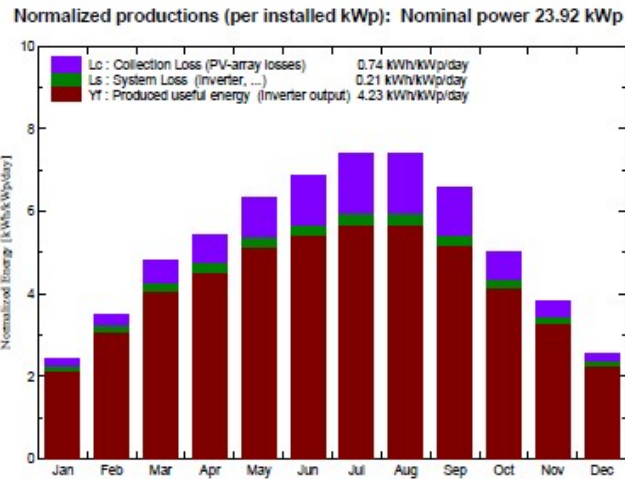


Figure 5.4: Micro inverter and shadowless system outputs

5.1.5 Micro Inverter in the First Shadow Density

Monthly system outputs are given in Figure 5.5.

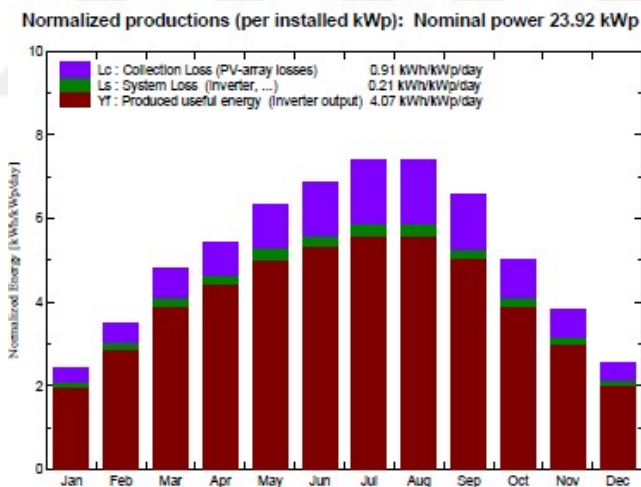


Figure 5.5: Micro inverter and system outputs at first shadow density

It is the system where inverter and panel losses are higher than shadowless system. In July and August, the ratio of production per installed kWp is about 5.5 kWh / kWp / day. When evaluated throughout the year, the produced useful energy is 4.07 kWh / kWp / day, system loss is 0.21 kWh / kWp / day and collection loss (PV-array losses)

is 0.91 kWh / kWp / day.

5.1.6 Micro Inverter in the Second Shadow Density

System outputs are shown in Figure 5.6.

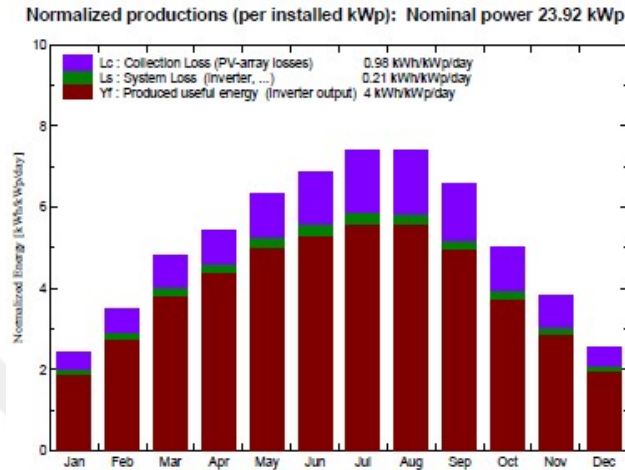


Figure 5.6: Micro inverter and system outputs at the second shadow density

It is the system with the highest loss of inverter and panel losses. In July and August, the ratio of production per installed kWp is about 5 kWh / kWp / day. When evaluated throughout the year, the produced useful energy is 4 kWh / kWp / day, system loss is 0.21 kWh / kWp / day and collection loss (PV-array losses) is 0.98 kWh / kWp / day. The maximum efficiency of the micro inverter used in these systems is 96%, and the efficiency of the string inverter is 98.7% [33-34]. Even though the total DC power is the same as the system, even with unshaded conditions, the efficiency of the string inverter is higher than the micro inverter. In all of the three systems, systems with string inverter are more efficient.

5.2 Conclusion and Discussion

Photovoltaic systems and emerging technologies will play more critical roles in the present and the future. In photovoltaic systems, problems such as shadow, high voltages, especially in DC cables and cable losses, panel alignment, and installation diffi-

Table 5.2: Performance rates

	Micro Inverter			Serial Inverter		
	Shadowless	1st Shadow Density	2nd Shadow Density	Shadowless	1st Shadow Density	2nd Shadow Density
Array nominal energy (at STC effic.) (kWh/year)	44060	42600	41550	44060	42610	41570
Energy injected into grid (kWh/year)	36900	35500	34889	38130	36710	36100
Losses (%)	19,4	20,0	19,1	15,6	16,1	15,2

culties are waiting to be solved. In particular, network-based system applications are still taking care of today, and work continues. Although there are many reasons for this, the most striking factor is that the payback period is shorter in grid connected systems. It is crucial to use micro inverter systems to produce electricity and to transmit excess energy to the grid in rooftop applications. The common goal of all technological developments is to make low-cost and low-risk systems available by keeping the annual generated energy at the highest level. In three common types of inverters, especially in roof applications, the micro inverter aims to prevent energy loss due to shadowing. In systems with string inverters, the energy loss increases due to the effect of the entire arm on the shadow of a single panel. In addition to energy loss, the panel becomes unavailable with a hot spot effect when there is a fixed shadow. This situation causes problems larger than power loss.

In this thesis, three different shade density analysis of micro inverter and string inverter systems are compared. Due to the high efficiency of the string inverters, the power outputs are higher than the micro inverter systems. However, because of the panels connected in series with a string inverter system, very high voltages constitute security risks. Another difference arises from the losses and costs of inverters, DC, and AC cables. Especially in string inverter systems, a large number of panels are connected in series and parallel with DC cables to the inverter. DC cables increase cable losses because they are more expensive and their usage is much more than AC cables. AC cables are cheaper and have fewer cable losses. [30]

When comparing efficiencies from the loss diagram, due to the inverter efficiencies of the micro inverters, systems with micro inverters are less efficient than the systems with string inverters. Other losses affect the system same. In the future works, efficiencies of the micro inverters should be increased.



REFERENCES

- [1] The Distribution of Turkey's Installed Capacity by Primary Energy Resources in 2017- Figure I.IV, "TEIAS – Türkiye Elektrik İletim A.Ş., " Internet: <https://www.teias.gov.tr/tr/i-installed-capacity>, 2018 [11 June 2019].
- [2] Enerji İşleri Genel Müdürlüğü, "Güneş Enerjisi ve Teknolojileri", Internet: <http://www.yegm.gov.tr/yenilenebilir/gunes-tekno.aspx>, 2019 [11 June 2019].
- [3] Turkey's Installed Capacity by Primary Energy Resources for the Years 2006 and 2017 – Figure I-II, "TEIAS – Türkiye Elektrik İletim A.Ş. ," Internet:<https://www.teias.gov.tr/tr/i-installed-capacity>, 2018 [11 June 2019].
- [4] C. Çetiner, Occasion, Topic: "Güneş Enerjisi Ders Notları" Şanlıurfa: Harran Üniversitesi, 2017.
- [5] H. Özgün, "Fotovoltaik Enerji Sistemleri, Temel Kavramlar ve Örnek Projelerle Fotovoltaik Güneş Enerjisi Sistemleri" (2nd Edition).Turkey, 2016 pp. 27-31.
- [6] M.H. Uzun, "Güneş Enerjisi Depolama Olanakları Ve Bir Yöntemin Değerlendirilmesi" Master's Thesis, T.C. Trakya Üniversitesi Fen Bilimleri Enstitüsü, Edirne, 2010.
- [7] Manienyan, V. Thambidurai, M. Selvakumar R., "Study on Energy Crisis and the Future of Fossil Fuels, Proceedings of SHEE 2009", Engineering Wing, DDE, Annamalai University, 2009.
- [8] Gazis, F.,Vokas G.A., Katsimardou I.J. and Kaldelis J.K., "Micro inverters for PV plants compared to the ordinary string or central inverters", The Conference for International Synergy in Energy, Environment, Tourism and contribution of Information Technology in Science, Economy, Society and Education, Piraeus, 2013.
- [9] Micro inverter vs String inverter, "Gozuk", Internet:<http://www.inverter.co/micro-inverter-vs-string-inverter-485719.html>, 2019 [11 June 2019].
- [10] Arráez-Cancelliere,O.A., Muñoz-Galeano, N. and Lopez-Lezama, J.M., "Performance and Economical Comparison between Micro-Inverter and String Inverter in a 5,1 kWp Residential PV-System in Colombia", IEEE, 2017, pp. 5-9.
- [11] Sharkawi, L. And Hassan, M., "Photovoltaic systems analysis taking into consideration the shadows effect", 2015 IEEE 8th GCC Conference and Exhibition, GCCCE 2015, Muscat, Oman,2015.
- [12] Krauter, S. And Bendfeld, J., "Cost, Performance, and Yield Comparison of eight different Micro-Inverters", 2015 IEEE 42nd Photovoltaic Specialist Conference (PVSC), Hyatt Regency - New Orleans,2015.

- [13] Famoso, F., Lanzafame, R., Maenza, S. and Scandura, P.F., “Performance comparison between micro-inverter and string-inverter Photovoltaic Systems, Energy Procedia v. 81” 69th Conference of the Italian Thermal Engineering Association, ATI 2014, Italia, 2015.
- [14] H. Özgün, Fotovoltaik Enerji Sistemleri, “Temel Kavramlar ve Örnek Projelerle Fotovoltaik Güneş Enerjisi Sistemleri (2nd Edition)”.Turkey, 2016 pp. 57-67.
- [15] Lecturer Kenan Özel, Ankara Üniversitesi Open Course Files 7. week, Topic: “Temperature And Photovoltaic Batteries Performance”, Ankara, 2019.
- [16] Solar Energy, “Photovoltaic Cells”, Internet:<https://web.itu.edu.tr/kaymak/PV.html>, 2019 [11 June 2019].
- [17] Enerji Atlası, “Solar Energy by Country”, Internet:<https://www.enerjiatlası.com/ulkelere-gore-gunes-enerjisi.html>, 2019 [11 June 2019].
- [18] World Energy Council, World Energy Resources, Solar 2016
- [19] T.C. Enerji ve Tabii Kaynaklar Bakanlığı, “Güneş”, Internet:<https://www.enerji.gov.tr/tr-TR/Sayfalar/Gunes>, 2019 [11 June 2019].
- [20] Şişman, N., “Türkiye’nin 2023 Yılında Toplam Elektrik Enerjisi Talebini Karşılama İçin Optimum Güneş Enerjisi Seçeneğinin Araştırılması”, Ph.D. Thesis, Eskişehir Osmangazi Üniversitesi, Eskişehir, 2018.
- [21] Yenilenebilir Enerji Genel Müdürlüğü, “Güneş Enerjisi Potansiyel Atlası (GEPA)”, Internet: <http://www.yegm.gov.tr/MyCalculator/Default.aspx>, 2018 [11 June 2019].
- [22] Photovoltaic Geographical Information System - Interactive Maps, Europe- PV Estimation, “Turkey sunshine duration”, Internet: <http://re.jrc.ec.europa.eu/pvgis/apps4/pvest.phpv>, 2019, [11 June 2019].
- [23] Photovoltaic Geographical Information System - Interactive Maps, Europe- PV Estimation, “PVGIS data for Turkey”, Internet: <http://re.jrc.ec.europa.eu/pvgis/apps4/pvest.phpv>, 2019, [11 June 2019].
- [24] Yılmaz, M., “Şebekeye Bağlı Fotovoltaik Sistemlerde Üretilen Enerjinin Yapay Sinir Ağları Kullanılarak Tahmini”, Master’s Thesis, Fırat Üniversitesi Fen Bilimleri Enstitüsü, Elazığ, 2014.
- [25] Donuk, K., “Güneş Takip Sistemi İle Güneş Enerjisinden Elektrik Enerjisi Elde Etme Yöntemleri Ve Optimum Verimin Belirlenmesi”, Ph.D Thesis, Marmara Üniversitesi, İstanbul, 2013.
- [26] Novergy Power Generation for Generations, “Layers”, Internet: <https://www.novergysolar.com/solar-cell-solar-panel-difference/layers/>, 2019 [11 June 2019].
- [27] GestEnergy, “Panel Parts and Modules”, Internet: <http://gest-energy.com/images/dosyalar/20140618121727-0.pdf>, version 1.9, 2019 [11 June 2019].

- [28] Youtube, “Plurawatt PV Modül Üretim Hattı”, Internet: https://www.youtube.com/watch?v=Bmddz_gUt_A, 2016 [11 June 2019].
- [29] Eruz, Ü.G., ”Güneş Paneli Çeşitlerinden Polikristal, Monokristal Ve Thin Film Panellerinin Karabük Şartlarında Verimlilik Karşılaştırılması”, Master’s Thesis, Karabük Üniversitesi, Karabük, 2015.
- [30] Ayetek Enerji, ”Solar Kablo Fiyatları Hakkında”, Internet: <http://www.ayetek.com/solar-kablo-fiyatları-hakkında/>, 2016 [11 June 2019].
- [31] PVEducation, “Hot Spot Heating”, Internet: <https://www.pveducation.org/pvcdrom/modules-and-arrays/hot-spot-heating>, 2019 [11 June 2019].
- [32] Güneş Sistemleri, “Sıcaklığın güneş hücreleri üzerindeki etkisi”, Internet: <http://www.gunessistemleri.com/fotovoltaik-sicaklik.php>, 2008 [11 June 2019].
- [33] Solar Inverters – ABB micro inverter system, “MICRO-0.25/0.3/0.3HV-I-OUTD 0.25kw to 0.3kw”, Internet: <https://library.e.abb.com/public/3b4b2359a4986e2685257dff005e1834/MICRO-0.25-0.3-0.3HV-Rev0.1.pdf>, 2015 [11 June 2019].
- [34] SMA, “SUNNY TRIPOWER 25000TL-JP”, Internet: <https://www.sma.de/en/products/solarinverters/sunny-tripower-25000tl-jp.html>, 2015 [11 June 2019].
- [35] Murty P.S.R., ”Chapter 9 - Lines and Loads” in Power Systems Analysis , 2nd ed., Edition), 2017, pp. 175-204.

APPENDIX A

APPENDICES

A.1 Serial Shadowless



Grid-Connected System: Simulation parameters

Project : Thesis

Geographical Site Ankara_g Country Turkey

Situation Latitude 39.9°N Longitude 32.9°E
 Time defined as Legal Time Time zone UT+2 Altitude 895 m
 Albedo 0.20

Meteo data: Ankara_g PVGIS CM SAF, satellite 1998-2011 - Synthetic

Simulation variant : Serial - shadowless

Simulation parameters

Collector Plane Orientation Tilt 30° Azimuth 0°

Models used Transposition Perez Diffuse Perez, Meteonorm

Horizon Free Horizon

Near Shadings Linear shadings

PV Array Characteristics

PV module Si-poly Model **PW-DC-260-P-60**
Original PVsyst database Manufacturer Plurawatt

Number of PV modules In series 23 modules In parallel 4 strings
 Total number of PV modules Nb. modules 92 Unit Nom. Power 260 Wp
 Array global power Nominal (STC) **23.92 kWp** At operating cond. 21.42 kWp (50°C)
 Array operating characteristics (50°C) U mpp 636 V I mpp 34 A
 Total area Module area **150 m²** Cell area 134 m²

Inverter Model **Sunny Tripower 25000TL-JP-30**
Original PVsyst database Manufacturer SMA

Characteristics Operating Voltage 390-800 V Unit Nom. Power 25.0 kWac
 Inverter pack Nb. of inverters 2 * MPPT 50 % Total Power 25 kWac

PV Array loss factors

Thermal Loss factor U_c (const) 20.0 W/m²K U_v (wind) 0.0 W/m²K / m/s
 Wiring Ohmic Loss Global array res. 320 mOhm Loss Fraction 1.5 % at STC
 LID - Light Induced Degradation Loss Fraction 2.0 %
 Module Quality Loss Loss Fraction -0.8 %
 Module Mismatch Losses Loss Fraction 1.0 % at MPP
 Incidence effect, ASHRAE parametrization IAM = 1 - bo (1/cos i - 1) bo Param. 0.05

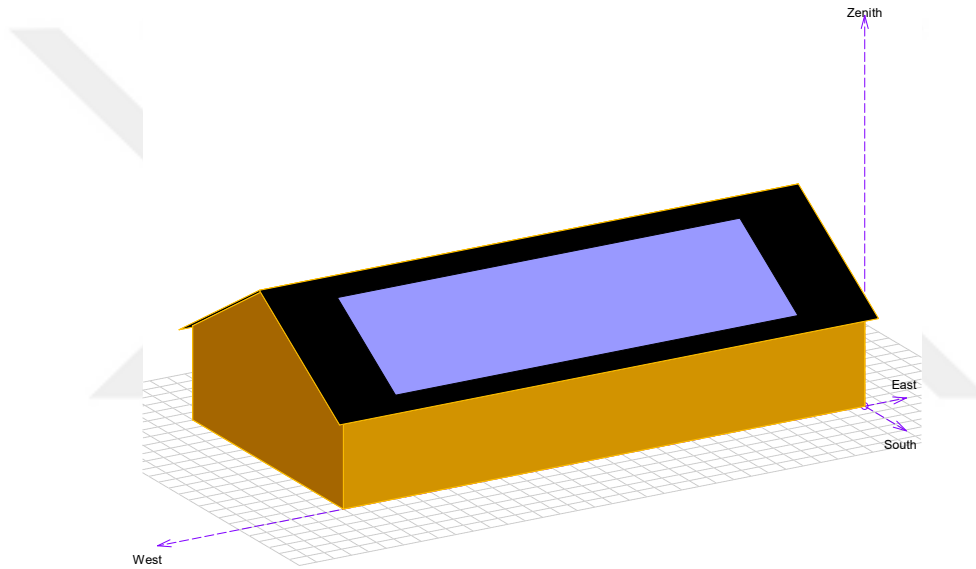
User's needs : Unlimited load (grid)

Grid-Connected System: Near shading definition

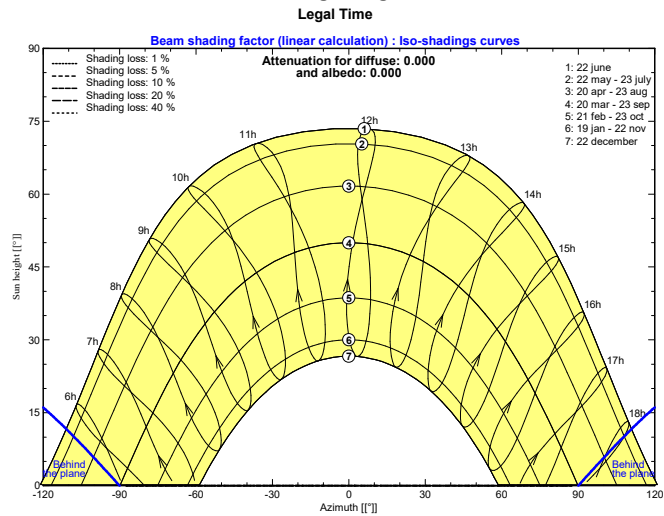
Project : Thesis
Simulation variant : Serial - shadowless

Main system parameters	System type	Grid-Connected		
Near Shadings	Linear shadings			
PV Field Orientation	tilt	30°	azimuth	0°
PV modules	Model	PW-DC-260-P-60	Pnom	260 Wp
PV Array	Nb. of modules	92	Pnom total	23.92 kWp
Inverter	Model	Sunny Tripower 25000TL-JP-30		25.00 kW ac
User's needs	Unlimited load (grid)			

Perspective of the PV-field and surrounding shading scene



Iso-shadings diagram



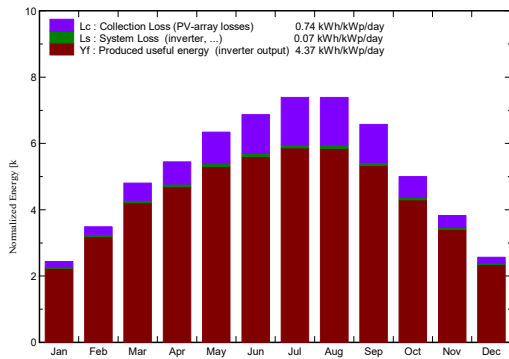
Grid-Connected System: Main results

Project : Thesis
Simulation variant : Serial - shadowless

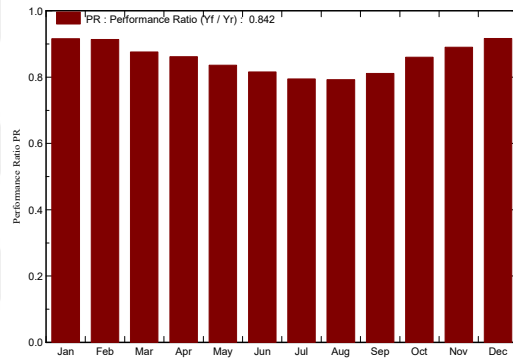
Main system parameters	System type	Grid-Connected		
Near Shadings	Linear shadings			
PV Field Orientation	tilt	30°	azimuth	0°
PV modules	Model	PW-DC-260-P-60	Pnom	260 Wp
PV Array	Nb. of modules	92	Pnom total	23.92 kWp
Inverter	Model	Sunny Tripower 25000TL-JP-30		25.00 kW ac
User's needs	Unlimited load (grid)			

Main simulation results	Produced Energy	38.13 MWh/year	Specific prod.	1594 kWh/kWp/year
System Production	Performance Ratio PR	84.2 %		

Normalized productions (per installed kWp): Nominal power 23.92 kWp



Performance Ratio PR



Balances and main results

	GlobHor kWh/m ²	T Amb °C	GlobInc kWh/m ²	GlobEff kWh/m ²	EArray MWh	E_Grid MWh	EffArrR %	EffSysR %
January	53.9	0.70	75.6	73.5	1.690	1.657	14.90	14.61
February	72.8	2.40	97.6	94.8	2.172	2.134	14.83	14.57
March	127.1	5.80	148.9	144.8	3.176	3.120	14.22	13.97
April	151.5	10.80	163.5	158.4	3.426	3.368	13.97	13.74
May	197.8	16.40	196.6	190.5	3.997	3.931	13.55	13.33
June	217.5	20.00	206.1	199.7	4.089	4.022	13.23	13.01
July	236.5	24.40	229.0	222.2	4.426	4.353	12.88	12.67
August	214.8	24.50	229.1	223.0	4.415	4.342	12.85	12.63
September	163.2	20.40	197.2	192.1	3.891	3.828	13.16	12.94
October	113.5	12.60	154.9	150.9	3.241	3.188	13.94	13.72
November	73.2	6.90	114.8	111.6	2.486	2.445	14.44	14.20
December	50.5	2.00	79.5	77.1	1.777	1.744	14.90	14.62
Year	1672.4	12.30	1892.8	1838.5	38.785	38.132	13.66	13.43

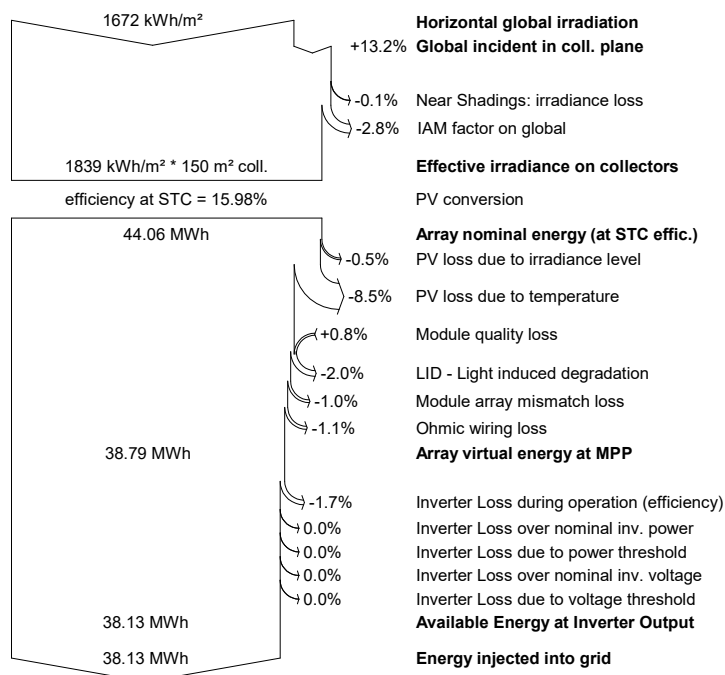
Legends: GlobHor Horizontal global irradiation
 T Amb Ambient Temperature
 GlobInc Global incident in coll. plane
 GlobEff Effective Global, corr. for IAM and shadings
 EArray Effective energy at the output of the array
 E_Grid Energy injected into grid
 EffArrR Effic. Eout array / rough area
 EffSysR Effic. Eout system / rough area

Grid-Connected System: Loss diagram

Project : Thesis
Simulation variant : Serial - shadowless

Main system parameters	System type	Grid-Connected	
Near Shadings	Linear shadings		
PV Field Orientation	tilt	30°	azimuth 0°
PV modules	Model	PW-DC-260-P-60	Pnom 260 Wp
PV Array	Nb. of modules	92	Pnom total 23.92 kWp
Inverter	Model	Sunny Tripower 25000TL-JP-30	25.00 kW ac
User's needs	Unlimited load (grid)		

Loss diagram over the whole year



A.2 Serial 1st Density



Grid-Connected System: Simulation parameters

Project :	Thesis		
Geographical Site	Ankara_g	Country	Turkey
Situation	Latitude 39.9°N	Longitude	32.9°E
Time defined as	Legal Time Time zone UT+2	Altitude	895 m
	Albedo 0.20		
Meteo data:	Ankara_g	PVGIS CM SAF, satellite 1998-2011 - Synthetic	

Simulation variant : Serial - 1st density

Simulation parameters

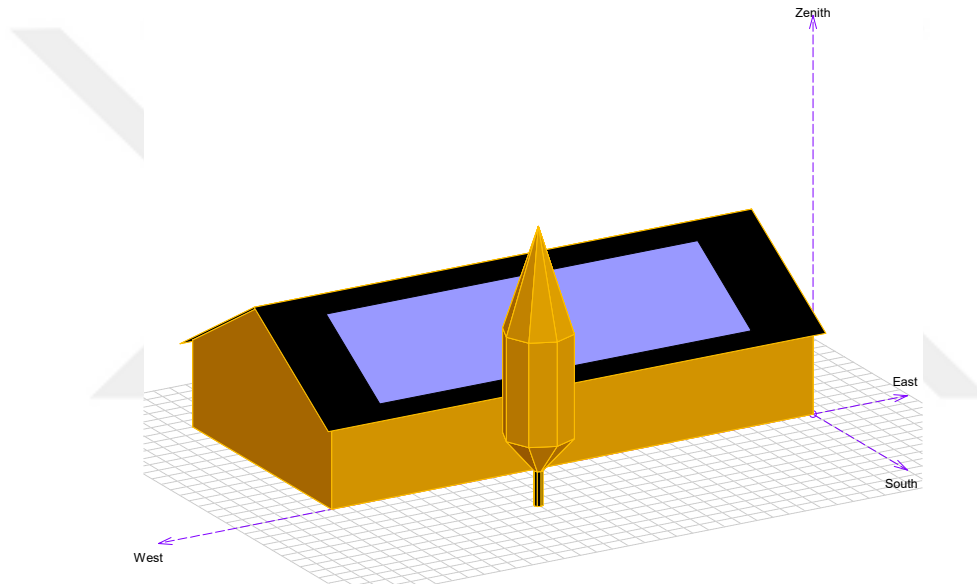
Collector Plane Orientation	Tilt	30°	Azimuth	0°
Models used	Transposition	Perez	Diffuse	Perez, Meteonorm
Horizon	Free Horizon			
Near Shadings	Linear shadings			
PV Array Characteristics				
PV module	Si-poly	Model	PW-DC-260-P-60	
<small>Original PVsyst database</small>	Manufacturer	Plurawatt		
Number of PV modules	In series	23 modules	In parallel	4 strings
Total number of PV modules	Nb. modules	92	Unit Nom. Power	260 Wp
Array global power	Nominal (STC)	23.92 kWp	At operating cond.	21.42 kWp (50°C)
Array operating characteristics (50°C)	U mpp	636 V	I mpp	34 A
Total area	Module area	150 m²	Cell area	134 m²
Inverter				
<small>Original PVsyst database</small>	Model	Sunny Tripower 25000TL-JP-30		
Characteristics	Manufacturer	SMA		
	Operating Voltage	390-800 V	Unit Nom. Power	25.0 kWac
Inverter pack	Nb. of inverters	2 * MPPT 50 %	Total Power	25 kWac
PV Array loss factors				
Thermal Loss factor	Uc (const)	20.0 W/m²K	Uv (wind)	0.0 W/m²K / m/s
Wiring Ohmic Loss	Global array res.	320 mOhm	Loss Fraction	1.5 % at STC
LID - Light Induced Degradation			Loss Fraction	2.0 %
Module Quality Loss			Loss Fraction	-0.8 %
Module Mismatch Losses			Loss Fraction	1.0 % at MPP
Incidence effect, ASHRAE parametrization	IAM =	1 - bo (1/cos i - 1)	bo Param.	0.05
User's needs :	Unlimited load (grid)			

Grid-Connected System: Near shading definition

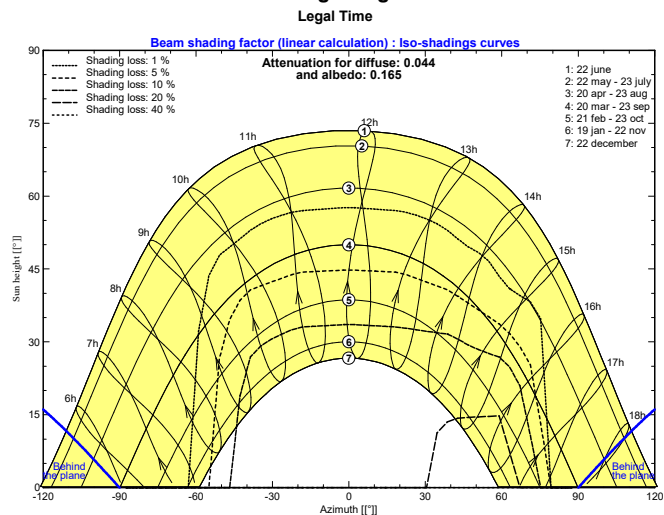
Project : Thesis
Simulation variant : Serial - 1st density

Main system parameters	System type	Grid-Connected		
Near Shadings	Linear shadings			
PV Field Orientation	tilt	30°	azimuth	0°
PV modules	Model	PW-DC-260-P-60	Pnom	260 Wp
PV Array	Nb. of modules	92	Pnom total	23.92 kWp
Inverter	Model	Sunny Tripower 25000TL-JP-30		25.00 kW ac
User's needs	Unlimited load (grid)			

Perspective of the PV-field and surrounding shading scene



Iso-shadings diagram



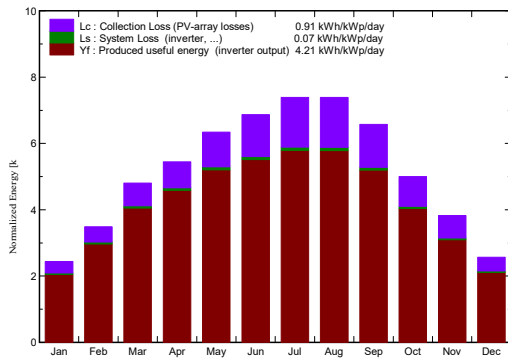
Grid-Connected System: Main results

Project : Thesis
Simulation variant : Serial - 1st density

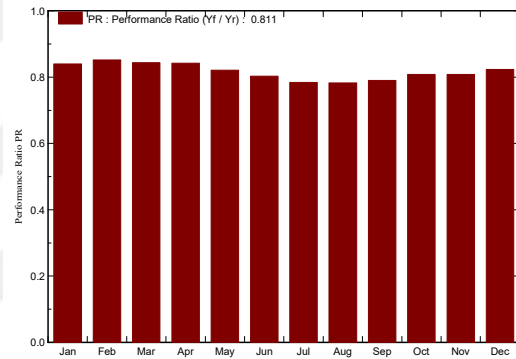
Main system parameters	System type	Grid-Connected		
Near Shadings	Linear shadings			
PV Field Orientation	tilt	30°	azimuth	0°
PV modules	Model	PW-DC-260-P-60	Pnom	260 Wp
PV Array	Nb. of modules	92	Pnom total	23.92 kWp
Inverter	Model	Sunny Tripower 25000TL-JP-30		25.00 kW ac
User's needs	Unlimited load (grid)			

Main simulation results	Produced Energy	36.71 MWh/year	Specific prod.	1535 kWh/kWp/year
System Production	Performance Ratio PR	81.1 %		

Normalized productions (per installed kWp): Nominal power 23.92 kWp



Performance Ratio PR



Balances and main results

	GlobHor kWh/m ²	T Amb °C	GlobInc kWh/m ²	GlobEff kWh/m ²	EArray MWh	E_Grid MWh	EffArrR %	EffSysR %
January	53.9	0.70	75.6	66.8	1.550	1.519	13.66	13.39
February	72.8	2.40	97.6	87.9	2.026	1.989	13.83	13.58
March	127.1	5.80	148.9	138.8	3.058	3.005	13.69	13.45
April	151.5	10.80	163.5	154.5	3.348	3.292	13.65	13.43
May	197.8	16.40	196.6	186.8	3.924	3.859	13.31	13.09
June	217.5	20.00	206.1	196.2	4.023	3.958	13.02	12.80
July	236.5	24.40	229.0	218.9	4.367	4.296	12.71	12.50
August	214.8	24.50	229.1	219.8	4.360	4.288	12.69	12.48
September	163.2	20.40	197.2	186.2	3.790	3.729	12.81	12.61
October	113.5	12.60	154.9	140.5	3.044	2.994	13.10	12.88
November	73.2	6.90	114.8	100.3	2.257	2.219	13.10	12.89
December	50.5	2.00	79.5	68.7	1.596	1.566	13.38	13.13
Year	1672.4	12.30	1892.8	1765.3	37.342	36.713	13.15	12.93

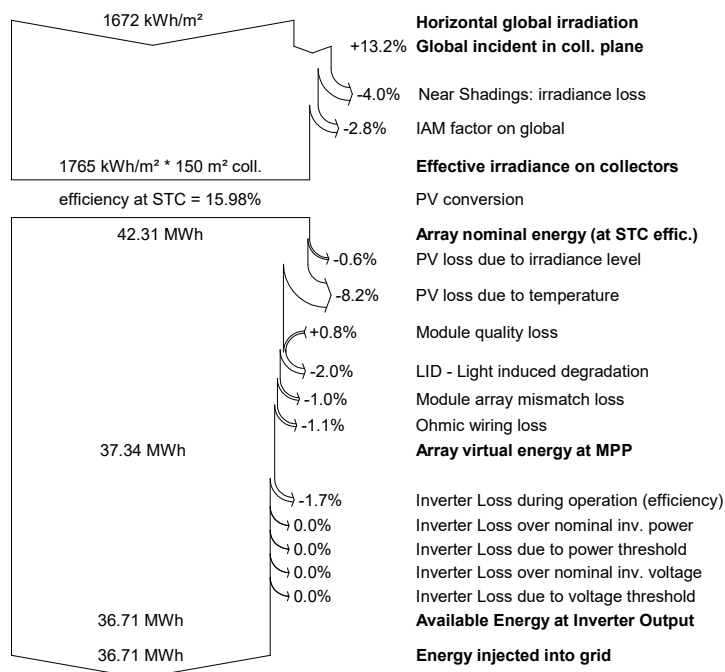
Legends: GlobHor Horizontal global irradiation
 T Amb Ambient Temperature
 GlobInc Global incident in coll. plane
 GlobEff Effective Global, corr. for IAM and shadings
 EArray Effective energy at the output of the array
 E_Grid Energy injected into grid
 EffArrR Effic. Eout array / rough area
 EffSysR Effic. Eout system / rough area

Grid-Connected System: Loss diagram

Project : Thesis
Simulation variant : Serial - 1st density

Main system parameters	System type	Grid-Connected	
Near Shadings	Linear shadings		
PV Field Orientation	tilt	30°	azimuth 0°
PV modules	Model	PW-DC-260-P-60	Pnom 260 Wp
PV Array	Nb. of modules	92	Pnom total 23.92 kWp
Inverter	Model	Sunny Tripower 25000TL-JP-30	25.00 kW ac
User's needs	Unlimited load (grid)		

Loss diagram over the whole year



A.3 Serial 2nd Density



Grid-Connected System: Simulation parameters

Project :	Thesis			
Geographical Site	Ankara_g	Country	Turkey	
Situation	Latitude	39.9°N	Longitude	32.9°E
Time defined as	Legal Time	Time zone UT+2	Altitude	895 m
	Albedo	0.20		
Meteo data:	Ankara_g	PVGIS CM SAF, satellite 1998-2011 - Synthetic		

Simulation variant : Serial - 2nd density

Simulation parameters

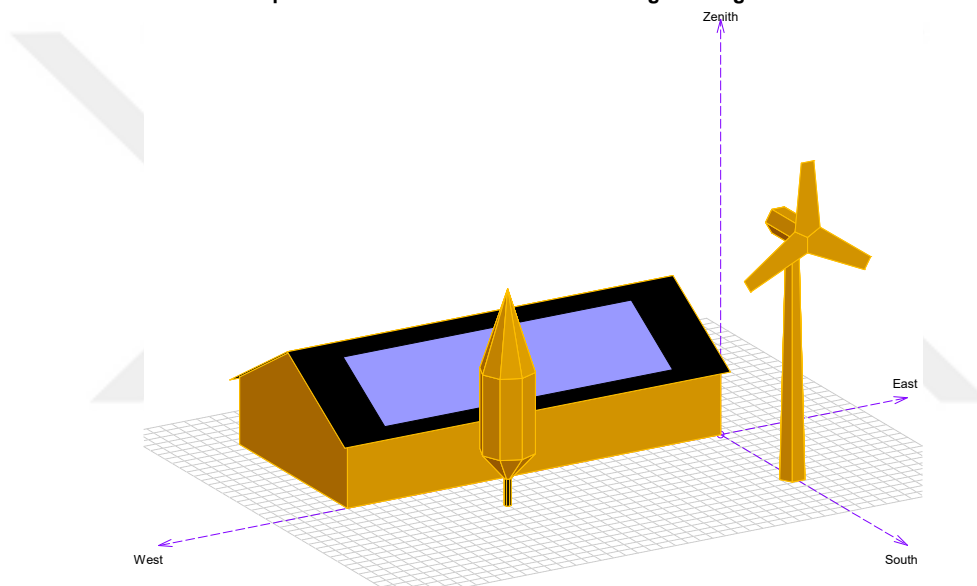
Collector Plane Orientation	Tilt	30°	Azimuth	0°
Models used	Transposition	Perez	Diffuse	Perez, Meteonorm
Horizon	Free Horizon			
Near Shadings	Linear shadings			
PV Array Characteristics				
PV module	Si-poly	Model	PW-DC-260-P-60	
<small>Original PVsyst database</small>	Manufacturer	Plurawatt		
Number of PV modules	In series	23 modules	In parallel	4 strings
Total number of PV modules	Nb. modules	92	Unit Nom. Power	260 Wp
Array global power	Nominal (STC)	23.92 kWp	At operating cond.	21.42 kWp (50°C)
Array operating characteristics (50°C)	U mpp	636 V	I mpp	34 A
Total area	Module area	150 m²	Cell area	134 m²
Inverter				
<small>Original PVsyst database</small>	Model	Sunny Tripower 25000TL-JP-30		
Characteristics	Manufacturer	SMA		
	Operating Voltage	390-800 V	Unit Nom. Power	25.0 kWac
Inverter pack	Nb. of inverters	2 * MPPT 50 %	Total Power	25 kWac
PV Array loss factors				
Thermal Loss factor	Uc (const)	20.0 W/m²K	Uv (wind)	0.0 W/m²K / m/s
Wiring Ohmic Loss	Global array res.	320 mOhm	Loss Fraction	1.5 % at STC
LID - Light Induced Degradation			Loss Fraction	2.0 %
Module Quality Loss			Loss Fraction	-0.8 %
Module Mismatch Losses			Loss Fraction	1.0 % at MPP
Incidence effect, ASHRAE parametrization	IAM =	1 - bo (1/cos i - 1)	bo Param.	0.05
User's needs :	Unlimited load (grid)			

Grid-Connected System: Near shading definition

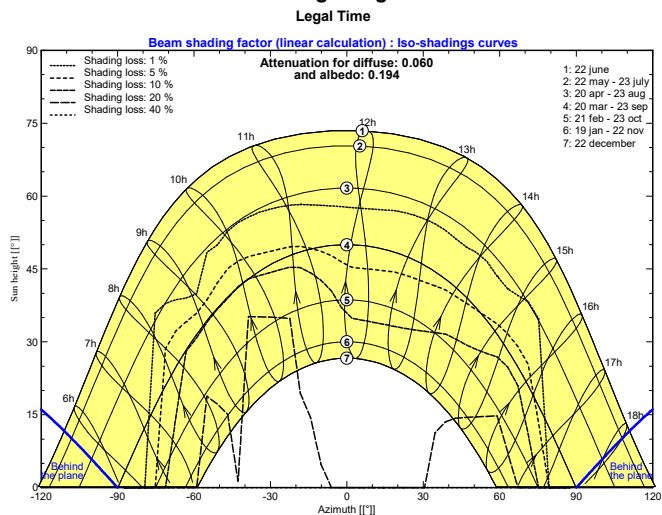
Project : Thesis
Simulation variant : Serial - 2nd density

Main system parameters	System type	Grid-Connected		
Near Shadings	Linear shadings			
PV Field Orientation	tilt	30°	azimuth	0°
PV modules	Model	PW-DC-260-P-60	Pnom	260 Wp
PV Array	Nb. of modules	92	Pnom total	23.92 kWp
Inverter	Model	Sunny Tripower 25000TL-JP-30		25.00 kW ac
User's needs	Unlimited load (grid)			

Perspective of the PV-field and surrounding shading scene



Iso-shadings diagram



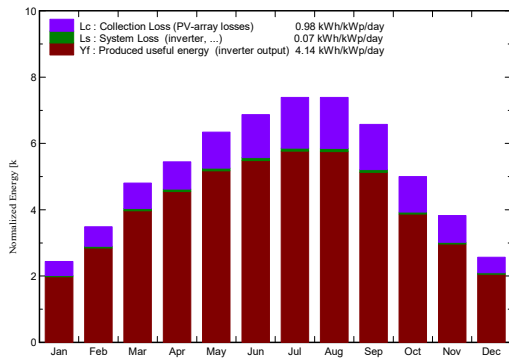
Grid-Connected System: Main results

Project : Thesis
Simulation variant : Serial - 2nd density

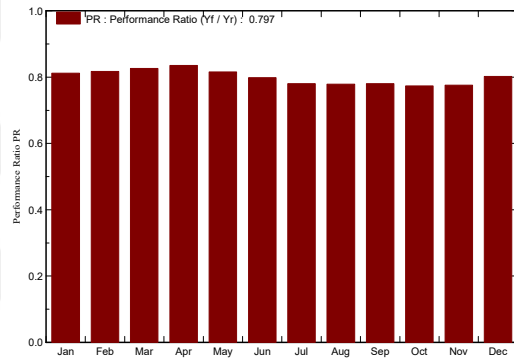
Main system parameters	System type	Grid-Connected		
Near Shadings	Linear shadings			
PV Field Orientation	tilt	30°	azimuth	0°
PV modules	Model	PW-DC-260-P-60	Pnom	260 Wp
PV Array	Nb. of modules	92	Pnom total	23.92 kWp
Inverter	Model	Sunny Tripower 25000TL-JP-30		25.00 kW ac
User's needs	Unlimited load (grid)			

Main simulation results	Produced Energy	36.10 MWh/year	Specific prod.	1509 kWh/kWp/year
System Production	Performance Ratio PR	79.7 %		

Normalized productions (per installed kWp): Nominal power 23.92 kWp



Performance Ratio PR



Balances and main results

	GlobHor kWh/m ²	T Amb °C	GlobInc kWh/m ²	GlobEff kWh/m ²	EArray MWh	E_Grid MWh	EffArrR %	EffSysR %
January	53.9	0.70	75.6	64.4	1.498	1.468	13.21	12.94
February	72.8	2.40	97.6	84.1	1.943	1.908	13.27	13.03
March	127.1	5.80	148.9	135.7	2.995	2.943	13.41	13.18
April	151.5	10.80	163.5	153.2	3.321	3.265	13.55	13.32
May	197.8	16.40	196.6	185.5	3.899	3.835	13.22	13.00
June	217.5	20.00	206.1	195.0	4.001	3.935	12.94	12.73
July	236.5	24.40	229.0	217.7	4.347	4.276	12.65	12.45
August	214.8	24.50	229.1	218.7	4.341	4.269	12.63	12.42
September	163.2	20.40	197.2	183.4	3.741	3.681	12.65	12.44
October	113.5	12.60	154.9	134.1	2.915	2.868	12.54	12.34
November	73.2	6.90	114.8	96.0	2.166	2.130	12.58	12.37
December	50.5	2.00	79.5	66.9	1.555	1.526	13.04	12.80
Year	1672.4	12.30	1892.8	1734.6	36.722	36.105	12.93	12.72

Legends: GlobHor Horizontal global irradiation
 T Amb Ambient Temperature
 GlobInc Global incident in coll. plane
 GlobEff Effective Global, corr. for IAM and shadings
 EArray Effective energy at the output of the array
 E_Grid Energy injected into grid
 EffArrR Effic. Eout array / rough area
 EffSysR Effic. Eout system / rough area

Grid-Connected System: Loss diagram

Project : Thesis
Simulation variant : Serial - 2nd density

Main system parameters	System type	Grid-Connected	
Near Shadings	Linear shadings		
PV Field Orientation	tilt	30°	azimuth 0°
PV modules	Model	PW-DC-260-P-60	Pnom 260 Wp
PV Array	Nb. of modules	92	Pnom total 23.92 kWp
Inverter	Model	Sunny Tripower 25000TL-JP-30	25.00 kW ac
User's needs	Unlimited load (grid)		

Loss diagram over the whole year



A.4 Micro Shadowless



Grid-Connected System: Simulation parameters

Project :	Thesis			
Geographical Site	Ankara_g	Country	Turkey	
Situation	Latitude	39.9°N	Longitude	32.9°E
Time defined as	Legal Time	Time zone UT+2	Altitude	895 m
	Albedo	0.20		
Meteo data:	Ankara_g	PVGIS CM SAF, satellite 1998-2011 - Synthetic		

Simulation variant : Micro - shadowless

Simulation parameters

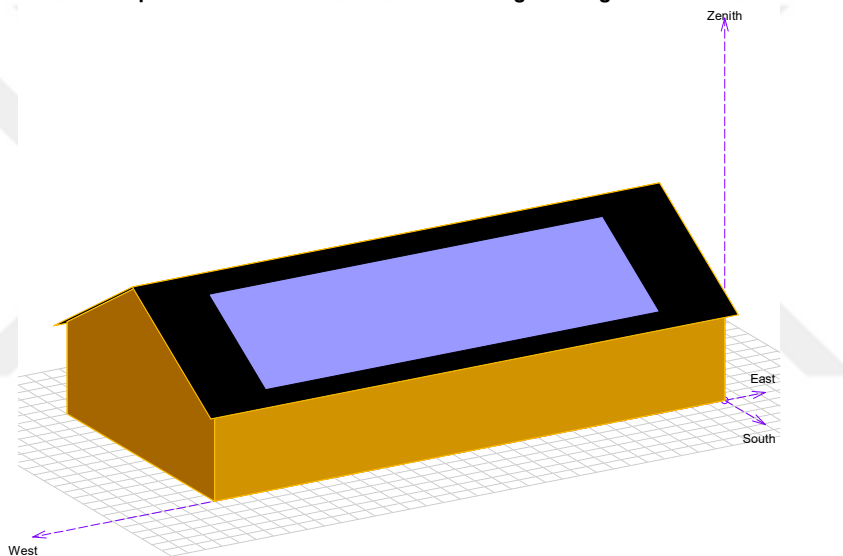
Collector Plane Orientation	Tilt	30°	Azimuth	0°
Models used	Transposition	Perez	Diffuse	Perez, Meteonorm
Horizon	Free Horizon			
Near Shadings	Linear shadings			
PV Array Characteristics				
PV module	Si-poly	Model	PW-DC-260-P-60	
<small>Original PVsyst database</small>	Manufacturer	Plurawatt		
Number of PV modules	In series	1 modules	In parallel	92 strings
Total number of PV modules	Nb. modules	92	Unit Nom. Power	260 Wp
Array global power	Nominal (STC)	23.92 kWp	At operating cond.	21.42 kWp (50°C)
Array operating characteristics (50°C)	U mpp	28 V	I mpp	774 A
Total area	Module area	150 m²	Cell area	134 m²
Inverter				
<small>Custom parameters definition</small>	Model	MICRO-0.25-I-OUTD-US-240		
Characteristics	Manufacturer	ABB		
	Operating Voltage	12-60 V	Unit Nom. Power	0.250 kWac
Inverter pack	Nb. of inverters	92 units	Total Power	23 kWac
PV Array loss factors				
Thermal Loss factor	Uc (const)	20.0 W/m²K	Uv (wind)	0.0 W/m²K / m/s
Wiring Ohmic Loss	Global array res.	0.60 mOhm	Loss Fraction	1.5 % at STC
LID - Light Induced Degradation			Loss Fraction	2.0 %
Module Quality Loss			Loss Fraction	-0.8 %
Module Mismatch Losses			Loss Fraction	1.0 % at MPP
Incidence effect, ASHRAE parametrization	IAM =	1 - bo (1/cos i - 1)	bo Param.	0.05
User's needs :	Unlimited load (grid)			

Grid-Connected System: Near shading definition

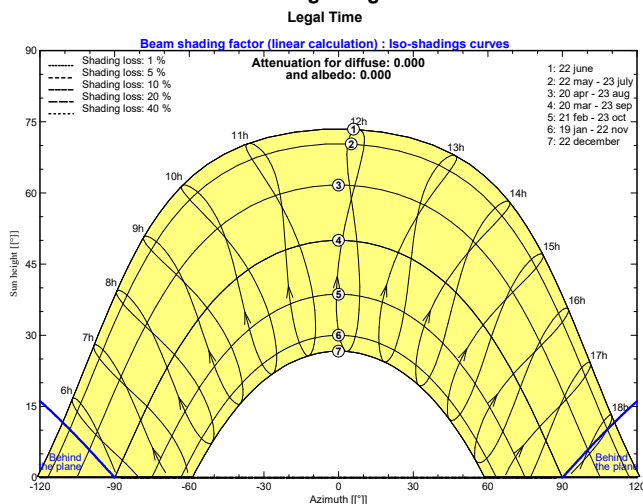
Project : Thesis
Simulation variant : Micro - shadowless

Main system parameters	System type	Grid-Connected		
Near Shadings	Linear shadings			
PV Field Orientation	tilt	30°	azimuth	0°
PV modules	Model	PW-DC-260-P-60	Pnom	260 Wp
PV Array	Nb. of modules	92	Pnom total	23.92 kWp
Inverter	Model	MICRO-0.25-I-OUTD-US-240		250 W ac
Inverter pack	Nb. of units	92.0	Pnom total	23.00 kW ac
User's needs	Unlimited load (grid)			

Perspective of the PV-field and surrounding shading scene



Iso-shadings diagram



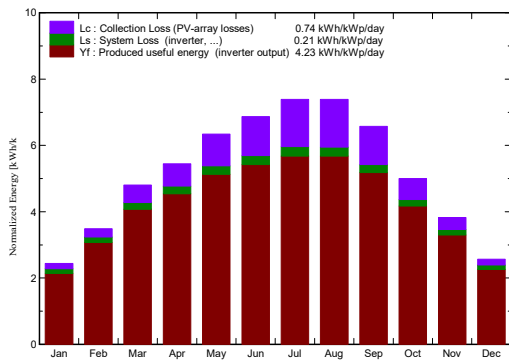
Grid-Connected System: Main results

Project : Thesis
Simulation variant : Micro - shadowless

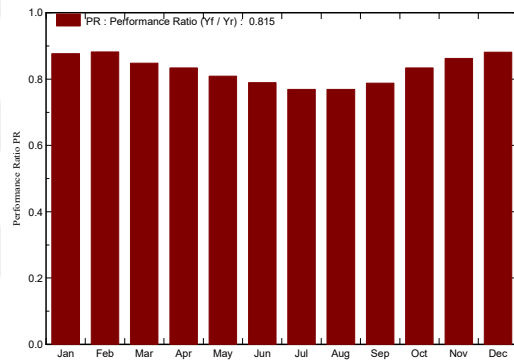
Main system parameters	System type	Grid-Connected	
Near Shadings	Linear shadings		
PV Field Orientation	tilt	30°	azimuth 0°
PV modules	Model	PW-DC-260-P-60	Pnom 260 Wp
PV Array	Nb. of modules	92	Pnom total 23.92 kWp
Inverter	Model	MICRO-0.25-I-OUTD-US-240	250 W ac
Inverter pack	Nb. of units	92.0	Pnom total 23.00 kW ac
User's needs	Unlimited load (grid)		

Main simulation results	Produced Energy	36900 kWh/year	Specific prod.	1543 kWh/kWp/year
System Production	Performance Ratio PR	81.5 %		

Normalized productions (per installed kWp): Nominal power 23.92 kWp



Performance Ratio PR



Balances and main results

	GlobHor	T Amb	GlobInc	GlobEff	EArray	E_Grid	EffArrR	EffSysR
	kWh/m ²	°C	kWh/m ²	kWh/m ²	kWh	kWh	%	%
January	53.9	0.70	75.6	73.5	1690	1586	14.90	13.98
February	72.8	2.40	97.6	94.8	2171	2060	14.83	14.07
March	127.1	5.80	148.9	144.8	3174	3021	14.21	13.53
April	151.5	10.80	163.5	158.4	3424	3260	13.97	13.29
May	197.8	16.40	196.6	190.5	3995	3803	13.55	12.90
June	217.5	20.00	206.1	199.7	4088	3891	13.22	12.59
July	236.5	24.40	229.0	222.2	4425	4213	12.88	12.26
August	214.8	24.50	229.1	223.0	4414	4213	12.84	12.26
September	163.2	20.40	197.2	192.1	3891	3717	13.15	12.57
October	113.5	12.60	154.9	150.9	3240	3091	13.94	13.30
November	73.2	6.90	114.8	111.6	2485	2368	14.43	13.75
December	50.5	2.00	79.5	77.1	1776	1676	14.89	14.05
Year	1672.4	12.30	1892.8	1838.5	38773	36900	13.66	13.00

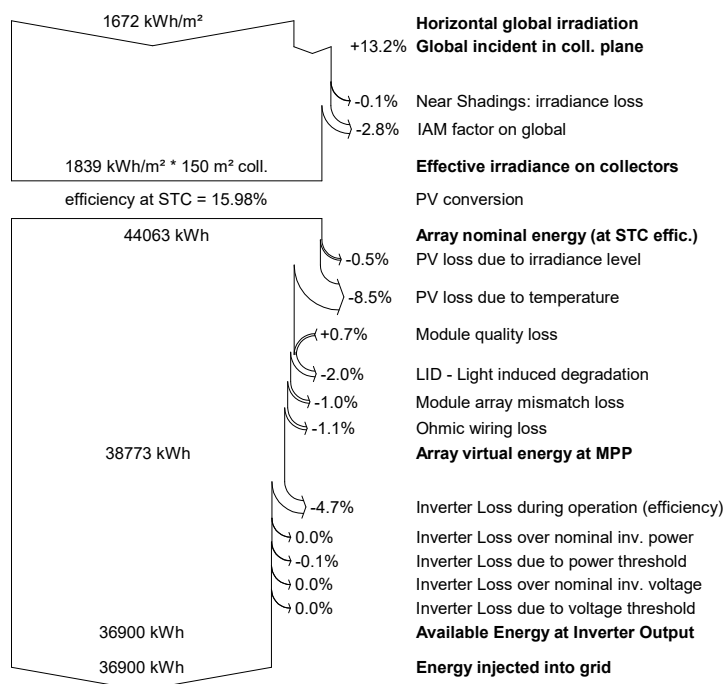
Legends:	GlobHor	Horizontal global irradiation	EArray	Effective energy at the output of the array
	T Amb	Ambient Temperature	E_Grid	Energy injected into grid
	GlobInc	Global incident in coll. plane	EffArrR	Effic. Eout array / rough area
	GlobEff	Effective Global, corr. for IAM and shadings	EffSysR	Effic. Eout system / rough area

Grid-Connected System: Loss diagram

Project : Thesis
Simulation variant : Micro - shadowless

Main system parameters	System type	Grid-Connected	
Near Shadings	Linear shadings		
PV Field Orientation	tilt	30°	azimuth 0°
PV modules	Model	PW-DC-260-P-60	Pnom 260 Wp
PV Array	Nb. of modules	92	Pnom total 23.92 kWp
Inverter	Model	MICRO-0.25-I-OUTD-US-240	250 W ac
Inverter pack	Nb. of units	92.0	Pnom total 23.00 kW ac
User's needs	Unlimited load (grid)		

Loss diagram over the whole year



A.5 Micro 1st Density



Grid-Connected System: Simulation parameters

Project :	Thesis		
Geographical Site	Ankara_g	Country	Turkey
Situation	Latitude 39.9°N	Longitude	32.9°E
Time defined as	Legal Time Time zone UT+2	Altitude	895 m
	Albedo 0.20		
Meteo data:	Ankara_g	PVGIS CM SAF, satellite 1998-2011 - Synthetic	

Simulation variant : Micro - 1st density

Simulation parameters

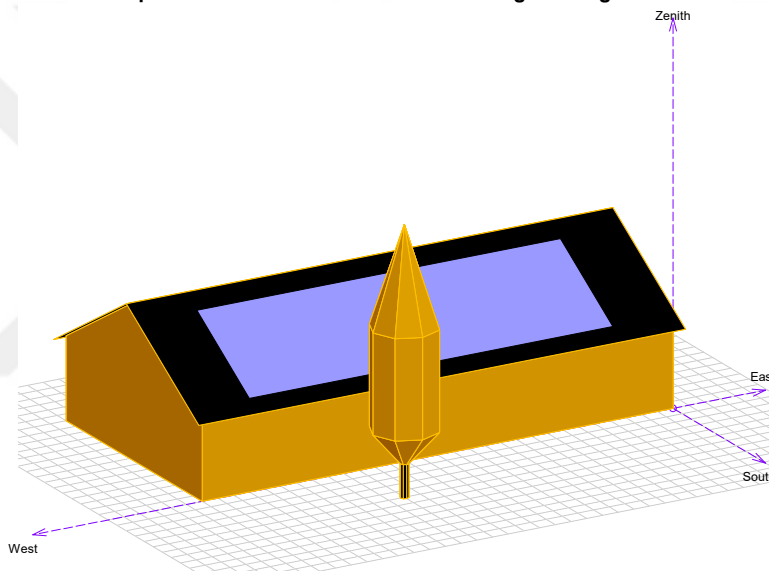
Collector Plane Orientation	Tilt	30°	Azimuth	0°
Models used	Transposition	Perez	Diffuse	Perez, Meteonorm
Horizon	Free Horizon			
Near Shadings	Linear shadings			
PV Array Characteristics				
PV module	Si-poly	Model	PW-DC-260-P-60	
<small>Original PVsyst database</small>	Manufacturer	Plurawatt		
Number of PV modules	In series	1 modules	In parallel	92 strings
Total number of PV modules	Nb. modules	92	Unit Nom. Power	260 Wp
Array global power	Nominal (STC)	23.92 kWp	At operating cond.	21.42 kWp (50°C)
Array operating characteristics (50°C)	U mpp	28 V	I mpp	774 A
Total area	Module area	150 m²	Cell area	134 m²
Inverter				
<small>Custom parameters definition</small>	Model	MICRO-0.25-I-OUTD-US-240		
Characteristics	Manufacturer	ABB		
	Operating Voltage	12-60 V	Unit Nom. Power	0.250 kWac
Inverter pack	Nb. of inverters	92 units	Total Power	23 kWac
PV Array loss factors				
Thermal Loss factor	Uc (const)	20.0 W/m²K	Uv (wind)	0.0 W/m²K / m/s
Wiring Ohmic Loss	Global array res.	0.60 mOhm	Loss Fraction	1.5 % at STC
LID - Light Induced Degradation			Loss Fraction	2.0 %
Module Quality Loss			Loss Fraction	-0.8 %
Module Mismatch Losses			Loss Fraction	1.0 % at MPP
Incidence effect, ASHRAE parametrization	IAM =	1 - bo (1/cos i - 1)	bo Param.	0.05
User's needs :	Unlimited load (grid)			

Grid-Connected System: Near shading definition

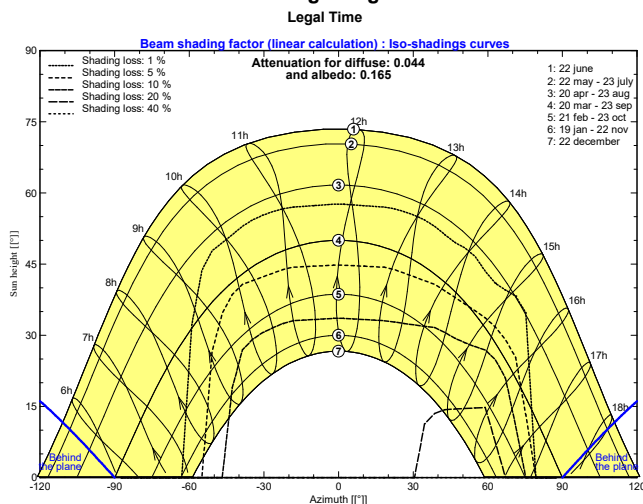
Project : Thesis
Simulation variant : Micro - 1st density

Main system parameters	System type	Grid-Connected		
Near Shadings	Linear shadings			
PV Field Orientation	tilt	30°	azimuth	0°
PV modules	Model	PW-DC-260-P-60	Pnom	260 Wp
PV Array	Nb. of modules	92	Pnom total	23.92 kWp
Inverter	Model	MICRO-0.25-I-OUTD-US-240		250 W ac
Inverter pack	Nb. of units	92.0	Pnom total	23.00 kW ac
User's needs	Unlimited load (grid)			

Perspective of the PV-field and surrounding shading scene



Iso-shadings diagram



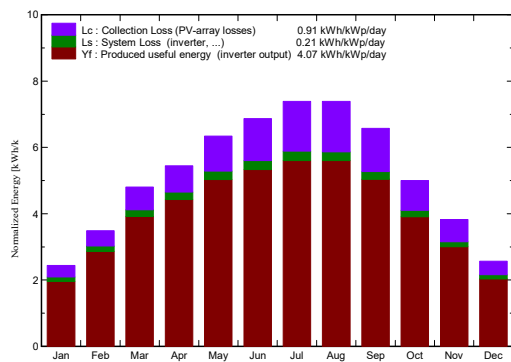
Grid-Connected System: Main results

Project : Thesis
Simulation variant : Micro - 1st density

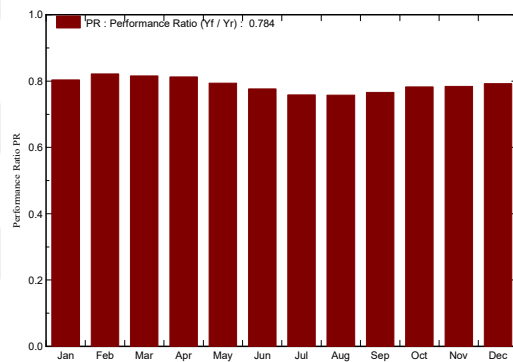
Main system parameters	System type	Grid-Connected	
Near Shadings	Linear shadings		
PV Field Orientation	tilt	30°	azimuth 0°
PV modules	Model	PW-DC-260-P-60	Pnom 260 Wp
PV Array	Nb. of modules	92	Pnom total 23.92 kWp
Inverter	Model	MICRO-0.25-I-OUTD-US-240	250 W ac
Inverter pack	Nb. of units	92.0	Pnom total 23.00 kW ac
User's needs	Unlimited load (grid)		

Main simulation results	Produced Energy	35500 kWh/year	Specific prod.	1484 kWh/kWp/year
System Production	Performance Ratio PR	78.4 %		

Normalized productions (per installed kWp): Nominal power 23.92 kWp



Performance Ratio PR



Balances and main results

	GlobHor	T Amb	GlobInc	GlobEff	EArray	E_Grid	EffArrR	EffSysR
	kWh/m ²	°C	kWh/m ²	kWh/m ²	kWh	kWh	%	%
January	53.9	0.70	75.6	67.0	1552	1453	13.68	12.81
February	72.8	2.40	97.6	87.9	2026	1919	13.83	13.10
March	127.1	5.80	148.9	138.7	3055	2905	13.68	13.01
April	151.5	10.80	163.5	154.2	3341	3179	13.63	12.96
May	197.8	16.40	196.6	186.7	3922	3732	13.30	12.65
June	217.5	20.00	206.1	196.2	4022	3827	13.01	12.38
July	236.5	24.40	229.0	218.8	4366	4156	12.71	12.10
August	214.8	24.50	229.1	219.4	4353	4153	12.66	12.09
September	163.2	20.40	197.2	185.9	3784	3614	12.79	12.22
October	113.5	12.60	154.9	140.6	3043	2901	13.09	12.48
November	73.2	6.90	114.8	100.7	2264	2154	13.15	12.51
December	50.5	2.00	79.5	69.0	1602	1507	13.43	12.64
Year	1672.4	12.30	1892.8	1765.1	37329	35500	13.15	12.50

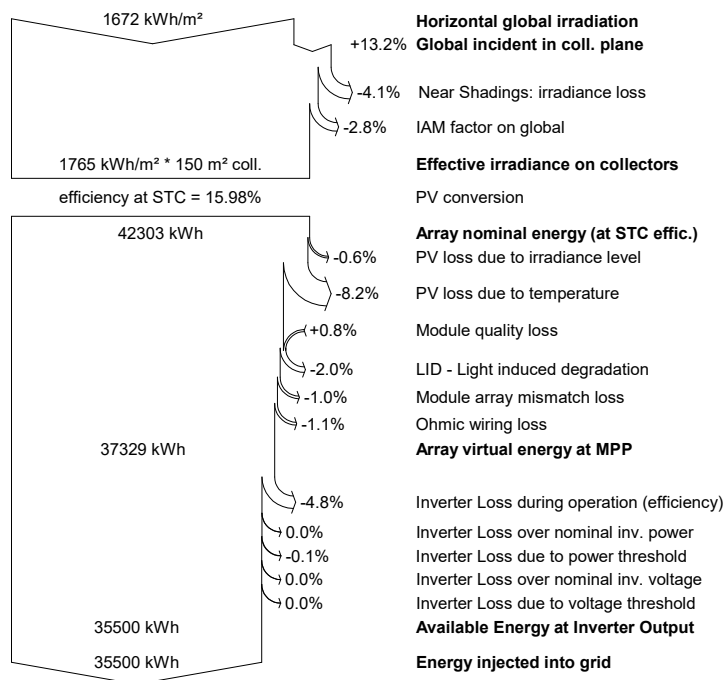
Legends:	GlobHor	Horizontal global irradiation	EArray	Effective energy at the output of the array
	T Amb	Ambient Temperature	E_Grid	Energy injected into grid
	GlobInc	Global incident in coll. plane	EffArrR	Effic. Eout array / rough area
	GlobEff	Effective Global, corr. for IAM and shadings	EffSysR	Effic. Eout system / rough area

Grid-Connected System: Loss diagram

Project : Thesis
Simulation variant : Micro - 1st density

Main system parameters	System type	Grid-Connected	
Near Shadings	Linear shadings		
PV Field Orientation	tilt	30°	azimuth 0°
PV modules	Model	PW-DC-260-P-60	Pnom 260 Wp
PV Array	Nb. of modules	92	Pnom total 23.92 kWp
Inverter	Model	MICRO-0.25-I-OUTD-US-240	250 W ac
Inverter pack	Nb. of units	92.0	Pnom total 23.00 kW ac
User's needs	Unlimited load (grid)		

Loss diagram over the whole year



A.6 Micro 2nd Density



Grid-Connected System: Simulation parameters

Project :	Thesis		
Geographical Site	Ankara_g	Country	Turkey
Situation	Latitude 39.9°N	Longitude	32.9°E
Time defined as	Legal Time Time zone UT+2	Altitude	895 m
	Albedo 0.20		
Meteo data:	Ankara_g	PVGIS CM SAF, satellite 1998-2011 - Synthetic	

Simulation variant : Micro - 2nd density

Simulation parameters

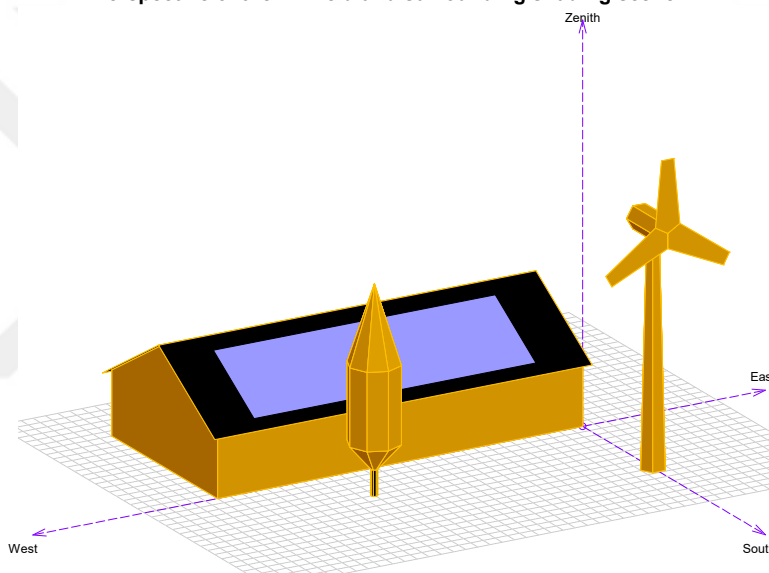
Collector Plane Orientation	Tilt	30°	Azimuth	0°
Models used	Transposition	Perez	Diffuse	Perez, Meteonorm
Horizon	Free Horizon			
Near Shadings	Linear shadings			
PV Array Characteristics				
PV module	Si-poly	Model	PW-DC-260-P-60	
<small>Original PVsyst database</small>	Manufacturer	Plurawatt		
Number of PV modules	In series	1 modules	In parallel	92 strings
Total number of PV modules	Nb. modules	92	Unit Nom. Power	260 Wp
Array global power	Nominal (STC)	23.92 kWp	At operating cond.	21.42 kWp (50°C)
Array operating characteristics (50°C)	U mpp	28 V	I mpp	774 A
Total area	Module area	150 m²	Cell area	134 m²
Inverter				
<small>Custom parameters definition</small>	Model	MICRO-0.25-I-OUTD-US-240		
Characteristics	Manufacturer	ABB		
	Operating Voltage	12-60 V	Unit Nom. Power	0.250 kWac
Inverter pack	Nb. of inverters	92 units	Total Power	23 kWac
PV Array loss factors				
Thermal Loss factor	Uc (const)	20.0 W/m²K	Uv (wind)	0.0 W/m²K / m/s
Wiring Ohmic Loss	Global array res.	0.60 mOhm	Loss Fraction	1.5 % at STC
LID - Light Induced Degradation			Loss Fraction	2.0 %
Module Quality Loss			Loss Fraction	-0.8 %
Module Mismatch Losses			Loss Fraction	1.0 % at MPP
Incidence effect, ASHRAE parametrization	IAM =	1 - bo (1/cos i - 1)	bo Param.	0.05
User's needs :	Unlimited load (grid)			

Grid-Connected System: Near shading definition

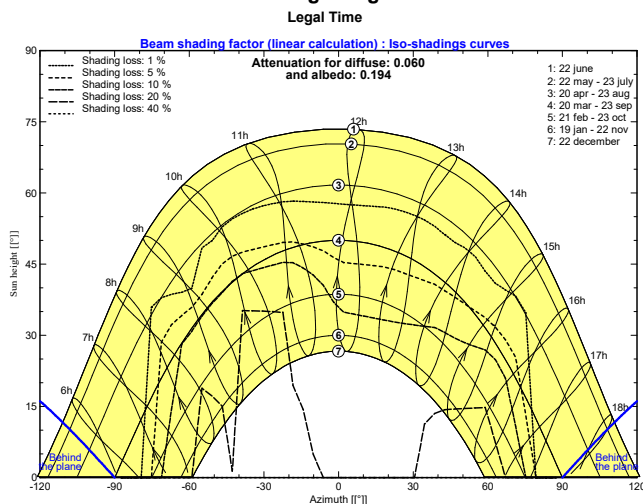
Project : Thesis
Simulation variant : Micro - 2nd density

Main system parameters	System type	Grid-Connected		
Near Shadings	Linear shadings			
PV Field Orientation	tilt	30°	azimuth	0°
PV modules	Model	PW-DC-260-P-60	Pnom	260 Wp
PV Array	Nb. of modules	92	Pnom total	23.92 kWp
Inverter	Model	MICRO-0.25-I-OUTD-US-240		250 W ac
Inverter pack	Nb. of units	92.0	Pnom total	23.00 kW ac
User's needs	Unlimited load (grid)			

Perspective of the PV-field and surrounding shading scene



Iso-shadings diagram



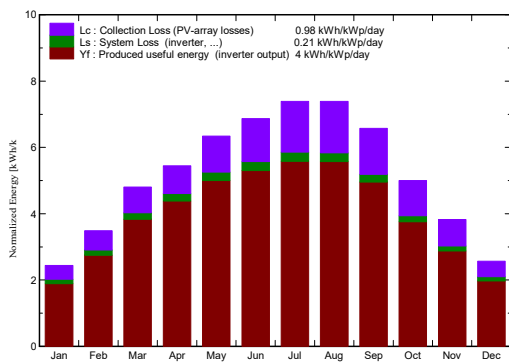
Grid-Connected System: Main results

Project : Thesis
Simulation variant : Micro - 2nd density

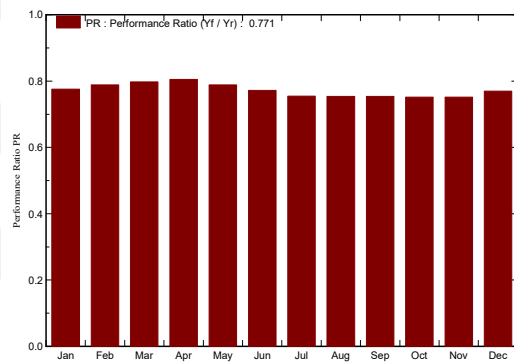
Main system parameters	System type	Grid-Connected	
Near Shadings	Linear shadings		
PV Field Orientation	tilt	30°	azimuth 0°
PV modules	Model	PW-DC-260-P-60	Pnom 260 Wp
PV Array	Nb. of modules	92	Pnom total 23.92 kWp
Inverter	Model	MICRO-0.25-I-OUTD-US-240	250 W ac
Inverter pack	Nb. of units	92.0	Pnom total 23.00 kW ac
User's needs	Unlimited load (grid)		

Main simulation results	Produced Energy	34889 kWh/year	Specific prod. 1459 kWh/kWp/year
System Production	Performance Ratio PR	77.1 %	

Normalized productions (per installed kWp): Nominal power 23.92 kWp



Performance Ratio PR



Balances and main results

	GlobHor	T Amb	GlobInc	GlobEff	EArray	E_Grid	EffArrR	EffSysR
	kWh/m ²	°C	kWh/m ²	kWh/m ²	kWh	kWh	%	%
January	53.9	0.70	75.6	64.6	1500	1403	13.22	12.37
February	72.8	2.40	97.6	84.3	1947	1842	13.29	12.58
March	127.1	5.80	148.9	135.5	2990	2842	13.39	12.73
April	151.5	10.80	163.5	152.6	3309	3147	13.49	12.84
May	197.8	16.40	196.6	185.4	3897	3707	13.21	12.57
June	217.5	20.00	206.1	195.0	3999	3805	12.94	12.31
July	236.5	24.40	229.0	217.7	4346	4137	12.65	12.04
August	214.8	24.50	229.1	218.2	4331	4133	12.60	12.03
September	163.2	20.40	197.2	182.6	3724	3556	12.59	12.02
October	113.5	12.60	154.9	134.6	2924	2786	12.58	11.99
November	73.2	6.90	114.8	96.4	2172	2065	12.61	11.99
December	50.5	2.00	79.5	67.0	1557	1465	13.06	12.28
Year	1672.4	12.30	1892.8	1733.8	36696	34889	12.92	12.29

Legends:	GlobHor	Horizontal global irradiation	EArray	Effective energy at the output of the array
	T Amb	Ambient Temperature	E_Grid	Energy injected into grid
	GlobInc	Global incident in coll. plane	EffArrR	Effic. Eout array / rough area
	GlobEff	Effective Global, corr. for IAM and shadings	EffSysR	Effic. Eout system / rough area

Grid-Connected System: Loss diagram

Project : Thesis
Simulation variant : Micro - 2nd density

Main system parameters	System type	Grid-Connected	
Near Shadings	Linear shadings		
PV Field Orientation	tilt	30°	azimuth 0°
PV modules	Model	PW-DC-260-P-60	Pnom 260 Wp
PV Array	Nb. of modules	92	Pnom total 23.92 kWp
Inverter	Model	MICRO-0.25-I-OUTD-US-240	250 W ac
Inverter pack	Nb. of units	92.0	Pnom total 23.00 kW ac
User's needs	Unlimited load (grid)		

Loss diagram over the whole year

